NANOTECHNOLOGY BASED APPROACHES FOR DETECTION AND QUANTIFICATION OF SAFFRON ADULTERATION

Thesis Submitted for the Award of the Degree of

DOCTOR OF PHILOSOPHY

in

Forensic Science

By

Tahir ul Gani Mir

Registration Number: 11816264

Supervised By

Dr Saurabh Shukla (26174)
Assistant Professor
Department of Forensic Science
School of Bioengineering and Biosciences,
Lovely Professional University, Phagwara,
Punjab- 144411, India

Co-supervised By

Dr Jaskaran Singh
Associate Professor
Department of Forensic Science
Geeta University, Naultha,
Panipat Haryana- 132145, India

LOVELY
PROFESSIONAL
UNIVERSITY

Transforming Education Transforming India

LOVELY PROFESSIONAL UNIVERSITY, PUNJAB

2024

DECLARATION

I, hereby declared that the presented work in the thesis entitled *"Nanotechnology based Approaches for detection and quantification of Saffron Adulteration"* in fulfilment of degree of **Doctor of Philosophy (Ph. D.)** is outcome of research work carried out by me under the supervision **Dr. Saurabh Shula** working as Assistant Professor in the Department of Forensic Science, School of Bioengineering and Biosciences, Lovely Professional University, Phagwara India. In keeping with general practice of reporting scientific observations, due acknowledgements have been made whenever work described here has been based on findings of another investigator. This work has not been submitted in part or full to any other University or Institute for the award of any degree.

Name of the scholar: Tahir ul Gani Mir
Registration No.: 11816264
School of Bioengineering and Biosciences,
Lovely Professional University, Phagwara, Punjab- 144411, India

CERTIFICATE

This is to certify that the work reported in the Ph. D. thesis entitled *"Nanotechnology based Approaches for detection and quantification of Saffron Adulteration"* submitted in fulfillment of the requirement for the reward of degree of **Doctor of Philosophy (Ph.D.)** in the Department of Forensic Science, School of Bioengineering and Biosciences, Lovely Professional University, Phagwara India is a research work carried out by Tahir ul Gani Mir is bonafide record of his/her original work carried out under my supervision and that no part of thesis has been submitted for any other degree, diploma or equivalent course.

(Signature of Supervisor)
Dr Saurabh Shukla (26174)
Assistant Professor
Department of Forensic Science
School of Bioengineering and Biosciences,
Lovely Professional University, Phagwara,
 Punjab- 144411, India

(Signature of Co-supervisor)
Dr Jaskaran Singh
Department of Forensic Science
Geeta University, Naultha, Panipat Haryana- 132145, India

Acknowledgement

I am immensely grateful to have the opportunity to express my heartfelt appreciation to those who have supported me throughout this journey of academic pursuit. I extend my deepest gratitude to my esteemed Supervisor **Dr Saurabh Shukla** and co-supervisor **Dr Jaskaran Singh** whose expertise, patience, and invaluable insights have been instrumental in shaping the direction and quality of this research. Your mentorship has not only enhanced my academic understanding but also inspired me to strive for excellence.

A special thanks is due to **Dr Neeta Raj Sharma**, Head of the School of Bioengineering and Bioscience, for her unwavering support, guidance, and encouragement. Her support and insights have been invaluable in shaping the course of this research.

I would also like to thank the members of **CRDP** and **RDC** for their thoughtful feedback, constructive criticism, and commitment to ensuring the academic rigor of this work.

I am indebted to **Lovely Professional University Phagwara Jalandhar Punjab** for providing the necessary resources, facilities, and academic environment that facilitated my research endeavors.

I would like to express my gratitude to my family and friends for their unwavering encouragement, understanding, and patience throughout this academic journey. Your belief in me has been a constant source of motivation, and I am truly blessed to have your support.

Last but not least, I extend my heartfelt thanks to all the participants, experts, and collaborators who generously shared their time and insights for this research. Your contributions have enriched the depth and significance of this work.

List of Figures

List of Tables

Abstract

Saffron is a highly valuable spice known as Golden Condiment or Red Gold, with the commercial part being the female Saffron filament or Saffron thread. Saffron plant is primarily produced in Greece, India (Kashmir J&K), Morocco, Italy, Iran, and Spain. Although other countries such as New Zealand, Japan, Israel, France, Egypt, Australia, Azerbaijan, and Switzerland are emerging as producers. In India saffron is cultivated in Kashmir (J&K). It has various medicinal properties, such as antidepressant, anti-inflammatory, and respiratory decongestant. The distinct qualities of Saffron can be ascribed to compounds like crocin, picrocrocin, and safranal. Several factors, including the time of harvesting, geographical conditions, storage, and the drying process, influence the overall quality of Saffron. It is common for Saffron to be adulterated, with substances like safflower, turmeric, and synthetic dyes often mixed with powdered Saffron. Globally, the market size of Saffron is expected to go high, which may lead to increase in cases of adulteration. Scientists are working on detecting and quantifying adulterants using various methods and techniques. Several methods have been employed for detection and estimation of saffron adulteration. However, these methods are based on instrumental techniques and require expertise in handling such instruments. Therefore, there is a need of cost effective, time efficient, selective and sensitive methods for detection and determination of adulteration in saffron.

Recently, nanotechnology has emerged as an important and significant tool for quality control. Nanotechnology plays a crucial role in enhancing food security through various applications such as various sensors for food analysis, and intelligent packaging. The primary purpose of employing nanotechnology in the food industry is to ensure food safety, preservation, and functionalization. To deliver high-quality and safe food products to consumers, it is essential to measure and monitor the stability of food components. Traditional methods such as spectrometric or chromatographic analyses are time consuming as well as labor intensive. Therefore, there is a growing need for the development of sensors that can quickly and accurately detect food components such as biogenic amines, ethylene concentrations, vitamins, volatile gases, and toxins. The detection of such components can serve as indicators of food quality.

In the present work, nanotechnological approach was used for the determination of saffron quality and detection of various adulterants in saffron. To develop sensitive nanomaterial-based techniques for detection and determination of saffron quality and detection of various

adulterants in saffron, this study is divided into three parts. In the first part commercial saffron samples were obtained from different geographical locations and instrumental techniques such as Uv-Vis spectroscopy and HPLC were used to investigate the levels of adulteration and quality of commercial saffron sold at different geographical locations. It was found that saffron sold at some commercial markets in Kashmir India, is either low grade or adulterated.

The second part of the research involved the synthesis of a molecularly imprinted polymer combined with quantum dots (MIP-CQDs) to accurately measure the amount of crocin in saffron. Crocin is a vital phytochemical in saffron, and its concentration directly determines the quality of the saffron. A higher concentration of crocin indicates better quality. The MIP-CQDs, an extremely sensitive optical nanosensor, was developed to detect crocin. To create the CQDs-MIP, APTES, TEOS, and carbon quantum dots were combined in the presence of gentibiose as template molecules. The synthesized nanosensor showed a remarkable detection limit of 1.3 μM and a linear range of 3.3-20.0 μM.

In the third part, Gold nanoparticle (AuNPs), Nitrogen doped Cardon Quantum Dots (NCQDs) and Sulphur-Doped Carbon Quantum Dots were synthesized for determination of saffron quality and detection of Methyl-orange (MO) and Sudan dye in saffron, respectively. AuNPs were synthesized using crocin itself as an reduction agent and the intensity of pink colored AuNPs was measured by spectrophotometer in order to establish the concentration of crocin. To assess the practical usefulness of the suggested assays for real sample analysis, they were utilized to measure the overall concentration of crocin in saffron. Saffron extract of different concentrations in water were used to observe the results. It was found that with the decrease in the concentration of saffron extract, the color intensity also decreased, which was confirmed by UV spectrophotometer. The results showed a recovery range of 98.28-99.12%. Saffron extract with different levels of adulteration with safflower (0%-100%) were also used for the synthesis of nanoparticles. It was found that samples with higher concentration of adulteration lowered the NP synthesis as the adulteration levels increased.

NCQDs were synthesized in order to detect MO in saffron. The NCQDs were synthesized using microwave synthesis technique, with succinic acid and gallic acid as carbon and nitrogen sources, respectively. Various characterization methods such as X-Ray photoelectron spectroscopy (XPS), fluorescence spectroscopy, transmission electron microscopy (TEM), X-Ray diffraction (XRD), and zeta potential analyzer were used to assess the properties of the NCQDs. The XRD and XPS spectroscopy showed that the chemical composition and

morphological features of the NCQDs were satisfactory. The investigation using TEM showed that the size distribution of the NCQDs is relatively narrow, ranging from 2 to 10 nm, with the most common size being 6 nm. The synthesized NCQDs displayed the highest intensity of fluorescence 340 nm of excited wavelength. These NCQDs were used as a fluorescent probe to detect MO, and they exhibited a limit of detection (LOD) 0.77 µM. Additionally, when applied to saffron samples, the NCQDs yielded satisfactory results, with a recovery range of 98.6% to 99.2%. These findings suggest that N-doped carbon quantum dots have promising potential in the detection of MO in saffron.

Similarly, citric acid and thiourea acid as a carbon and sulphur source to conduct a straightforward one-step microwave synthesis of SCQDs. For the characterization of as-synthesized SCQDs, several methods such as fluorescence spectroscopy, XPS, XRD, and zeta potential analyzer were utilized. XRD and XPS spectroscopy are used to examine the chemical composition and morphological aspects. These SCQDs were found to have maximum distribution at 7 nm, according to zeta size analyser examinations. The SCQDs exhibited the highest fluorescence intensity (FL intensity) when excited at a wavelength of 340 nm. These synthesized SCQDs proved to be an effective fluorescent probe for detecting Sudan I in saffron samples, with a LOD of 0.77 M. These synthesized SCQDs were employed as an efficient fluorescent probe for the detection of Sudan I in saffron.

Chapter 1

1.1. Introduction

Saffron is a well-known spice obtained from the dried stigmas of *Crocus sativus* L. flowers. It is currently the most expensive spice and is commonly known as "Red Gold" (Mir *et al*., 2022; Shahi *et al*., 2016). *Crocus sativus* is an angiosperm plant belonging to the Asparagales family and blooms in the autumn, remaining dormant throughout the summer (Saxena, 2010). The flower of the *Crocus sativus* is solitary, purple, with six petals, three stamens, one style, and three red-orange stigmas (Figure 1.1). It is mainly distributed in the and Western Asia and Mediterranean Europe. Saffron from Iran accounts for almost 90% of global production (Husaini *et al*., 2010). The ideal growing environments for saffron are warm subtropical climates and well-drained sandy soils (Razak *et al*., 2017; Saxena, 2010). Saffron has been historically used as a spice; however, literature also justifies its use in ethnomedicine. Saffron has been used in traditional medicine to treat conditions including constipation, mucus membrane inflammation, depression, respiratory congestion, increased appetite, coughing, menstrual flow stimulation, lactation stimulation, and cramp relief (Sharma *et al*., 2020). Saffron has been used as an expectorant, emmenagogue, and adaptogenic agent in Ayurvedic medicine (Gohari *et al*., 2013). Greeks used saffron to cure wounds, acne, and other skin conditions (Mollazadeh *et al*., 2015). Saffron has been used to produce yellow or saffron dyes for dying clothes, painting, and other artistic endeavors (Yildirim *et al*., 2020). Saffron is highly antioxidant, and because of its moisturizing properties, it is widely used in perfumery and cosmetic products and in the prevention of skin cancer. Saffron is used in Various sunscreens and lotions as a UV absorbent agent, thus protecting skin from harmful radiations from the sun. Traditionally saffron soaked with basil leaves is used for the treatment of several skin conditions such as acne. Saffron extract along with olive oil or coconut oil helps to improve blood circulation in face skin. Saffron extract can also be used to treat rashes or redness of face (Mzabri et al., 2019a).

Medicinal plants are considered a valuable and essential approach to promoting health due to their minimal occurrence of negative effects. Saffron is rich in more than 300 volatile and nonvolatile compounds, including crocin, safranal, picrocrocin, monoterpenes, aldehydes, and various carotenoids with medicinal benefits (Winterhalter and Straubinger 2000; Melnyk., *et al,.* 2010). The analysis of saffron extract has unveiled a range of phytochemicals, with the

most significant bioactive elements being crocin, crocetin, safranal, and picrocrocin. These phytochemicals, such as picrocrocin, crocin and safranal, have been acknowledged for their positive impact on health (Mykhailenko et al,. 2019; Pandita., 2021). They possess the capability to treat several health disorders, including gastrointestinal issues (Milajerdi and Mahmoudi., 2014), cardiovascular disease (Kamalipour and Akhondzadeh., 2011), insulin resistance (Xi *et al.,* 2007), depression (Siddiqui *et al.,* 2018), premenstrual syndrome (Beiranvand *et al.,* 2016), insomnia (Taherzadeh *et al.,* 2020), anxiety (Shafiee *et al.,* 2018), tumors (Bolhassani *et al.,* 2014), etc. Additionally, saffron's antioxidant properties suggest its potential benefits in cancer treatment (Papandreou *et al.,* 2006; Dai and Mumper 2010; Gismondi *et al.,* 2012). Saffron finds extensive applications in both traditional medicine and modern pharmacology (Shahi *et al.,* 2016). Consequently, it is crucial to conduct toxicity studies on saffron and its metabolites. Recent years have witnessed several clinical studies examining the toxicity of saffron and its metabolites.

Figure 1.1- Saffron cultivation: *Crocus* Plant (a), *Crocus* flower with stigma (b), Harvesting saffron from *Crocus* flower (c), freshly harvested saffron (d), dried and processed saffron (e)

1.2. Chemical Composition/ Phytochemistry of Saffron

The primary components of saffron consist of varying percentages of nitrogenous matter, sugars, water, volatile oil, soluble extract, fiber, and overall ash (Table 1.1). Saffron is also a source of important vitamins such as riboflavin and thiamin, along with a small amount of β-carotene. Riboflavin is the predominant vitamin in saffron, with concentrations ranging from 56 to 138 ng/g. Thiamine concentrations in saffron ranging from 0.7 to 4 g/g (Christodoulou *et al*., 2015). In addition, it has been found that the petroleum ether extract of saffron contains important fatty acids such as linolenic and linoleic acids. A variety of sterols, including, stigmasterol, campesterol and beta-sitosterol, as well as ursolic, palmitoleic, and oleanolic may be found in saffron. In addition to these acids, saffron contains sterols, palmitoleic acid, ursolic acid, oleanolic acid, and oleic acid (Kosar *et al*., 2017).

Saffron is rich in volatile, nonvolatile, and aromatic compounds. These compounds include hydrophilic and hydrophilic proteins, carbohydrates, minerals, vitamins, gums, pigments, mucilage, saponins, alkaloids, crocins, safranal, picrocrocin, crocetin, and other compounds in traces (Kosar *et al*., 2017). The primary components found in the reddish-colored stigmatic lobes of saffron consist of crocetin and its related glucosidic derivatives. (Ghanbari *et al*., 2019). The presence of picrocrocin is the main component of the saffron that imparts a bitter taste to the saffron. Upon hydrolysis, it is crystallized it produces safranal and glucose (Anastasaki *et al*., 2009).

1.2.1. Apocarotenoids

The oxidative cleavage of the principal carotenoids by oxygenases gives apocarotenoids as products. The involved enzymes, CCDs (Carotenoid cleavage oxygenases), are known to recognize the double bonds and thus cleave one or two double bonds (Gohari *et al*., 2013). The primary metabolites of saffron include crocin, picrocrocin, safranal and crocetin (Table 1.2). The genus *Crocus* has a tremendous amount of crocins. Its molecular weight is 976.96 g/mol having $C_{44}H_{70}O_{28}$ as the chemical formula (Seifi and Shayesteh, 2020). Crocin is a quite peculiar compound of carotenoids with *cis* and *trans* diester that are water-soluble gentiobiose commonly utilized as a coloring agent in various medicines and foods (Pandita, 2021a). Crocin is made of trans-crocetin di-D gentiobiosyl and gives saffron its orange-yellow color (Ahrazem *et al*., 2015; Mir *et al*., 2022). Crocins maybe either monoglycosyl polyene or diglycosyl polyene ester of crocetin. The presence of esterified gentiobioses in crocin makes it the perfect coloring agent for a variety of foods and cuisines. Crocetin is a peculiar olefin conjugate that is unsaturated in nature and classified as a lipophilic carotenoid having 328.4g/mol as

molecular weight and 285℃ degree as the melting point. Different forms of crocetins (crocetin-I, alfa-crocetin, gamma-crocetin, crocetin-II) are formed by the degradation and/or cleavage of zeaxanthin on 8`,8/7 double bonds (Cuttriss *et al*., 2011). Crocetin is present in saffron in the form of glycosides in saffron as 94%, while 6% are present as free crocetin (Giaccio., 2004).

Crocetin is hydrophobic and oil-soluble in nature. It is a conjugated polyene dicarboxylic acid designed to enhance the distinctive pleasant aroma of saffron. Crocetin is a member of the carotenoid family, a group of natural dyes, but it does not possess the provitamin function (Caballero-Ortega *et al.*, 2004). Unlike most carotenoids, crocetin belongs to a small subgroup characterized by the presence of acid and carboxylic groups, which cannot be incorporated into the overall chemical structure. Specifically, crocetin is referred to as 8,8-diapo-8,8-caroteneic acid and features a symmetrical arrangement of seven double bonds and four methyl groups, forming a diterpenic structure. Its chemical composition is denoted as $C_{20}H_{24}O_4$, with a molecular weight of 328.4 (Caballero-Ortega *et al.*, 2004). Crocetin (due to its chemical structure) is referred to primarily for its antioxidant properties and is an essential component of saffron in ongoing research (Gohari *et al*., 2013; Pandita., 2021)

The pungent flavor of saffron comes from a bitter glucoside called picrocrocin. Picrocrocin has the chemical formula $C_{16}H_{26}O_7$ and is known scientifically as *4-(-D-glucopyranosyloxy)-2,6,6 trimethyl-cyclohexane* carbaldehyde. Picrocrocin with 330.37 g/mol molecular weight is a glycoside acting as the precursor substance for safranal (Escribano *et al*., 1996). It is a second major compound in saffron with a monoterpene nature. On the other hand, safranal is a 150.21 g/mol molecular weight compound chemically a glycon of picrocrocin and a monoterpene aldehyde (Shafat., *et al*., 2021). The samples of Iranian saffron were subjected to GCMS analysis; the results showed a string of aromatic active compounds in the form of safranal, dihydro-oxophorone, and 4-ketoisophone (Jalali-Heravi *et al*., 2009). The presence of apocarotenoids in the saffron stigma is quite regulated. The peak value concerning the accumulation of apocarotenoids is achieved as the red stigmas develop. Five different genes have been studied that are involved in the biosynthesis of carotenoids, expression of associated genes, and cleavage activities (Iman Yousefi Javan and Yousef Hosseinzadehgonabad, 2017). Picrocrocin is broken down into glucose and safranal during the drying process of saffron after harvest

Safranal is a cyclic terpenic aldehyde with the chemical formula $C_{10}H_{14}O$ (m.w.= 150; e.p.70 OC/1 mm) and the IUPAC name *(2, 6, 6 trimethy l-1,3 cyclohexadien 1*

carboxaldehyde). Safranal is a volatile oil and gives distinctive aroma to saffron (Gismondi *et al*., 2012). Safranal may account for as much as 70 percent of the volatile fraction of saffron. The freshly harvested stigma has no distinctive aroma. After being harvested, saffron is processed and dried. The combined action of enzymes and heat on picrocrocin results in the production of D-glucose and a free molecule of safranal. The resulted safranal has a distinct aroma that gives the spice a characteristic aroma (Caballero-Ortega *et al*., 2004).

1.2.2. Flavonoids

The glycosylation of flavonols at 3,7 and 4-OH positions in *Crocus sativus* results in the formation of a string of flavonols (E. Karimi *et al*., 2010). Three glucosides having a kaempferol nature have been reported viz "*kaempferol 7-O sophoroside (K$_7$OS), kaempferol 3,7,4 triglucoside, and kaempferol 3-O sophroside 7-O glucopyranoside (K$_3$OS$_7$OG)*" (Carmona *et al*., 2007). Each of them increases with the development of stigma of *Crocus*. At the point of anthesis, the relative quantitative levels of K$_7$OS reach maximum while K$_3$OS$_7$OG reach the maximum level at the time of scarlet, also known as the scarlet-stage (Dhar *et al*., 2017). Gallic acid and pyrogallol are two flavonoids that have been isolated from the stigma of saffron, while galangin, kaempferol and quercetin have been isolated from the fresh petals of the saffron. The identified flavonoids in ethyl acetate, diethyl ether, and some aqueous fractions include taxifolin 7-O hexose (T7OH), 4-methyl ether dihydrokaempferol-3-O-deoxyhexoside (4MEDK3ODH), and naringenin-7-O-hexoside (N$_7$OH). The other flavonoids have been isolated using methanolic extract (Trapero *et al*., 2012). The isolated flavonoids include kaempferol and quercitin glycosidic derivates as the main compounds in combination with acetylated and methoxylated derivatives. Almost 21 different isorhamnetin, myricetin, naringenin, tamarixentin, kaempferol, and taxifolin have been isolated and characterized in tepals (Mottaghipisheh *et al*., 2020).

1.2.3. Saponins and miscellaneous compounds of saffron
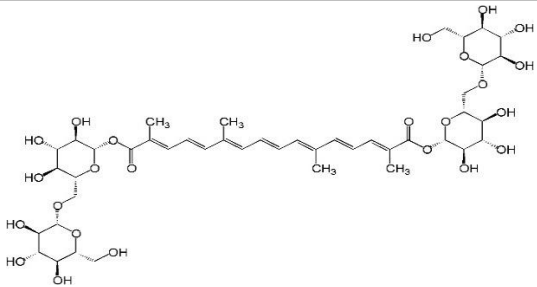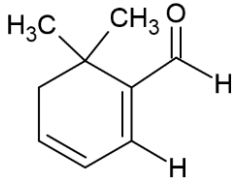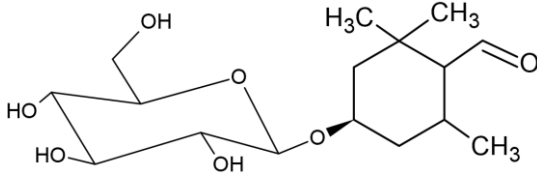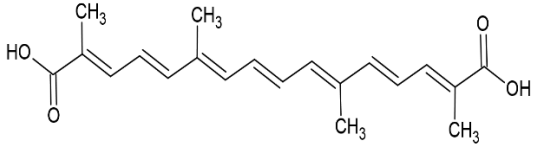
Saponins are abundantly found in many plants and plant products. These are chemically terpenoids with a wide range of bioactivities in the form of antimicrobial, antioxidant, allelopathic, herbicidal, and insecticidal properties(Rubio-Moraga *et al*., 2013). The name saponin is taken from the Latin word soap because of foam producing property of the surfactants (Cardone *et al*., 2020). Based on the chemical nature, the saponins are classified into triterpenoid and steroidal saponins(Rubio-Moraga *et al*., 2011). In *Crocus sativus*, two saponins of triterpenic nature have been characterized in corm that includes azafrine-1 and

azafrine-2. Chemically azafrine-1 possesses 3-O-β-D-glucopyranose iduronic echinocystic acid as prosapogenin. Azafrine1 and azafrine-2 are present in the outer part of corms, which makes them important for the plant's defense system. Salicylic acid, catechol, cinnamic acid, vanillin, gentisic acid, cinnamic acid, caffeic acid are syringic acid are some other compounds of phenolic nature found in the corms of saffron(Keller *et al*., 2019). The compound with volatile nature found in corms of saffron includes hexadecanoic acid, palmitic acid, octadecadienoic acid, pentadecane, eicosane, etc. (Rubio-Moraga *et al*., 2011).

Table 1.1- Primary composition of saffron

Component	Mass Percentage
Water-soluble components	*53.00%*
Protein	*12.00%*
Lipid	*12.00%*
Gum	*10.00%*
Water	*10.00%*
Pentosan	*8.00%*
Pectins	*6.00%*
Starch	*6.00%*
Nonvolatile oil	*6.00%*
Inorganic matter	*6.00%*
Fibers	*5.00%*
Alfa-crocin	*2.00%*
Volatile oils	*1.00%*
Other carotenoids	*1.00%*

Table 1.2- Chemical Structure and characteristic properties of Nonvolatile metabolites of Saffron

Metabolite	Chemical Structure	Characteristic Property
Crocin		Crocin ($C_{44}H_{64}O_{24}$) is a carotenoid chemical compound which is meant for the characteristic colour of saffron
Safranal		Safranal ($C_{10}H_{14}O$) is a chemical compound isolated from saffron responsible for the saffron aroma
Picrocrocin		Picrocrocin ($C_{16}H_{26}O_7$) is meant for the bitter taste of saffron.
Crocetin		Crocetin ($C_{20}H_{24}O_4$) is a natural apocarotenoid dicarboxylic acid in the flower of saffron.

1.3. Grades of Saffron and ISO 3632 (International Organization of Standardization

The level and potency of saffron differ based on the quantity of style connected to the red stigma. The saffron's age also plays a role. As the color and flavor concentrate in the red stigmas, saffron becomes less effective when more style is present. Saffron originating from Iran, Spain, and Kashmir are classified based on the ratios of red stigma to yellow styles (see Figure 1.1). The ISO 3632 certification assures consumers that the saffron they buy is genuine and safe to eat. Based on the following factors, Saffron is classified into grades I, II, and III by ISO 3632: 1. Moisture level (dried) 2. Crocin (color) 3. picrocrocin (bitterness) 4.

Safranal (aroma). The quantities of these key compounds are used to determine the saffron quality (Table 1.2). A higher concentration of these compounds implies to greater quality of saffron. The highest quality saffron is graded in group I by ISO-3632, which means direct readings of absorbance of E1% aqueous solution of saffron at 440, 330, and 257 nm for crocin, safranal, and picrocrocin, respectively are greater than 190, 20, and 70, respectively

1.4. Adulteration in saffron

Saffron adulteration refers to the deliberate addition of inferior substances to high-quality saffron, resulting in a decline in its overall quality and altering its original characteristics, such as color, smell, taste, and nutritional value. This deceptive practice poses significant health risks as harmful substances may be intentionally added, aiming to deceive consumers and maximize economic gain. Adulterants can be either accidental or intentional.

There are primarily two categories of adulterants: those that come from nature, also known as biological adulterants, and those that are created artificially, also known as synthetic or chemical adulterants. Adulterants derived from natural sources include, among other things, shredded and colored meat fibers, turmeric, and numerous floral components acquired from a wide variety of flowers. Detecting and evaluating saffron that has been adulterated with natural chemicals may be a difficult task since it might be difficult to detect the adulterants. Adulterants that are made by chemicals include things like liquid glycerin, inorganic salts, nylon fibres, and a wide variety of dyes. Powdered saffron is frequently adulterated with the use of several kinds of synthetic colors. Adulteration techniques also include unethical business practices, such as mislabeling turmeric as "Indian Saffron," combining saffron of inferior grade with saffron of premium quality and selling artificially colored saffron that has had its quality damaged by the use of chemical means. Cheaper saffron sourced from various geographical origins may be fraudulently marketed as high-quality brands, extending the fraudulent activity across international boundaries. To counter adulteration and protect the integrity of their own saffron, many countries have regulatory bodies that issue a Protected Designation of Origin (PDO) status. Overall, saffron adulteration is a serious concern as it compromises the quality of the product, poses health hazards, and undermines the trust of consumers. Efforts are being made to combat this issue through improved detection methods, stricter regulations, and the establishment of PDO status to confirm the genuineness and origin of saffron.

Chapter 2

Review of Literature

Saffron, also known as *red gold*, is considered as the expensive spice worldwide. It is obtained from flowers (stigma) of the *Crocus sativa* (Saxena., 2010). Saffron, originating from the Arabic term azaferan, solely blossoms during autumn and remains inactive throughout the summer. *Crocus sativa* belongs to the Asparagales family and is an angiosperm plant. The flower of Crocus is solitary, purple, with six petals, three stamens, one style, and three red-orange stigmas. The Mediterranean–Europe, and Western Asia are the leading distributors of saffron. Iran supplies around 90% of total worldwide saffron output (Husaini *et al*., 2010). Saffron is highly expensive for its golden hue, flavor, and aromatizing properties. It is also used as a potent natural substance that offers numerous health advantages. The spice's remarkable ability, along with its essential elements, to protect against toxins of both natural and chemical origins has significantly enhanced its significance. Due to its exorbitant cost and high demand from pharmaceutical companies, there is an alarming prevalence of illicit trade and adulteration associated with saffron in recent times (Karimi *et al*., 2016; Varliklioz *et al*., 2017).

2.1. Pharmaceutical significance of saffron and its phytochemicals

Plant-derived phytochemicals are considered a potential therapeutic agent with minimum side effects compared to chemically manufactured medications (Mgbeahuruike *et al*., 2017; Akhtar *et al*., 2021; Khurshid Wani *et al*., 2021). Various studies have emerged to explore the therapeutic applications of saffron (Table 2.1). Besides being used as a popular spice, Saffron has also been found to be significant in treating of various diseases, including asthma (Zilaee et al., 2019a), depression (M. Siddiqui et al., 2018), menstruation disorders (Rajabi *et al*., 2020), cardiovascular disease (Razavi and Hosseinzadeh, 2017), digestive ailments (Ashktorab *et al*., 2019), cancer (Samarghandian and Borji, 2014), insomnia (Lopresti *et al*., 2020) and several other disorders. The presence of phytochemicals like crocetin, safranal, and crocins in saffron is considered to be associated with the therapeutic benefits of this spice (Mykhailenko *et al*., 2019). Saffron has been found to be an effective gastrointestinal modulator for preventing gastrointestinal atonia (Naeimi *et al*., 2019) and a major therapeutic agent for female genitals (Milajerdi *et al*., 2016). Chronic bronchitis and other respiratory conditions may be effectively treated with safranal. It acts on alveoli through the vagus nerves, making coughing less severe (Mahmoudabady *et al*., 2013). Crocin, an analgesic, has been recommended for dysmenorrhea as it helps slow down uterine contractions (Sadi *et al*., 2016). On the other hand,

21

Picrocrocin has been shown to have a tranquilizing property and thus induce a sedative impact on lumbar and spasm pains (Khazdair *et al*., 2015). Even though compounds of saffron are significantly effective, crocetin has shown more remarkable pharmaceutical activities because this ensures the oxygen transport speed, which makes it useful in the treatment of atherosclerosis (Hatziagapiou and Lambrou, 2018), hemorrhages (Gutheil *et al*., 2011), alveolar hypoxia (Xi and Qian, 2018), arthritis (Hamidi *et al*., 2020), and tumors (Siavash *et al*., 2010; Bukhari *et al*., 2018).

2.1.1. Anticancer properties

Cancer is one of the deadliest diseases that are prevalent across the globe. Several *in vivo* and *in vitro* studies have been conducted to examine the anticancer properties of different plants, including saffron (Wani *et al.,* 2022). Bathaie *et al.,* (2013) examined the effects of saffron extract (SE) on gastric cancer induced by MNNG (1-methyl-3-nitro-1-nitrosoguanidine). The administration of SE demonstrated the ability to inhibit cancer growth, with more than 15 percent of treated rats showing normal conditions. Crocin, a component of saffron, has been found to suppress the proliferation of colorectal cancer cells without adversely affecting normal cells (D'Alessandro *et al*., 2013). Animal experiments have also shown that saffron reduces DEN (diethylnitrosamine)-induced hepatic dyschromatic nodules, indicating its potential to alleviate DEN-induced stress in rats (Amin *et al*., 2011). In investigating pancreatic cancer invasion, in vitro studies administered crocetin, a compound found in saffron, to cancer cells. Analysis using H-(3)-thymidine and flow cytometry revealed inhibition of proliferation (Zhang *et al*., 2013). Given the increasing prevalence of breast cancer, preventive measures are crucial. Chen *et al.,* (2019) studied the effects of crocetin, the primary component of saffron, on invasive cancer cells (MDA-MB-231) using the WST-1 assay. The results demonstrated inhibition of MDA-MB-231 invasiveness through MMP regulation.

Saffron and its active constituents play a significant role in inhibiting tumor development and progression. Numerous studies on animal models have confirmed the substantial contribution of saffron and its plant-based compounds in preventing various types of tumors. Oral administration of saffron extract has been shown to enhance the lifespan of mice with sarcoma-180, Ehrlich ascites carcinoma, and Dalton's lymphoma ascites tumors (Nair *et al*., 1991; Amin *et al*., 2011; Zhang *et al*., 2013; Khazdair *et al*., 2015).

2.1.2. Antioxidant properties

Due to the peculiar chemical nature of crocin, saffron has been studied as an important antioxidant agent (Srivastava *et al*., 2010). A bleaching assay on crocin was also framed because of its antioxidant potential (Bathaie *et al*., 2011). One of the studies carried out the comparative studies of tomatoes, carrots, and saffron stigmas for their antioxidant activity using methanol and water as solvents. The studies showed a higher antioxidant potential of saffron than the other two (Giaccio, 2004; M. Siddiqui et al., 2018). Kanakis *et al.,* (2007) evaluated the saffron for its antioxidant property as well and reported safranals' activity lower than that of BHT (Butylated hydroxyl toluene) and Trolox, while crocetin showed comparable results (Kanakis *et al*., 2007). The antioxidant property of dimethyl-crocetin was found to be dose-dependent, having 40 ug/ml as a peak value, while the synergistic effect gave saffron presented saffron as a better antioxidant agent. The scavenging effect of crocin was found to be higher, at 50% for 500ppm solution and 65% for 1000 ppm solution, while safranal has 34% for 500 ppm solution (Assimopoulou *et al*., 2005). The scavenging property is attributed to the hydrogen donating ability towards DPPH radical. The scavenging of free radicals by saffron-associated compounds defends the cells against oxidative stress (Amarowicz and Pegg, 2019; Assimopoulou *et al*., 2005). Crocin has demonstrated efficacy in the preservation of sperm during cryoconservation, making it a viable option for neurodegenerative conditions due to its antioxidant properties. Additionally, it aids in reducing lipid peroxidation caused by Reactive oxygen species (ROS) in liver cells (Uttara *et al.*, 2009, Mehri *et al.,* 2015).

2.1.3. Antimicrobial properties

Microbes are omnipresent and adapt to fluctuating environments, including antibiotic-contaminated sites, through a series of cellular and molecular pathways (Wani *et al*., 2021, 2022). The side effects and antibiotic resistance has been a major concern while dealing with antibiotics (Ventola, 2015). This has compelled scientists around the globe to look for novel antimicrobial agents with a good range of safety and efficacy (Fair and Tor, 2014; Wani *et al*., 2022). Food poisoning is one of the common health issues caused by eating foods contaminated with harmful microbes (Hernández-Cortez *et al*., 2017). Using antimicrobial agents or certain preservatives helps us prevent microbial growth, thereby preventing food poisoning (Arshad and Batool, 2017). The methanolic extracts of the saffron petal have shown antimicrobial activity against *B. cereus, E-coli, S. aureus,* and *, S. dysenteriae* at the concentration of 1000mg/ml with a zone of inhibition ranging from 12-22mm. However, using the solvents like chloroform and water, the activity lessens to some extent (Asgarpanah *et al*., 2013). Several

researchers have also mentioned the anti-fungal properties of saffron-derived safranal and crocin (Rameshrad *et al*., 2018).

2.1.4. Anticonvulsant activity

The anticonvulsant effect of saffron was examined in mice utilizing pentylenetetrazole (PTZ) and max electroshock seizure (MES) tests in both aqueous (0.08-0.8 g/kg) and ethanolic extracts (20-40 mg/kg). In the test for PTZ, delayed initiation of tonic convulsions was observed; however, it failed to offer complete mortality protection. In the case of MES tests, it was observed that both aqueous and ethanolic extracts decrease the tonic seizure duration. Using PTZ-induced convulsions in rats, the anticonvulsant effects of crocin and safranal have been investigated. Safranal (0.15 and 0.35 mg/kg, IP) has been found to decrease the length of seizures, delay the inception of tonic convulsions, and prevent mortality in mice (Hosseinzadeh *et al*., 2001). Saffron demonstrated a considerable dose-dependent antiepileptic activity in a PTZ-induced seizure model at dosages of 400 and 800 mg/kg (Sunanda *et al*., 2014). IP administration of safranal (0.15 and 0.35 ml/kg) in mice has been found to reduce the duration of PTZ-induced seizures and delay the onset of tonic convulsions; however, IP administration of crocin (200 mg/kg.) failed to show anticonvulsant activity (Hosseinzadeh and Sadeghnia, 2005; Hosseinzadeh and Sadeghnia, 2007).

Table 2.1- some of the studies on the therapeutic applications of Crocus sativa and its metabolites

Saffron Metabolite	Animal Model/ Cell line	Mode of Action	References
Aqueous extract of saffron	*Modified well-plate test*	Reduction in the inhibition zone of growth against S. faecalis, S. aureus, and E. coli	(Cenci-Goga *et al*., 2018)

Ethanolic extract of Crocin and saffron	*DPPH and lipid-peroxidation assays*	Antihemolytic activity assessed using the phospho-molybdenum method	(Zengin *et al.*, 2019)
Ethanolic and methanolic extracts of saffron	*DPPH ferric reducing antioxidant-power assays*	High antioxidant activity at 300 μg/mL	(Karimi *et al.*, 2010)
Saffron/aqueous extract	*Bronchial epithelial cells*	Antioxidant activity resulting in decreased peroxynitrite ion generation and cytochrome c release	(Bukhari *et al.*, 2015)
Crocetin	*Rats*	Antioxidant properties leading to decreased oxidative stress and ROS levels in brain of rat	(Yoshino *et al.*, 2011)
Saffron	*BALB-c mice*	Neuroprotective effects, reduction in ROS levels, and enhanced antioxidant effect in a murine model of MPTP induced Parkinson's disease	(Purushothuman *et al.*, 2013)
Aqueous extract of saffron	*STZ-induced diabetic rat*	Antihyperglycemic effects resulting in reduced glucose levels, decreased lipids and	(Samarghandian *et al.*, 2017)

		cholesterol, enhanced glutathione level, and decreased inflammatory cytokines	
Aqueous and ethanolic extracts of Saffron	*Rats and guinea pigs*	Antihypertensive activity leading to a dose dependent decrease in blood pressure	(Fatehi *et al*., 2003)
Crocetin	*Mice with benzo(a)pyrene-induced lung carcinoma*	Antitumor activity accompanied by increased activity of glutathione metabolizing enzymes and enzymatic antioxidants, and suppression of proliferating cell formation	(Magesh *et al*., 2006)
Crocetin	*Mice with benzopyrene-induced lung cancer*	Antitumor activity resulting in decreased formation of proliferating cells	(Magesh *et al*., 2009)
Zhejiang saffron	*Mice with xenograft tumor*	Antitumor activity accompanied by increased apoptosis	(Liu *et al*., 2014)
Saffron/aqueous infusion	*Mice with DMBA-induced skin carcinogenesis*	Antitumor activity resulting in decreased formation of proliferating cells	(Das *et al*., 2004)

Saffron	*Rats with PTZ-induced seizures*	Anticonvulsant effects with a frequency-dependent reduction in seizures	(Sunanda *et al*., 2014)
Safranal	*Rats with PTZ-induced seizures*	Anticonvulsant effect	(Hosseinzadeh and Talebzadeh, 2005)
Crocetin	*Mice*	Protection against retinal damage	(Ohno *et al*., 2012)
Saffron extract in water	*Rats*	Modulation of brain neurotransmitters with a dose dependent enhance in dopamine and glutamate levels	(Ettehadi *et al*., 2013)
Aqueous extract of Crocus sativus L.	*Rats with STZ-ICV-induced Alzheimer's disease*	Anti-Alzheimer effects including the amelioration of cognitive deficits, enhanced memory, and metabolic improvements	(Khalili *et al*., 2010)
Saffron/honey syrup	*Mice with aluminum chloride-induced neurotoxicity*	Alleviation of neurotoxicity associated with aluminum chloride exposure	(Shati *et al*., 2011)

27

Aqueous extract of saffron	*Rats with diazinon-induced neurotoxicity*	Neuroprotective effects resulting in reduced neuronal damage, oxidative stress, and inflammation	(Moallem *et al.*, 2014)

2.2. Methods of Saffron adulteration and its detection

Saffron is indeed expensive spice and owing to limited production and the high demand for this spice, it remains susceptible to illicit trade and adulteration (Thakar and Sharma, 2018). Adulteration of saffron is mainly done by adding safflower, maize silk, marigold floret, horsehair, grassroots, stamens of saffron, red dried silk fiber, etc. These kinds of adulterants resemble saffron in color and texture. Sugar, potassium hydroxide, borax lactose, glycerin, fats, glucose, starch, etc., are mainly added to increase weight. Adulteration is not only done by adding a foreign substance to the saffron but also mixing different grades is one of the common methods of adulteration. The powdered form of saffron is more likely to be adulterated. Usually, turmeric and other powders resembling saffron are blended and sold in the markets with powdered saffron (Figure 2.1) (Nazari and Keifi, 2007). Saffron is frequently adulterated due to its high market value. This practice has a long history, dating back around 600 years, driven by economic motives. Various methods are used to adulterate saffron, such as mixing it with older or lower-quality saffron, adding other plant parts like styles and stamens, and using substances to increase weight, such as glycerin, olive oil, honey, or syrup. Chemicals like starch, sodium borate, potassium nitrate, and lactose, as well as mixing with other flowers like safflower and marigold, are also common. Other types of saffron with shorter stigmas, animal materials, turmeric, paprika, and synthetic dyes such as Allura Red and Tartrazine have been used as adulterants as well.

Efforts to improve saffron adulteration detection methods include advancements in chromatographic, spectroscopic, immunological, electrophoretic, molecular (DNA-based), and sensor-based techniques. Despite several review articles on these methods, comprehensive reviews comparing their effectiveness are scarce. This review aims to fill that gap by summarizing current detection methods and discussing their advantages and disadvantages. Physical methods, such as analyzing morphology, flavor, colorimetry, moisture content, and ash, are basic yet effective ways to assess saffron purity. Microscopic examination and

immersing saffron in water to observe color release are examples. Diphenylamine (DPA) solution can detect nitrate adulteration by changing color when saffron is added. Techniques like tristimulus colorimetry help identify synthetic dyes. These methods are simple, easy to use, and do not require sample preparation, making them suitable for primary analysis. However, they lack sensitivity, accuracy, specificity, and reproducibility, and cannot quantify adulterants.

The ongoing adulteration of saffron has badly affected the production and economy of saffron cultivators. Various instrumentation methods are available to detect adulterations in saffron. (Lozano *et al.,* 1999) carried HPLC analysis on Mancha, Rio, and Sierra grades of Iranian saffron, and ten different metabolites were found in the saffron extract. Each chromatograph depicted at three wavelengths (250, 310 and 440), and it was concluded that Mancha showed the highest concentration for all sec-metabolites followed by Rio and Siera (Lozano et al., 1999a). Sujata *et al.,* (1992) used TLC, HPLC, and Gas chromatography to check the authenticity of saffron. Crocin, picrocrocin, and crocetin were resolved using TLC and HPLC analysis; however, safranal was evaluated using Gas chromatography. In TLC analysis n-butanol, Acetic acid, and water (4:1:1) were used as mobile phase and R_f (Retention factor) was calculated as 0.63, 032, and 0.98 for crocin, picrocrocin, and crocetin respectively. In HPLC analysis, the extract of pure saffron in 80 % ethanol was passed through a cartridge eluted with 100 % acetonitrile and R_t was obtained. It was found that R_t of crocin, picrocrocin, and crocetin was 13.5, 14-18, and 18 respectively. Gas chromatography was used to resolve safranal. Nitrogen at a flow rate of 30 ml/min was used and it was found that safranal could be resolved into a sharp peak at a rate of 3.6 minutes (Sujata *et al*., 1992). Semiond *et al.,* (1996) studied the isotopic analysis and identification of saffron using Supercritical Fluid Extraction (SFE). Safranal metabolites obtained from saffron of different origins were analyzed and a difference was found between synthetic and natural safranal. Moreover, it was found that SFE allowed various volatile compounds to be selectively extracted from saffron under optical conditions. It is a quicker and safer way to extract volatile saffron compounds (Semiond *et al*., 1996).

In another study, Thermal-desorption Gas Chromatography-Mass Spectrometry was used for analyzing the authenticity of Spanish saffron and found that major components of the aromatic composition are safranal. The fingerprint of the chromatograph was obtained for genuine and fake saffron, which were different. In adulterated saffron, a chromatograph peak appeared, which was not produced by pure saffron fingerprint. Such fingerprint [*m/z*- 121 (100),91 (50),

107 (40), 79 (33), 105 (31), 77 (28), 135 (22), 93 (20), 122 (16), 65 (10)] was similar to compound 2,6,6-trimethyl cyclohexane-carboxaldehyde, and it could be concluded that if beta-cyclocitral peak appears in chromatograph fingerprint, the saffron was adulterated (Alonso *et al.*, 1998). Zalacian *et al.*, (2005) used a testing tool for various colorant identification. This method was based on removing crocins from the sample by precipitation before the adsorption of colorants on a Polyamide Solid-phase Extraction (SPE) cartridge. Elution with methanol-ammonia solution was performed and after washing identification process was carried out with a Uv-Vis Spectrophotometer (Zalacain *et al.*, 2005). In another study, Sequence-Characterized Amplified Regions (SCARs) were employed to detect adulteration with specific agents using various food products containing saffron. The use of SCAR markers proved to be an effective, quick, and low-cost screening method for authenticating saffron-containing food products (Torelli *et al.*, 2014). The HPLC process for identifying, detecting and quantifying saffron metabolites was studied by Haghighi *et al.*, (2007) to detect adulterants like colored styles of Crocus sativa, safflower red beet, etc. The chromatograms were obtained at desired wavelengths showed the presence of adulterants in saffron (Haghighi *et al.*, 2007). Gonzalo *et al.*, (2007) developed a method for HPLC-DAD to simultaneously classify crocins and picrocrocin in aqueous saffron spice extracts. This method was able not only to determine crocin and picrocrocin but also to detect water-soluble colorants in saffron. Application of Proton Transfer Reaction-Mass Spectrometry (PTR-MS) in saffron quality control was studied by Nikolaos *et al.*, (2014). A minute quantity sample was used to capture volatile fingerprints. IPTR-MS/chemometry was examined to detect fresh addition of low-quality saffron to fine quality. Heidarbeigi *et al.*, (2015) developed an electronic nose system coupled with an artificial neural network to detect adulteration in saffron. This was the first approach towards the detection of adulteration using sensors. The electronic nose could detect complex odors via an array of sensors. The specimen odors are drawn into the electronic nose chamber and then passed through the sensor array process, resulting in a reversible physical change or chemical alteration in the sensing material associated with electrical properties like conductivity (Heidarbeigi *et al.*, 2015). Ordoudi *et al.*, (2014) researched a multi-step method for detecting saffron fraud. HPLC, UV – Vis, FT-IR, and NMR were used to examine the saffron fraud. UV – Vis and FT-IR data were used to reveal the artificial colors used. NMR was used to identify others. The identification of authentic saffron by using a molecular genetic approach was investigated by Ma *et al.*, (2000). After analysis, they found that the nucleotide sequence of all

the samples were distinct and different and served as a marker for authentic identification of pure saffron from counterfeit saffron (Ma *et al*., 2001).

Javanmardi (2011) studied the petals of the safflower plant that are mostly used as an adulterant of saffron. They employed DNA analysis (RAPD) to detect adulteration in saffron. DNA from safflower petals and saffron were extracted and after analysis shows two monomorphic bands (500 and 700 bp) present in safflower were found to be absent in saffron (Javanmardi *et al*., 2011). Luana magi *et al.,* (2011) studied the spectroscopic method to determine the safranal content in the saffron. To check the quality of saffron spice, this quantitative safranal study was based on non-polar solvent extraction followed by spectrometric analysis. Ultrasound-assisted safranal extraction was performed and UV-Vis spectrophotometric analysis showed satisfactory results in the performance of repeatability, linearity, and recovery (Maggi *et al*., 2011). Karimi *et al.,* (2016) used FTIR spectroscopy with pattern recognition to differentiate between pure saffron and those samples adulterated with various food adulterants. the FTIR spectrum was obtained for all the samples and it was found that three region bands corresponding 1800-1830, 2600-2900 and 3700-3850 nm were responsible for recognizing true saffron from adulterated ones (Karimi *et al*., 2016). Soffritti *et al.,* (2016) in their study, isolated DNA from the saffron sample, adulterated sample, and possible adulterants, then from isolated DNA new markers were developed to recognize genuine saffron from fake or adulterated saffron. This method could recognize saffron from a mixture with a low percentage of adulterants (Soffritti *et al*., 2016).

In another study, non-target screening of volatile compounds was performed on 38 authentic saffron samples and 25 samples of potential adulterants (safflower, calendula, capsicum, and turmeric) using headspace solid-phase microextraction followed by gas chromatography coupled to high-resolution mass spectrometry (HS-SPME-GC-HRMS). Chemometric analysis using Principal Component Analysis (PCA) and Partial Least Squares Discriminative Analysis (PLS-DA) successfully separated authentic saffron from potential adulterants. Significant marker compounds for each plant and saffron were tentatively identified. Target screening of these markers in model mixtures enabled detection of adulterants at levels as low as 2% w/w. (Filatova *et al.,* 2024). In another study, using near-infrared hyperspectral imaging (NIR-HSI) and chemometrics for fast and cost-effective detection and quantification of adulteration in saffron stigmas has been found to be highly effective. In this study, adulterated samples were prepared with Crocus sativus styles in concentrations of 20–90%. Spectral data were pre-

31

treated using standard normal variate (SNV) and multiplicative scatter correction (MSC), with variable reduction by Principal Component Analysis (PCA) and Partial Least Squares (PLS). Classification was performed using Linear Discriminant Analysis (LDA), Partial Least Squares Discriminant Analysis (PLS-DA), Support Vector Machine (SVM), and Multi-Layer Perceptron (MLP) models, achieving correct classification rates of 95.6%–100%. Quantification was done using PLS, PCA, SVM, and MLP regression models, with the MLP model showing excellent predictive capabilities (coefficient of determination for prediction (R^2p) of 0.97, Root Mean Squared Error of Prediction (RMSEP) of 4.3%, and Residual Predictive Deviation (RPD) of 5.4). These findings highlight the potential of NIR-HSI and chemometrics for rapid, nondestructive detection and quantification of saffron adulteration (Malavi et al., 2024).
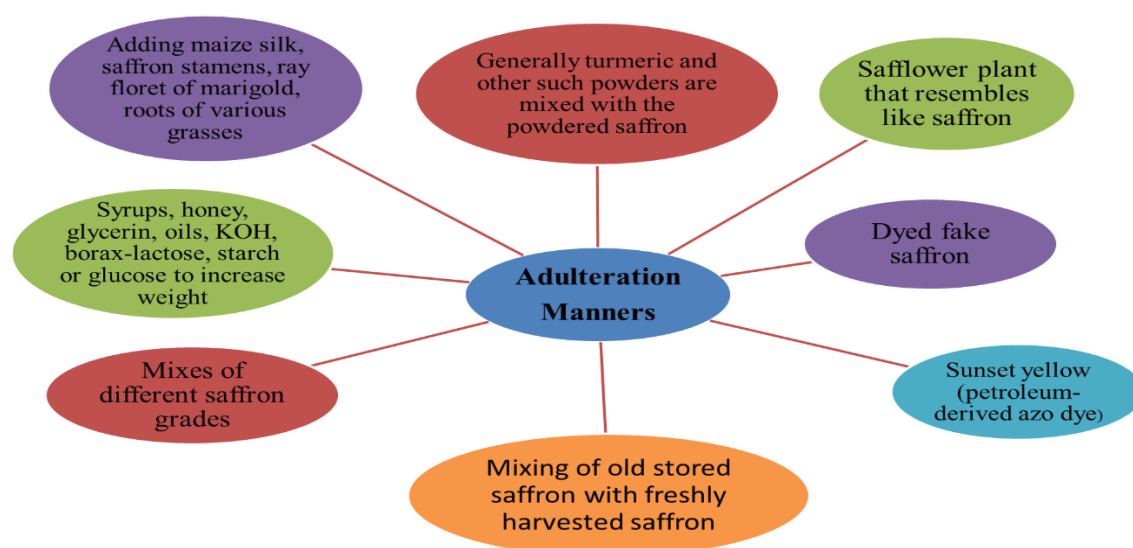
Figure 2.1- Manners of Adulterating saffron.

Methyl orange [(MO) *dimethylaminoazobenzenesulfonate*] is the most prevalent artificial colour used as an adulterant in saffron (Ashok *et al*., 2017). It is mostly used in powdered saffron and imparts orange colour to the stigmas of various flowers used as adulterants in saffron. MO is also employed in various foodstuffs where saffron is used as a colouring ingredient. When dissolved in water, it displays a vivid orange hue and has a high colourability. MO contains aromatic and -N=N- groups (Figure 2.2), which are extremely poisonous, teratogenic, and carcinogenic (Haque *et al*., 2021; Wu *et al*., 2021). In order to regulate the sale of unhealthy saffron or adulterated saffron and to ensure food quality and safety, the development of an inexpensive, environmentally friendly, quick and dependable technique for the detection of MO in adulterated saffron and other foodstuffs has been the centre of interest

for several researchers across the globe. Several methods have been proposed to detect the presence of several organic dyes in saffron HPLC, NMR, Capillary Electrophoresis and so on have widely been used in the detection of dyes in saffron and other foodstuffs (Kumari et al., 2021b). Although these approaches were quantitative, they were time-consuming, required enormous sample volumes, produced a lot of waste, and required bulky and costly gear. As a result, a simple and sensitive approach for identifying dyes in foodstuff is widely desired.

The addition of illegal and banned additives such as MO, Sudan I, melamine, and tetrazine in a foodstuff has posed a threat to human health (Guo *et al*., 2021; Thangaraju *et al*., 2021; Visciano and Schirone, 2021). CDS have been employed for sensing various pollutants such as Rhodamine 6 G (Rh6G) (Bogireddy *et al*., 2020), Methylene Blue (MB) (Atchudan *et al*., 2020), Bromophenol blue (BrPB) (Sahu *et al*., 2021) and MO (Atchudan *et al*., 2020). Xu *et al.,* introduced an environmentally friendly method for synthesizing carbon quantum dots (CQDs) through a hydrothermal process. These CQDs were used as a fluorescence probe to selectively and sensitively detect tartrazine in steamed bread, candy, and honey (Xu *et al.*, 2015). Yang *et al.,* (2020) focused on synthesizing N, Cl-doped fluorescent CQDs with a quantum yield (QY) of 60.52%, which were utilized for tartrazine detection in beverages. Molecularly imprinted polymer (MIP)-based CQDs were employed by Zoughi *et al.,* (2021) for the detection of tetrazine in saffron. Anmei *et al.*, (2018) utilized cigarette filters as a carbon source to synthesize CQDs for detecting Sudan I in chili and tomato samples. Hu *et al.,* (2019) employed Au@CQDs for the detection of melamine in milk, achieving a limit of detection (LOD) of 3.6 nmol-1. MO is a banned food additive, and Zulfajri *et al.,* (2019) synthesized CQDs from fruit extract of Averrhoa carambola via a hydrothermal process, successfully detecting MO in water samples.

Sudan I, commonly used as a coloring agent in various industrial applications, has been found to be carcinogenic and harmful to public health due to its DNA-binding intermediates that promote gene mutation (Chen *et al.*, 2014; Singh *et al.*, 2021). Despite restrictions on its use as a food additive, Sudan I is still illegally employed, particularly in ketchup, causing concerns among consumers (Haughey *et al.*, 2015; Reile *et al.*, 2020). Analytical methods like HPLC, GC-MS, and immunoaffinity chromatography (IAC) have been used to detect Sudan I, but they have limitations such as expensive equipment, time-consuming procedures, and maintenance costs (Chailapakul *et al.*, 2008; He *et al.*, 2007; Li *et al.*, 2010). To address these challenges, fluorescence-based approaches have gained attention due to their simplicity, cost-

effectiveness, high sensitivity, and time-saving qualities (Fang *et al.*, 2016; Anmei *et al.*, 2018). However, existing fluorescence probes often require complex fabrication techniques, expensive chemicals, and may have drawbacks like toxicity and hydrophobicity. Researchers have explored doping CQDs with other elements to enhance their fluorescence intensity and specificity for target elements (Manzoor *et al.*, 2009; Nsibande and Forbes, 2016; Chiu *et al.*, 2016; Sobiech *et al.*, 2021). In our study, we synthesized CQDs for the detection of MO and Sudan dye in saffron, and a comprehensive review of CQDs is provided in the later part of this chapter.
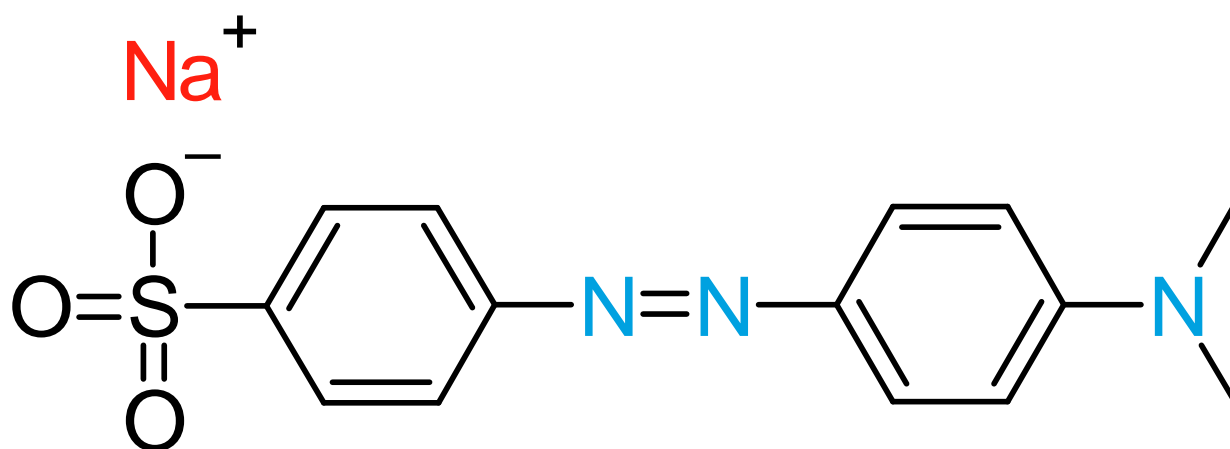
Figure 2.2.- Chemical structure of methyl orange

2.3. An Overview of Molecularly Imprinted Polymers

Polyakov introduced the Molecularly imprinting technique first in 1931. This technique involves the formation of specific binding sites with similar sites to that of the template molecule. Molecularly imprinting polymers (MIPs) involves target samples, functional monomers, and cross-linker for polymerization reaction (Chen *et al*., 2011). The monomer has an active group capable of combining with the template via covalent and non-covalent interactions. Some commonly used monomers are itaconic acid, hydroxy methacrylate, acrylic acid, acrylamide, etc. The crosslinker helps develop the film layer by binding the functional group around the imprinted molecule and forming a high crosslinked polymer. Some crosslinkers are ethylene glycol, dimethyl acrylate, divinylbenzene etc.

2.3.1.   Mechanism of MIPs

 The MIPs has been studied generally with two mechanisms: reversible covalent binding and non-covalent binding. Covalent binding was introduced by *Wuff* in 1972, while non-covalent

interaction was employed by *Mosbach* in 1981 between template molecules and functional monomers (Dickey, 1949). The dummy molecule in covalent binding is linked by covalent interaction with specific functional monomers, such as in 4-vinyl phenylboronic acid and 4-vinyl benzylamine (Yin *et al*., 2005). We require a similar template molecule with identical functional monomers for the formation of reversible covalent interactions. Therefore, templates suitable for such covalent imprinting are insufficient, and the process becomes hectic. Non-covalent imprinting techniques overcome such limitations (Chen *et al*., 2011). The polymeric matrix possessing a functional monomer can then rebind the template via the same non-covalent interactions after polymerization, so a various and wide range of applicative compounds can be synthesized. Besides the process mentioned above, a further factor in non-covalent MIPs is their uniformity in operation since we require only mixing monomers and templates with a suitable solvent in the presence of the initiator. In recent times, for the synthesis of MIPs, Non-covalent imprinting is more favoured (Yin *et al*., 2005). It has become a general synthesis strategy for molecularly branded technology. It is now the most broadly used technique to synthesize molecular imprinted binding site interactions based on the non-covalent interaction of the target molecule with functional monomers before polymerization (Shea and Sasaki, 1989). The synthesis usually follows free-radical bulk polymerization with a crosslinking monomer.

For the Formation of a MIP, the template and available monomer interaction are essential.(H. Li *et al*., 2021; Rimmer, 1998; Zhou *et al*., 2019). During the bond interaction, active monomer interaction with the crosslinker and solvent is also crucial (Hirayama *et al*., 2002). Methacrylic acid is specifically used to synthesize the crocin-specific MIP, and during the interaction, a crosslinker and solvents with weak interactions are used. Some other functional monomers are shown in Table 2.2. Crosslinker plays an important role in the design of MIPs. Interlinkage of the crosslinker with the template is less studied. The interaction of the crosslinker with the investigated molecule determines the selectivity of MIPs. Some crosslinkers have been mentioned in Table 2.3.

Porogenic solvent plays a significant role in the preparation of MIPs. Porogenic solvents tend to interact with a different template, functional monomers, and crosslinker (Haupt and Mosbach, 2000). The kind and concentration of porogenic solvents influence the depth of noncovalent contacts besides the shape of the polymer, which has a direct impact on MIP synthesis (Ansell *et al*., 1996). To begin with, the sample molecule, monomer, initiator, and

crosslinker must all be solvable in porogenic solvents. Furthermore, the solvent should create large pores, and to decrease the barriers during the complex organization between the monomer, imprint molecule, porogenic solvent should be of medium polarity.

Table 2.2. Common monomers used in MIP
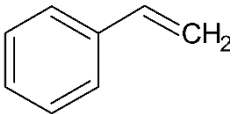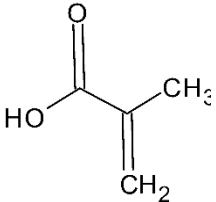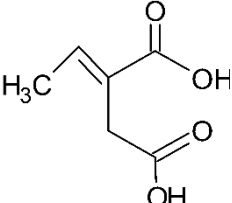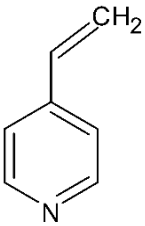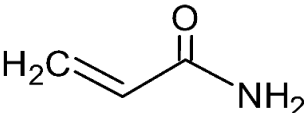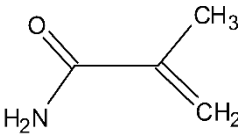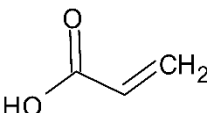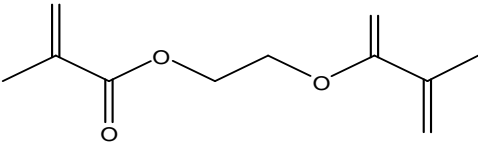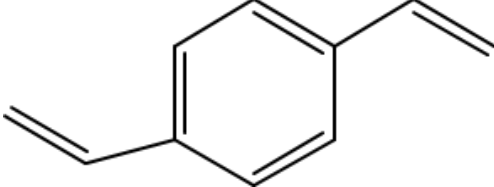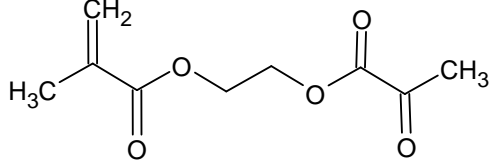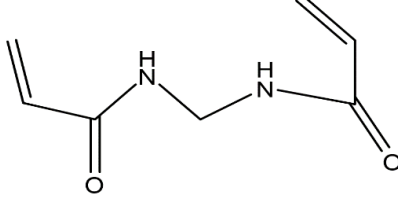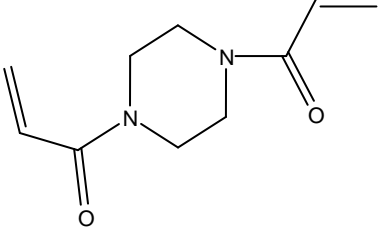
Monomer	Chemical structure	Chemical Formula
Styrene		C_8H_8
Methacrylic acid		$C_4H_6O_2$
Itaconic acid		$C_6H_6O_4$
4-vinyl pyridine		C_7H_7N
Acrylamide		C_3H_5NO
Methacrylamide		C_4H_7NO
Acrylic acid		$C_3H_4O_2$

Table 2.3.- Common crosslinkers used in MIP

Crosslinker	Chemical structure	Chemical formula
Ethylene glycol dimethyl acrylate		$C_{10}H_{14}O_4$
Divinyl benzene		$C_{10}H_{10}$ or $C_6H_4(CH{=}CH_2)_2$
Ethylene glycol dimethacrylate		$C_{10}H_{14}O_4$
N'N-methylenediacrylamide		$C_7H_{10}N_2O_2$
1,4 diacryloyl piperazine		$C_{10}H_{14}N_2O_2$

2.3.2. Preparation Methods of MIP

MIPs are commonly synthesized through chemical methods. In this process, a functional monomer in a solution forms a complex with the template molecule, establishing a connection through either covalent or noncovalent interactions. The relationship between the template molecule and the functional monomer involves different modes of interactions and rearrangements, including covalent, non-covalent, and semi-covalent imprinting.

Covalent imprinting is favored when creating stable polymers to ensure an even distribution of binding sites throughout the polymer structure. Conversely, noncovalent imprinting relies on weaker binding interactions such as dipole interaction, ionic contact, and hydrogen bonding between the template and functional monomers. Semi-covalent imprinting techniques combine both covalent and noncovalent interactions, where the target molecule connects to the monomer through noncovalent interaction, and polymerization occurs through covalent contacts as part of the molecular imprinting process. MIPs use a variety of methods to obtain high levels of selectivity (Kriz *et al*., 2011). The most commonly used approaches for the preparation of MIPs are described below:

2.3.2.1. Bulk Polymerization

Bulk polymerization, which involves dissolving the monomer in a non-reactive solvent, is the best approach for producing MIP. The bulk polymer is mechanically crushed to produce tiny particles that are then sieved into appropriate size scales, typically in the micro-meter range (Baggiani *et al*., 2005). This approach is the one of the common, and it has a lot of appealing features, especially for beginners. It is quick and does not require any expensive equipment or particular operator abilities (Sellergren *et al*., 2002). Although bulk polymerization is a basic and uncomplicated procedure, it has several disadvantages. After the ultimate sieving process, the particles recovered have an uneven shape and size. Some interactions are lost during grinding, resulting in poor chromatographic performance and low MIPs adsorption loading capacity compared to theoretical values.

Furthermore, the crushing and sieving technique is a time-consuming operation. It results in a large waste of valuable polymers, estimated to be between 50 and 75 % of the original amount of bulk material. This process uses many template molecules, but it could only use a part of the polymer as a packing material. Lastly, bulk polymerization cannot be undertaken without the risk of overheating the unit because of its exothermic character. Using digoxin as a template, Bulk MIP was synthesized through non-covalent interaction (González *et al*., 2006). The bulk

polymers were made under different circumstances, using different functional monomers (methacrylic acid or 2-vinyl pyridine) and pyrogenic solvents (acetonitrile or dichloromethane. The binding affinity, specificity, chemical, and thermal capabilities of bulk polymerized produced MIP is related to surface morphology (O'Mahony *et al*., 2006).

2.3.2.2. Multi-step Swelling Polymerization

Serval efforts have been put forward to synthesize imprinted stationary phases with small size, higher efficiency, and mass transmission properties (Lei and Tong, 2005; Tamayo *et al*., 2005). To synthesize homogeneous spherical particles, the multiphase swelling approach has been applied (Hosoya *et al*., 1996; Haginaka and Sakai, 2000; Haginaka and Kagawa, 2002; Nakamura *et al*., 2005). Direct preparation of particles in the form of spherical beads with the regulated size is possible. The multistep swelling process creates chromatographically suitable particles that are substantially monodisperse in size and shape (Sambe *et al*., 2005).

2.3.2.3. Suspension Polymerization

Suspension polymerization produces an assembly of spherical particles and evenly formed microspheres when the solution is sufficiently diluted. It is a simple process for preparing printed polymers without mechanical contact. In suspension polymerization, perfluorocarbon solvents have been examined to avoid the interference described above in the Multi-step swelling method (Zhang *et al*., 2003). Uniform molecular imprinted microspheres with efficient chromatography and great selectivity have been prepared using suspension polymerization even at high flux rates. However, the application and feasibility of this approach are limited by the usage of a perfluorocarbon solvent and a fluorinated surfactant (Pang *et al*., 2005). In comparison to the protein control, selectivity analysis demonstrated greater identification capacity for protein templates. In addition, compared to those made directly using inverse-phase suspension polymerization, the imprinting beads showed a faster adsorption rate and better regeneration capability.

2.3.2.4. Precipitation Polymerization

This technique is used to create microspherical MIPs with uniform size, extending a vast surface area by regulating their composition. Precipitation polymerization involves the coagulation of nano-gel beads due to oligomer recovery from the surrounding solution (Downey *et al*., 2001). By altering the polymerization conditions, near-monodispersed spherical beads with fine-tuned size and porosity may be made. MIP-based competition assays (Surugiu *et al*., 2001; Ye *et al*., 2002) and capillary electro-chromatography (de Boer *et al*.,

2002) have described this approach. Precipitation polymerization has also been identified as having a potentially useful method for producing molecularly imprinted beads of chromatography grade (Li *et al*., 2003).

Ye and Puoci *et al.,* (2001) have created molecular imprinted microspheres using precipitation-polymerization (Ye *et al*., 2001). Despite the excellent yield, the preparation technique necessitates using a large number of target molecules due to the high dilution factor. Ho *et al.,* 2005) synthesized morphine MIPs by precipitation polymerization (Ho *et al*., 2005). The precipitation polymerization process is a viable approach for producing MIP to create uniform particles. These particles prepared via precipitation polymerization provide more precise recognition that binds affinity in detecting morphine. Furthermore, the rebinding of MIP in a solution composed of morphine via precipitation polymerization has shown a better performance (Baggiani *et al*., 2005).

2.3.2.5. Surface-Imprinting Polymerization

Surface coating of MIPs film over prepared beads has been introduced as an exciting and comprehensive technique for obtaining chromatography-level imprinted materials. This technique uses different methods to coat chromatography-grade porous silica with thin imprinted layers to determine , radical polymerization occurs on the bead surface (Rückert *et al*., 2002; Sellergren *et al*., 2002). Sreenivasan *(2006)* created a printed layer on the surface of commonly used polymers distinct to certain molecules without changing bulk properties (Sreenivasan, 2006). To synthesize ultra-thin metal ion MIP films, *Piacham et al.,* (2005) employed surface-initiated radical polymerization. To monitor polymer growth, polymer sheets were produced on a gold-coated quartz crystal. For this reason, it is simple to check the width of MIP film to be under 50 nm, allowing the quartz crystal resonator on the base of the MIP to detect and identify the targeted analyte (Araki *et al*., 2005; Piacham *et al*., 2005; Say *et al*., 2005).

2.3.2.6. Monolithic-Imprinted Polymerization

The monolithic-molecularly imprinted polymer is synthesized through one-step process called in-situ free radical polymerization, which take place inside chromatographic column. This approach is uncomplicated and avoids the challenges associated with the labor-intensive tasks of sieving, crushing, and column packing. The advantages of a monolithic column and imprinted molecular technique is projected to increase division and allow direct interpretation with a high rate and execution following in–situ polymerization. In-situ polymerization has

been used by *Matsui et al.,* to create molecularly imprinted monoliths (Liu *et al*., 2005; Matsui *et al*., 1995). They employed permeable solvents, cyclohexanol and 1-dodecanol, to dissolve the desired substance, monomer, crosslinkers, and initiators. Subsequently, they separated the gas and placed the liquid onto a stainless-steel column. After polymerization, a combination of acetic acid and methanol was used to fully remove the porogenic solvent and template. The monolithic molecularly imprinted approach has attracted a lot of attention because of its ease of synthesis, high selectivity, small template size, high sensitivity, and quick transport speed. Monolithic molecularly imprinted stationary phases have grown in popularity as a method of preparing stationary chromatographic phases in recent years (Fairhurst *et al*.,2004)

Table 2.4- Different techniques of polymerization, their advantages and limitations

Method	Advantages	Limitations
Suspension Polymerization	Highly reproducible outcomes, higher purity of the polymer obtained, spherical particles, aside from the initiator and chain transfer reagent, no further additions are required.	Complicated system for phase partitioning Many imprinted processes are incompatible with water, requiring the use of specialist surfactant polymers.
Bulk Polymerization	Polymerization is simple to perform, universal, and no special skills or advanced instrumentation are required. Low viscosity due to the suspension, Easy heat removal due to the high heat capacity of water	Grinding, sieving, and column packing are time-consuming processes. Particles are irregular in size and shape. Low efficiency
Multi-step swelling polymerization	Excellent particle for performing HPLC	Procedures are complicated
In-situ polymerization	In-situ and single-step preparation Great porosity and cost-effective	For each new template system, extensive optimization is required.
Surface polymerization	Uniform binding properties, elimination of contamination of the product with, re-usability of the template in further applications, ease of the procedure	Complicated and time-consuming
Precipitation polymerization	Microspheres with imprints, High yield and universal size	The dilution factor is high.

2.3.2.7. Synthesis of MIPs for various compounds

Molecularly imprinted nanospheres have been synthesized from quercetin, and the reaction was proceeded by precipitation polymerization to obtain nano-sized materials with spherical shapes (Curcio *et al*., 2012). The synthesis involves methacrylic acid and EGDMA as a monomer and crosslinker respectively. Bisphenol is one of the synthetic organic compounds used in the production of polycarbonate plastics. Polycarbonate plastics have widespread use, which leads to human exposure. Bisphenol has harmful effects on the human body as it disrupts the endocrine system. The MIP has been used as a sorbent for bisphenol preconcentration from food samples (Kubiak *et al*., 2020).

Diclofenac serves as a widely employed nonsteroidal anti-inflammatory drug, functioning as an analgesic. The molecularly imprinted polymer (MIP) has been synthesized through a non-covalent interaction strategy, utilizing diclofenac as the template molecule. The synthesis process entails incorporating 0.55 mmol of diclofenac as the template, along with 02 mmols of methacrylic monomer dissolved in 7 ml of a chloroform-toluene mixture within a test tube. Subsequently, the solution is allowed to incubate at room temperature for 30 minutes. Next, an initiator consisting of 12 mmol of EGDMA and 0.06 mmol of AIBN is introduced. Ultrasonication is employed for a duration of 5 minutes. The test tube is then sealed using nitrogen gas and placed within an oven for a period of 20 hours to facilitate the completion of the reaction. Following this, the resulting polymer monolith is finely ground and passed through 200 mesh sieves. To conclude, methanol is utilized to thoroughly cleanse the imprinted polymer until no diclofenac is detected via HPLC analysis. (Mohajeri *et al*., 2012).

Fluconazole, a crucial antifungal medication, is classified as an azole drug. Extracting fluconazole has been accomplished using the MIP technique. This entails utilizing EGDMA as a crosslinker, methacrylic acid as a monomer, and fluconazole as a template. The monomer and template self-assemble within the MIP and subsequently polymerize on the surface of the crosslinker. Afterwards, the template is eliminated, resulting in the formation of a cavity that matches the shape and size of the original template (Madikizela *et al*., 2017)

2.4. Quantum dots

Quantum dots (QDs) are minuscule luminescent nanocrystals, typically varying in size from 2 to 10 nanometers (Drbohlavova *et al.*, 2009). These 3D nanoparticles, known as QDs, have their size and dimensions altered by a quantum confinement effect. QDs can be classified based

on the materials used, such as metals or semiconductors (Ferancová and Labuda, 2008; Maxwell *et al.*, 2020). Additionally, QDs can be derived from metalloids like silicon-based QDs, which have been utilized in various studies. Quantum confinement effects are responsible for the advantageous qualities that set QDs apart from bulk solids (Ghanem *et al.*, 2004). When electron confinement occurs in the x-direction while allowing free movement in the other two directions, it results in two-dimensional (2D) structures known as quantum wells. One-dimensional (1D) structures, referred to as quantum wires, are obtained when the carriers are restricted in two directions, and confinement in three dimensions leads to the formation of QDs or quantum boxes (Fujioka *et al.*, 2008).

QDs can be classified as planar, vertical, or self-assembled, depending on the quantum confinement of electrons. Planar and perpendicular QDs are commonly studied and produced by patterning specific metal electrodes or gates on a 2D electron gas cover. Electronic confinement in planar and perpendicular QDs typically begins with dimensions around 100 nm, with a size of around 10 nm. Self-assembled QDs (usually 10nm in size) exhibit uniformity in composition, improved spectral purity, and can be easily modified in structure for specific applications. Pyramidal QDs find significant applications in laser technology (Mićić and Nozik, 2002; Matagne and Leburton, 2003). Often described as "artificial atoms," QDs possess both continuous and discrete energy gaps and can modulate their bandgaps accurately by varying their size (Missous., 2006). They are typically synthesized from elements belonging to groups II-VI or III-V. QDs are considered one of the leading nanoparticles in bioscience, with potential applications in various economic sectors and health-related products. Several strategies have been developed for QD synthesis, with two commonly proposed techniques: top-down processing and bottom-up approaches.

Top-down processing involves the breakdown of bulk materials into nano-sized structures or particles, constituting a modification of methods utilized for the synthesis of larger particles. Top-down synthesis depends on miniaturizing the original bulk material to achieve the desired structure with suitable properties. Common approaches in top-down methods include X-ray lithography, molecular beam epitaxy, ion implantation, and e-beam lithography to obtain QDs. However, materials produced through the top-down method may have imperfect surface particles, such as clusters of contaminants and structural imperfections (Bertino *et al.*, 2007). To minimize surface imperfections, an alternative and cost-effective approach has been developed.

The bottom-up approach involves the self-assembly of materials from individual atoms and molecular clusters. This technique is still in its early stages of commercial production of nanopowders. Bottom-up techniques have been used to prepare fluorescent nanoparticles, employing methods like organometallic chemical synthesis, reverse-micellar route, wet chemical sol-gel synthesis, precipitation synthesis, hydrothermal synthesis, and electrochemical deposited template-assisted sol-gel. Colloidal QDs are formed through the self-assembly of particles in a solution, allowing for controlled size and shape with specific geometries.

Bottom-up methods can be broadly divided into two types: (a) wet-chemical methods, which involve the precipitation of individual or mixed solutions with precise parameter control. The wet chemical method is especially useful for synthesizing 2D nanomaterials, which cannot be easily produced through top-down approaches (Burda *et al.*, 2005; Nsibande and Forbes, 2016). Fabrication of 2D nanomaterials and high controllability are unique features associated with the wet chemical method (Leonardi *et al.*, 1998; Valizadeh *et al.*, 2012). (b) Vapour-phase methods are another approach for producing QDs, where layers are formed through an atom-by-atom process by heteroepitaxial growth of strained atoms. Generally, QDs grow as uniform, epitaxial layers in the vapour-phase method (Kurtz *et al.*, 2000). This method involves synthesizing nanomaterials through molecular beam epitaxy, sputtering methods of film deposition, and liquid metal ion sources (Swihart, 2003).

2.4.1. Quantum dot-based sensors

Nano-sensors have been created utilizing QDs instead of conventional inorganic or organic fluorescent dyes due to their superior performance (Chakraborty 1999; Zhang et al. 2015; Zhou et al. 2019). QDs exhibit distinctive optical characteristics, such as a high fluorescence quantum yield (QY), a broad range of excitation wavelengths, a narrow emission spectrum, and excellent photostability. These attributes make them highly suitable for sensor applications (Chakraborty 1999; Zhang et al. 2015). The emission spectrum and wavelength of QDs can be adjusted by varying their particle size and chemical composition. QDs have been extensively employed in diverse fields, including chemical sensing, biosensing, bioimaging, nanomedicine, photocatalysis, and electrocatalysis (Chakraborty 1999).

2.5. Strategies to develop MIPs based QDs Sensors

2.5.1. Silica-Based MIP-QDs Sensors

In recent years, there has been significant attention given to the use of silica in order to enhance the efficiency of quantum dots (QDs) (Bossi *et al.*, 2020; Huang *et al.*, 2023). Silica-based QDs are notable for their UV-Vis transparency, which helps in protecting the QDs from photochemical degradation and improves their optical properties. Additionally, the crosslinked morphology of silica is well-developed and lends itself to the creation of recognition sites

QDs that are coated with silica are commonly prepared using the sol-gel method, which is a straightforward and cost-effective approach for producing various nanomaterials and modifying polymer surfaces. MIPs created from silica-based nanomaterials offer selected cavities and exhibit long-term stability due to the thermal and mechanical properties of silica-based materials. Moreover, sol-gel-based MIPs facilitate the efficient extraction of template molecules from the polymer matrix (Leung *et al.*, 2001; Annamma and Beena, 2011; Kia *et al.*, 2016; Moein *et al.*, 2019; Kalogiouri *et al.*, 2020).

2.5.2. Hybrid inorganic-organic MIP-QDs Sensors

The advantages of silica-based QDs are accompanied by certain limitations, viz their limited porosity and chemical functionality (Li *et al*., 2018). To overcome these limitations, researchers have developed hybrid molecularly imprinted polymer-quantum dots (MIP-QDs) that combine organic and inorganic components. This hybrid approach provides a wide range of functional monomers and crosslinkers, resulting in enhanced QD efficiency compared to silica-based QDs. The organic imprinted polymer selectively recognizes and binds to the template molecule (Li *et al*., 2018). Various scientific sources present different synthesis methods for hybrid inorganic-organic QDs. For instance, in one study, FeSeQDs were utilized as a sensor and support material in an optical quantum dot sensor for detecting cyfluthrin (insecticide). The composite was prepared using a reverse microemulsion process, involving the hydrolysis of tetraethyl orthosilicate (TEOS) with a solution containing 2,2'-azobisisobutyronitrile (AIBN), TEOS, TritonX100, cyclohexane, FeSeQDs, and ammonia. Subsequently, a prepolymerization mixture comprising the template, the monomer APTES, the secondary monomer (MAA), and the crosslinker EGDMA were combined with the QD sensor and heated to initiate polymerization (Li *et al*., 2018).

2.5.3. Organic MIP-QDs Sensors

Organic MIPs have emerged as a potential alternative to silica in the specific synthesis of MIP-QDs (Chao *et al*., 2014). When compared to silica-based MIPs, MIPs based on acrylate have shown enhanced selectivity and specificity in the production of acrylate on CdTe QDs as

fluorescent sensors, as well as tetracycline-imprinted polymeric silicates (Chao *et al*., 2014). The increased fluorescence observed in acrylate-based MIPs can be attributed to the stronger bond activity between the target molecule and the acrylate-based polymer (Chao *et al*., 2014).

Although less attention has been given to organic MIP-QDs, they hold promise as highly efficient catalysts. Typically, the synthesis of organic MIP-QDs involves chain-growth polymerization of crosslinkers and monomers in the presence of a radical initiator. Prior to imprinting, the QDs are functionalized with a binding anchor like 4-vinyl pyridine (Wei *et al*., 2016). Currently, there is ongoing development of a MIP-GQDs fluorescent nanosensor for methamphetamine detection.

2.6.5. Extraction of crocin using MIPs

Since saffron is a costly spice, several efficient extraction methods have been devised to achieve a significant yield of crocin and other metabolites. The extraction process used is determined by parameters such as the required purity of the crocin extract, the scale of extraction, the available equipment, and the desired efficiency. Table 2.5 details the many techniques that have been discovered to extract crocin from saffron. The application of a MIP based on a gentiobiose template is one such method (Figure 2.3). A solution of 0.5 mmol of gentiobiose and 4 mmol of methacrylamide in 10 ml of dimethyl sulfoxide has been employed to prepare the gentiobiose MIP (Gent-MIP) and 10 mg of 2,2-azo-bis-iso-butyronitrile and 20 mmol of ethylene glycol dimethacrylate was added to the solution. After 10 minutes of contact with oxygen-free nitrogen, the resultant solution was hermetically sealed. To finish the polymerization reaction, the sealed tube was heated to 50 °C for 24 hours. The resulting polymer was then sieved through a 200-mesh for final preparation (Mohajeri *et al*., 2010).

 Gent-MIP and nonimprinted polymer (NP) has been studied for crocin binding in aqueous conditions. The results indicated that, compared to the nonimprinted polymer, the Gent-MIP had increased affinity for towards crocin throughout the board. The Gent-MIP performed well as sorbent in a SPE procedure for removing impurities and concentrating crocin from a methanolic saffron extract.

Table 2.5- Different extraction techniques for crocin and their advantages/disadvantages

Technique	Parameter/principle	Advantages	Disadvantages
Crystallization technique	Simple and efficient method for extraction of crocin. Crystals are obtained by storing the extract at -5°C. Ethanol (80%) is ideal for extraction. This technique is based on the nature of the crystallizing substance, the concentration, the temperature, agitation, and the impurities present in the solution.	Simple and widely used, high purity	Yield is limited by phase equilibria, energy consumption, generally only purifies one component.
Solvent-Based Extraction Technique	Generally, the soxhlet method is employed for extraction. 80% ethanol (v/v) is the ideal solvent for this method	Low energy consumption, high production capacity, simple continuous operation, simplicity of automation	Time and solvent consumption, the impurity may be present
Ultrasound-assisted Extraction	UAE is characterised by ultrasonic effects caused by acoustic cavitations. Vibration and acceleration of the particles in the solid and liquid phases cause solute to rapidly infiltrate from the solid phase into the solvent. Crocin can be separated and extracted from saffron by UAE using water and ethanol as solvents	Eco-friendly. commercially viable tool for large-scale samples, easy to handle and time-efficient High-quality yield, reduced solvent consumption	The active component of ultrasound is limited in the proximity of the ultrasonic emitter. The attenuation of ultrasonic waves is aided by the presence of scattered phases.
Supercritical Fluid Extraction	Crocin can be extracted from saffron with supercritical CO_2. Solutes extraction conditions can be optimized by response surface methodology for maximum recovery.	Eco-friendly, Solvent (Carbon dioxide) is cost-effective. Solvent recycling is possible for all methods, high speed of analysis, and pure extraction yield may be obtained.	Specialized tools or equipment are required. Improper solvent selection results in the loss of desirable compounds. High analytical cost
MIPs-SPE based extraction	Using gentiobiose as a template, MIPs can be synthesized and used in SPE for the extraction of crocin from saffron	High affinity and selectivity for the target molecule, simple preparation, great stability, high resistance to pressure and temperature	Template-functional monomer interaction is less strong,
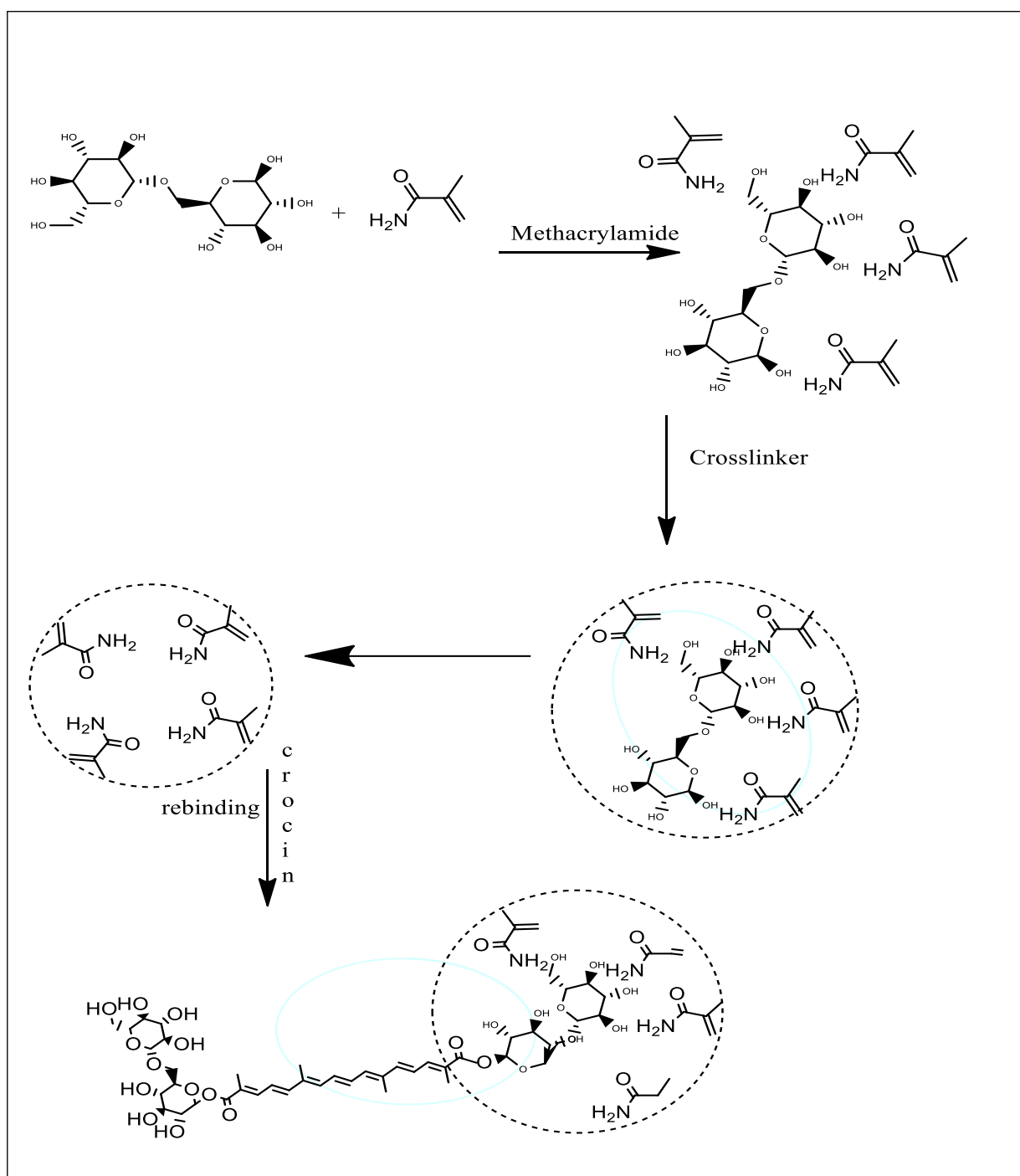
Figure 2.3 - Schematic representation of Extraction of Crocin using gentiobiose as a template.

2.6. Strategy for employing MIPs-QD sensors for extraction and detection of crocin

MIP embedded with QDs has a lot of applications, and QD sensors can be prepared with MIPs as recognizing elements towards the template (Li *et al*., 2010). This method has detected a nanolevel concentration of 9 *nm* targent molecules. MIPs with silica-embedded QDs can be used in pesticide sensing. Trace detection of λ-cyhalothrin pestcide in water has been done with

MIPs-CdSe-QDs modified in silica spheres (Ren *et al*., 2015). Pentachlorophenol, an organochloride pesticide widely used as a wood preservative, has been detected with ZnS; M^{2+} imprinted with a MIP (Wei *et al*., 2016). However, to make the separation easy, Fe_3O_4 nanoparticles were incorporated to induce supramagnetic properties in the MIP matrix under the influence of external magnetic field is applied (Wang *et al*., 2009). This signal transducer could detect pentachlorophenol down to 0.5 µM. Pentachlorophenol has been selectively adsorbed in the presence of other aromatic compounds by Fe_3O_4 nanoparticles loaded MIP matrix. The OVDAC/CdTe fluorescent sensor has been successfully used to determine λ-cyhalothrin in river water samples.

A similar strategy can be employed to extract, preconcentrate, and detect crocin using QD embedded MIPs (Figure 2.4). Different extraction methods are employed for the extraction of crocin from the extract, and different spectroscopic and chromatographic techniques like TLC, UV, HPLC, NMR, MS, and HPLC are currently used to characterize crocin. There is a shortage of data on MIPs for the extraction of crocin. Crocin has been extracted with different methods and solvents (ethanol/water), but currently, MIPs became an interesting and desired area for the extraction of the target molecule. The MIPs is a simple synthesis method with high selectivity and specificity for the template molecule. The synthesis is simple and can be performed easily with less expensive instruments or skills. MIPs has the unique capacity of generating recognition cavities towards the analyte, and these cavities are complementary in shape, size, and functionality to the template. MIP can be synthesized for the extraction of crocin using crocin as a template. Different monomers and crosslinkers can be tried for better and specific extraction of crocin from the complex mixture. The functional monomer can be applied for the hydroxyl interaction of crocin like acrylic acid. The derivatives and stability of the polymer can be maintained with the help of suitable crosslinkers and for the reaction initiation. AIBN, an initiator, can be used for free radical polymerization. The stability and adsorption rate can be studied with the help of instrumental analysis. However, to improve the selectivity of MIP for an analyte, MIPs can be embedded in the QDs. QDs draws a significant role in the selective and sensitive determination of an analyte. Therefore, MIPS embedded with QDs can simultaneously extract, preconcentration, and detect crocin from the extract.
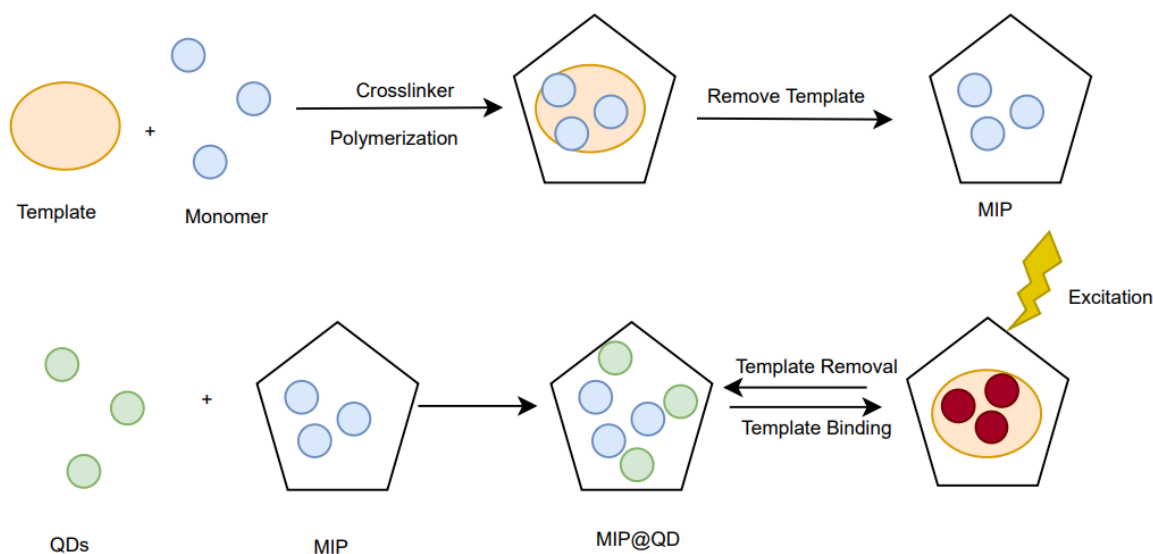
Figure 2.4.- Scheme for using MIPs and QDs complex for detection of Crocin

MIPs have exceptional resistance to high temperatures and pressures, acid and alkali, making them ideal as sensitive materials for sensors to identify desired samples analytically. The high selectivity and affinity for the target molecule employed in the imprinting process are the major advantages of MIPs. Recently, studies have suggested combining MIPs with QDs established and optimising them to provide extremely selective and sensitive detection systems. MIPs coated with QDs are extensively utilised in different areas, including environmental contaminant analysis, food quality and safety, sample separation and enrichment, etc. The combination of MIPs and QDs has been suggested as a promising material in the production of optical sensors.

Crocin is the major metabolite present in saffron, and it has been used as a therapeutic agent for decades. The extraction of crocin by various methods using ethanol as a solvent has already been performed in the literature. Different spectroscopic and chromatographic techniques have been used to characterize crocin like TLC, NMR, UV, MS, and HPLC. QDs, owing to their extensive applications in nanotechnology, pharmaceuticals and the increasing trend of being environment friendly, have become a centre of interest. Therefore, QDs embedded in MIPs have the potential to simultaneously extract and detect crocin from saffron.

2.7. Gold nanoparticles as an approach for detection of adulteration

Adulteration is a major threat in various industries, including food, cosmetics, and pharmaceuticals (Parmar *et al*., 2022). The practice of adding foreign ingredients to a product, which lowers the quality of the product and often puts customers' health at risk, is termed "adulteration" (Handford *et al*., 2016). Thus, it has become a major issue in these fields to create reliable and sensitive methods of detecting adulterants. Recently, nanotechnology has emerged as a promising approach for detecting adulteration (Inbaraj and Chen, 2016; Ravichandran, 2010). Various nanomaterials have been synthesized for detection of various adulterants in various food stuff. Nanomaterials have unique physical and chemical characteristics due to their nanometer-scale dimensions. These properties may be used to develop extremely specific and sensitive detection methods for adulterants (Ravindran *et al*., 2021). The principle of SPR underpins the use of nanomaterials for the sensitive and selective detection of adulterants. SPR is a phenomenon that occurs when light interacts with a nanoparticle, resulting in the excitation of surface electrons. This excitation causes the formation of a plasmon, which changes the surrounding medium's index of refraction (Kooyman; 2008; Jana *et al*., 2016). This change in refractive index can be monitored and utilized to detect adulterants. In recent years, gold nanoparticles (AuNps) have garnered considerable attention in the scientific community. AuNPs have been utilised to identify adulteration in a variety of food (Mecker *et al*., 2012; Kumar *et al*., 2014; Chaisiwamongkhol *et al*., 2020).

Chemical analysis is a procedure that makes use of analytical techniques. Methods such as UV-Vis Spectroscopy (Ordoudi *et al*., 2017), HPLC (Sabatino *et al*., 2011), GCMS (Aiello *et al*., 2020), and Infrared Spectroscopy (S. Karimi *et al*., 2016) are all examples of such chemical approaches. These approaches can detect the presence of adulterants in saffron by assessing its chemical composition. HPLC is often preferred over other analystical techniques because of its ability to quantitatively and qualitatively identify adulterants by separating and measuring the various components of the spice (Maggi, *et al*., 2020). The chemical structure of the spice's constituents can be determined by using GCMS or MS. This is also a very sensitive and selective method identifying various adulterants. Since this approach can determine the chemical structure of the individual components, it is possible to detect adulterants in very low concentrations. It can detect adulterants by determining the chemical composition of the spice's constituent parts (Kaavya *et al*., 2020).

PCR is a DNA-based technique used to quantify adulteration in saffron. The saffron DNA of the different components of the spice may be amplified using the very sensitive PCR. The adulterants may then be recognized at very trace levels (Soffritti *et al*., 2016). In this study, AuNPs were synthesized using saffron extract and employed as a means for calorimetrically detecting the adulteration of saffron. The Au-NPs were synthesized under various conditions in the presence of saffron extract acting as a reducing agent, resulting in the formation of pink-colored nanoparticles. This approach enables the identification of saffron quality and identification of adulterants.

Objectives

1. Investigation of pure and adulterated saffron by various instrumental techniques.
2. Synthesis of Molecularly Imprinted Polymer encapsulated with Quantum Dots for detection of Crocin.
3. Development of nanomaterial-based methods for quantification and detection of various adulterants in saffron

Chapter 3

Material and Methodology

3.1. Chemical and reagents

- **Sigma Aldrich (Merck):** Crocin ($C_{44}H_{64}O_{24}$) Safranal ($C_{10}H_{14}O$), Tetra chloroauric acid ($HAuCl_4$), Succinic acid ($C_4H_6O_4$), Gallic acid ($C_7H_6O_5$), Citric acid ($C_6H_8O_7$), Thiourea (CH_4N_2S), Sudan I ($C_{16}H_{12}N_2O$), Methyl orange ($C_{14}H_{14}N_3NaO_3S$)

- **BioMall:** Picrocrocin

- **LobaChemie:** HPLC-grade reagents (methanol, acetonitrile), L-serine, L-tryptophan , L-threonine, Vitamin B6, Vitamin B1, Vitamin C, Copper chloride ($CuCl_2$), Magnesium sulfate ($MgSO_4$), Nickel sulfate ($NiSO_4$), Sodium chloride (NaCl), Potassium chloride (KCl), Sodium hydroxide (NaOH), Hydrochloric acid (HCl)

- **SRL Chemical:** Phosphate citrate buffer, Tetraethyl orthosilicate (TEOS) Aminopropyltriethoxysilane (APTES), Potassium bromide (KBr), Potassium iodide (KI)

3.2. Material and methodology

3.2.1. Objective 1- Investigation of pure and adulterated saffron by various instrumental techniques.

The primary objective of this research was to estimate the quality range and apocarotenoid content of commercial saffron in Kashmir using UV-Vis spectrophotometry and HPLC analysis. Saffron in India is cultivated and commercialized in Kashmir. The main local commercial zones of saffron in Kashmir are Srinagar, Pampore and Budgam. Besides local markets, the saffron in Kashmir is also commercialized by government-operated commercial emporiums (e.g., Government Kashmir Art Emporiums). A total of 31 samples were used for this study. 24 samples of saffron were collected from Kashmir, among which 06 samples were collected from Government operated commercial emporiums (KAE), 06 samples were collected from the local market of Srinagar (SXR), 06 samples were collected from Pampore (PAM) district, and 06 samples were collected from Budgam (BUD). The samples collected were supposed to be yielded from the crop year 2019 and processed in 2020 as per their packing. Besides these samples, 04 samples were collected from Afghanistan (AFG), and 02 samples were collected from Iran (IRN). The samples collected from KAE, AFG and IRN had

an origin certificate and were assured free from any adulteration. One standard sample was collected from Sigma (SIG). Crocin and safranal standards were obtained from Sigma. Picrocrocin was obtained from BioMall. HPLC-grade reagents (methanol, acetonitrile) were obtained from LobaChemie.

3.2.1.1. Determination of floral waste content

About 1 g of each sample were taken, and each filament was spread on the paper. With the help of forceps, different floral waste components were separated, and the samples were weighed again. The floral waste was taken in shoe glass and weighed. The floral waste content of the sample (*wF)* was expressed as per ISO guidelines as a percentage by mass, using the relation:

$$wF = (m_2 - m_1) \; x \; 100/m_o \; \%$$

Where m_0 = mass, in *grams*, of the test portion; m_1 = mass, in *grams*, of the shoe glass; m_2 is the mass, in grams, of the shoe glass containing the floral waste.

3.2.1.2. Determination of volatile and moisture content

The samples collected were collected and examined for their authenticity by ISO 3632 guidelines for conducting UV-Vis spectroscopy. To calculate E_1 %, first, the moisture content of all the samples was calculated. 01 gram of saffron from each sample were placed in a Petri dish and kept in the oven for 18 hours at 70 ^{0}C. After that, samples were weighed again to measure the moisture and volatile matter content (*wMV)* and is expressed as-

$$wMV = (m_0 - m_1) \; x \; 100/m_0 \; \%$$

where m_0 = in grams of the test portion; m_1 = mass in grams of the dry residue

3.2.1.3. UV-vis spectroscopy

The UV-Vis spectroscopy for samples was performed according to ISO guidelines with slight modifications in order to get a greater yield of apocarotenoid compounds. In brief, the procedure involved the extraction of dried saffron samples weighing 100 mg. This was achieved by using a mortar and pestle with 5 ml of cold ethanol solution (50% v/v). The resulting extract was then transferred to a 50 ml tube with a screw cap, and an additional 20 ml of the same ethanol solution was added. To facilitate the process, the tubes were subjected to 20 minutes of sonication on ice, followed by a 15-minute centrifugation at 4000 rpm. Afterward, the mixture underwent two washes using 5 ml of the ethanol solution. To analyze

the supernatant, a spectrophotometric technique was employed. For analysis purposes, the supernatant (1 ml) was diluted to 5 ml using 50% ethanol solution. A standard curve was plotted using crocin, safranal, and picrocrocin absorption values at 440 nm, 330 nm, and 257 nm, respectively. Using a Shimadzu spectrophotometer (equipped with a 1 cm route quartz cell), absorbance was recorded at 440 nm, 330 nm, and 257 nm directly from 100-fold-diluted sample supernatants. A UV-Vis scan was also obtained to observe peaks in samples of different geographical locations. The results obtained were used to measure E_1 % of aqueous saffron extract using the following relation.

$E_{1\%}\ 1\ cm = (A \times 10000/ [(M \times (100\text{-}H)]$

3.2.1.4. HPLC analysis

To perform HPLC analysis, we conducted the extraction of saffron samples in powdered form, weighing 50 mg each. The extraction process involved utilizing a 10 ml solution of 50% methanol-water (v/v). This extraction took place in the dark at 4 °C and lasted for 24 hours, during which continuous stirring was maintained using a magnetic stirrer. Following the extraction, the samples underwent centrifugation at 5000 rpm for 30 minutes. The resulting supernatant was then collected and filtered using 0.2 µm syringe filters.

Before the analysis, 2-nitroaniline was added as an internal standard to each sample to quantify crocin, picrocrocin, and safranal (Caballero-Ortega et al., 2007). The analysis was conducted using a Shimadzu HPLC system equipped with a photo-diode-array detector. The mobile phase consisted of 50% ethanol and 15% acetonitrile (v/v). Detection was achieved with an injection volume of 20 μl, a flow rate of 1 ml/min, and a run time of 35-40 minutes. Crocin, picrocrocin, and safranal were detected at wavelengths of 440 nm, 250 nm, and 330 nm, respectively. For quantification, a calibration curve was constructed for the internal standard, spanning concentrations from 0.125 to 1.0 mg ml^{-1}. The quantification of the components relied on the molecular absorption coefficient of each peak obtained at their respective maximum absorbance wavelength. The R^2 values for the calibration curve ranged from 0.9722 to 0.9890. The results were expressed in mg per gram of saffron stigmas.

3.2.1.5. Statistical analysis

One-way ANOVA used to compare mean and Duncan's Multiple Range Test (DMRT) to assess significance using IBM SPSS (version-20). Two tailored Pearson correlations between apocarotenoid levels with floral waste content and moisture levels were done using IBM SPSS (v. 20). The results were also analyzed using the multivariate analysis technique principal

component analysis (PCA) using Origin-2021b (version-9.8b). PCA is a dimensionality-reduction technique often used to decrease the dimensionality of big data sets by converting a large collection of variables into a smaller one that still retains most of the information in the large set.

3.3. Objective 2- Synthesis of Molecularly Imprinted Polymer encapsulated with Quantum Dots for detection of Crocin.

In this study, MIPs embedded with QDs has been employed for detection of Crocin concentration in saffron.

3.3.1. Synthesis of CQDs and MIPs

To synthesize carbon quantum dots (CQDs), a sophisticated method known as thermal pyrolysis, as outlined in Dong et al.'s work (2012), was employed. In this approach, 4.0 grams of citric acid powder underwent heating to 180°C until the solution underwent a color change to yellow. The subsequent cooling to room temperature followed the protocol specified by Ahmadi *et al.* (2019). The characterization of the CQDs involved various techniques, such as X-ray Diffraction (XRD), fluorescence spectroscopy (FS), X-ray Photoelectron Spectroscopy (XPS), Fourier-Transform Infrared Spectroscopy (FT-IR) and Transmission Electron Microscopy (TEM).

Subsequently, the CQDs underwent further modification. Initially, 5 ml of APTES was introduced to the CQDs, followed by the addition of 0.05 grams of gentiobiose, dissolved in 70% methanol (v/v). Afterward, optimized volumes of TEOS and a catalyst solution (100 μL), prepared with 0.036 grams of NH4F, 9.2 ml of NH4OH, and 20 ml of water, were incorporated into the mixture. The resulting blend underwent stirring for 60 minutes at 35°C to generate the MIP-CQDs. After centrifugation and washing with a mixture of deionized water and methanol, the MIP-CQD nanocomposite was obtained. For the synthesis of CQDs-NIP, the same procedure was followed, excluding the gentiobiose template.

3.3.2. Characterization of CQDs and MIPs

The morphology of CQDs was studies through TEM, while the zeta potential and particle analyzer (Malvern) were used to determine the surface charge and average diameter. Fluorescence spectroscopy (FL) was carried out using a Perkin Elmer fluorescence spectrophotometer with a 5/5 μM slit. FTIR spectra, spanning 400-4000 cm−1, were captured using an FTIR spectrophotometer (SHIMADZU AIM-8800). To investigate the crystalline

structure of the compound, X-ray Diffraction (BRUKER D8 ADVANCE) was utilized. The absorption spectra were captured using a UV–Vis double beam spectrophotometer (UV-1900I-SHIMADZU. SEM was employed to investigate the morphology of MIP and NIP. XPS analysis was conducted to determine the elemental composition of CQDs. Ultra-pure DI water was utilized in all experiments. Gentiobiose was used as template for the synthesis of MIP as crocin being a large molecule, it is not possible to use Crocin itself as a template. Structurally, Crocin is made up of two Gentiobiose molecules therefore, gentiobiose was used as a template

3.3.2.1. Preparation of fluorescent probe for detection of crocin

To prepare the fluorescent probe, dried MIP-CQDs powder (0.5 g) was sonicated for 03 h in a 200 ml-volumetric flask containing buffer (BR), then cooled at room temperature, and 1 ml of the solution was transferred into a quartz cuvette, and it was then mixed with 3 ml of a BR buffer solution. The varying concentration of crocin 2μm to 200 μm was prepared in 70% ethanol and 100 μL added to the fluorescent quartz and fluorescence spectrum was measured for each concertation. Same procedure was applied for NIP-CQDs for comparative analysis.

3.3.2.2. Collection and Sample collection and preparation:

Samples of saffron were procured from local markets situated in Pampore, Kashmir, India. Pampore, a district in Kashmir, has gained recognition for its exceptional saffron cultivation. To ensure the presence of any impurities, the collected samples underwent analysis employing the ISO-3632 technique. These samples were then finely ground to a powder consistency with the assistance of a mortar and pestle. Approximately 100 mg of the ground sample was placed into a screw-capped test tube, followed by the addition of 100 ml of water. The resulting mixture underwent sonication for a duration of 30 minutes, and subsequent centrifugation for around 30 minutes at a speed of 10000 rpm. The supernatant obtained after centrifugation was then filtered and properly stored at a temperature of 4°C.

3.4.   Objective 3- Development of nanomaterial-based methods for quantification and detection of various adulterants in saffron

3.4.1. Sample preparation and instrumentation

Saffron sample was grinded into a powder using a mortar and pestle and 100 mg sample was taken into a screw-capped test tube, and 100 ml of water was added. The mixture was sonicated for 30 minutes and centrifuged for approximately 30 minutes at 10000 rpm. The resulting supernatant saffron extract (SE) was filtered and stored at 4°C for analysis. To verify the shape of AuNPs, the morphology was confirmed using a FE-SEM. The surface-charge and average diameter of the AuNPs were determined by analyzing the zeta sizer from Malvern. The FTIR spectra of NCQDs were captured using an FTIR spectrophotometer in the 400-4000 cm^{-1} range. The technique was employed to investigate the crystalline structure of the compound. Finally, the absorption spectrum was measured by using UV–Vis double beam spectrophotometer.

3.4.1.1.Synthesis of AuNPs

The tetra-chloroauric acid (HAuCl$_4$) and crocin were mixed together in an acidic solution and the solution's pH, which was initially close to 3 due to the presence of HAuCl$_4$, was raised to 10 by increasing the pH fallowed by incubation at 40 ºC for 6 hours. This increase in pH triggered a reaction, resulting in the synthesis of nanoparticles. The development of a pink color visually confirmed the synthesis of nanoparticles. Different parameters were examined to determine their impact on the size and quantity of AuNPs produced.

3.4.1.2. Optimization of Synthesis procedure

Gold ions were employed in concentrations spanning from 0.5 to 5 mM, along with crocin serving as a reducing agent. The experiments involved different time intervals (ranging from 10 minutes to 10 hours), pH values (ranging from 2 to 12), and temperatures (ranging from 20 to 60 °C). Changes in the color of the solutions were observed over time by employing a UV-Vis spectrophotometer, specifically within the wavelength range of 520-560 nanometers. Following the synthesis process, the solutions were subjected to three rounds of centrifugation lasting 15 minutes each, at a speed of 10,000 rpm. Subsequently, the synthesized solutions were washed using deionized water to effectively separate pure AuNPs.

3.4.2. Synthesis of NCQDs for detection of MO in saffron

The morphology of NCQDs was validated using TEM. Zeta potential and particle analyzer were used to determine the surface charge and average diameter of NCQDs. A Perkin fluorescence spectrophotometer with a 5/5 nm slit was employed for FL spectroscopy. FTIR spectra of NCQDs within the 400-4000 cm^{-1} range were recorded using an FTIR spectrophotometer. XRD was employed to investigate the crystalline structure of the compound.

3.4.2.1. Preparation of NCQDs

To NCQDs, we utilized a microwave-assisted approach with succinic acid as the carbon source and gallic acid as the nitrogen source. Initially, 1 gram of succinic acid and 0.7 gram of gallic acid were dissolved in 5.0 mL of deionized water. The solution was then heated using a household microwave oven (700 W) for 10 minutes, yielding a brown material. After cooling at room temperature, the mixture was redissolved in 10 mL of deionized water. To eliminate unreactive and large particles, the solution underwent centrifugation at 10000 rpm for 20 minutes. The resulting supernatant was subsequently filtered and stored for characterization and potential future applications.

3.4.2.2. Optimization of prepared NCQDs

The effect of pH Values (4-10) on NCQDs was investigated in order to determine their fluorescent behavior for different pf values. The pH of NCQDs was adjusted using 0.1 mM HCL and NaOH solution. The optimized time required for quenching of the FL intensity of NCQDs upon interaction with MO was also monitored at different time intervals.

3.4.2.3. Preparation of the fluorescent probe for MO using NCQDs

For selective interaction of NCQDs with MO, 100 μL MO solutions with different concentrations (02- 200 μM) were added into an Eppendorf tube containing 800 μL of NCQDs (pH. 8 with phosphate buffer). The FL spectrum was obtained at an excitation wavelength of 340 nm after 3 minutes of incubation time.

3.4.2.4. Preparation of saffron samples

Approximately 100 mg of the ground sample was placed into a screw-capped test tube, followed by addition of 100 ml of water. The resulting mixture underwent sonication for a duration of 30 minutes, and subsequent centrifugation for around 30 minutes at a speed of 10000 RPM. The supernatant obtained after centrifugation was then filtered and properly stored at 4°C for future utilization.

3.4.2.5. Detection of MO in saffron by NCQDs

The detection of MO in saffron was performed by spiking different concentrations of MO (5-75 μL) to saffron extract (100 μL) and NCQDs were added to the make final volume of 500 μL. The fluorescence spectrum of spiked samples was taken, and the recovery percentage was calculated using the following relation-

$$R=[(C_3-C_2)/C_1] \times 100\%$$

Where R= recovery percentage, C_1= Added concentration of MO, C_2= Real MO concentration already present in the sample, and C_3= Concentration of MO found after adding standard MO.

3.4.3. Synthesis of SCQDs for detection of Sudan I in saffron
3.4.3.1. Synthesis of SCQDs

The SCQDs were synthesized by microwave assisted method using citric acid and thiourea as as carbon and sulphur source respectively (Chang, 2022; Rani *et al*., 2023). Citric acid and thiourea were dissolved in 10ml of distilled water and then stirred on a magnetic stirrer until completely dissolved. A microwave oven set to 450W was used to irrigate the solution for 10 minutes. The resultant brown material was dissolved in 10 ml of water and centrifugation at 15000 rpm was carried out for 30 minutes and then filtered. The resultant solution was allowed to dry for 03 days at room temperature. After that, the material was once again dissolved in water (20 ml) and filtered again. The resulting suspension containing SCQDs was collected for further characterization and use.

3.3.3.3. Optimization of prepared SCQDs

The aim of optimization was to improve the performance of SCQDs through optimization. Specifically, the fluorescent behavior of SCQDs at different pH values (ranging from 2 to 10) was studied by adjusting the pH using solutions of 0.1 mM HCL and NaOH. Additionally, the time required for efficient quenching of SCQDs' FL intensity upon interaction with Sudan I was monitored at different intervals to determine the optimal timing.

3.3.3.4. Preparation of the FL probe for Sudan I using SCQDs

In order to develop a FL probe for Sudan I, SCQDs were used for their selective interaction with the target molecule. To achieve this, different concentrations of Sudan I solution (ranging from 02 to 150 μM) were added to an Eppendorf tube containing 800 μL of SCQDs in a phosphate buffer solution at pH 8. After incubating the mixture for 3 minutes, fluorescence spectra were obtained by exciting the sample at a wavelength of 340 nm. This process allowed

for the creation of a fluorescent probe that was able to selectively detect Sudan I through its interaction with SCQDs. The resulting fluorescence spectra could then be analyzed for determination of the Sudan I concentration in the sample.

3.3.3.5. Preparation of saffron samples

The saffron samples were then ground into a powder using a mortar and pestle, and approximately 100 mg of the resulting powder was placed in a screw-capped test tube. Next, 100 ml of water was added to the test tube, and the mixture was sonicated for 30 minutes before being centrifuged for about 30 minutes at 10000 rpm. The resulting mixture underwent sonication for a duration of 30 minutes, and subsequent centrifugation for around 30 minutes at a speed of 10000 RPM. The supernatant obtained after centrifugation was then filtered and properly stored at 4°C for future utilization.

3.3.3.6. Detection of Sudan I in saffron samples using SCQDs

To detect the presence of Sudan I in saffron, different concentrations of Sudan I (ranging from 5-75 µL) were added to 100 µL of saffron extract, followed by the addition of SCQDs to achieve a final volume of 500 µL. The fluorescence spectrum of the resulting samples were obtained, and the recovery percentage was calculated using the formula:

$$R = \left[\frac{C_3 - C_2}{C_1}\right] x \ 100\%$$

where R represents recovery percentage, C_1 represents spiked concentration of Sudan I, C_2 is the real concentration of Sudan I already present in the sample, and C_3 is the concentration of Sudan I found after adding standard Sudan I. By calculating the recovery percentage, the accuracy and precision of the method for the detection of Sudan I in saffron could be possible.

Chapter 4

Results and Discussion

4.1. Objective I- Investigation of pure and adulterated saffron by various instrumental techniques.

The determination of floral waste in the samples was performed by physical separation of floral waste and then measuring its weight. The floral waste in the samples varied in range, with samples obtained from SXR and BUD showing a high range of floral waste. KAE samples and sigma samples showed the lowest range of floral waste, while IRN and AFG samples showed a medium to low range of floral waste. Floral waste in the Sigma sample was not detected (Table 4.1). The moisture/volatile matter content was performed to analyze samples had been properly dried and processed. The average moisture level in KAE samples was found to be 6.26 %. Samples from SXR, BUD and PAM showed high levels of moisture and volatile content matter (12.45 %, 7.90 %, and 7.26 %, respectively). The average moisture and volatile content in the AFG and IRN samples was 6.35 % and 542 %, respectively, while in the SIG sample, it was found to be 4.49 % (Table 4.1).

Apocarotenoid content (E_1 %) was determined using UV-Vis spectrophotometry. The main objective of this measure analysis was to analyze the quality range of commercial saffron sold in Kashmir. One-way ANOVA and DMRT were used to compare means and assess the level of significance. The results showed significant variation in all the samples (Table 4.1). Results showed that average crocin content varied from 198.5 in KAE samples, 135.16 in SXR samples, 184.5 in PAM samples, 166 in BUD samples, 197.25 in AFG samples, 200.5 in IRN samples and 203 in standard. Based on crocin content, it was found that among 31 samples, 14 samples fell in category I, 09 fell into category II, 05 fell in category III and 03 were counterfeit or adulterated samples as they showed E1 % less than 110. Similarly, picrocrocin expressed as direct reading of the absorbance at 257 nm showed an average concentration of 36.5 in KAE samples, 23.83 in SXR, 33 in PAM, 28.16 in BUD, 34 in AFG, 38.5 in IRN and 32 in SIG sample (Table 4.2). The safranal content in 29 samples was found to be above 20, thus falling in the optimum range under ISO criteria. 03 samples resulted in a safranal content range below 20, which is not optimal as per ISO guidelines. The floral waste and moisture/volatile content in saffron samples were negatively correlated with crocin content values (-0.87, -0.81, respectively). The results were analyzed using PCA analysis. PC1 (76.23 %) and PC2

(18.06 %) accounted for 94.29 % of the total variance of the data. The coefficient for both the principal components is given in Table 4.4. A biplot of samples was obtained to distinguish between adulterated and pure saffron (Figure 4.1). The findings of this study coincided with previous studies by Nehviet et al., (2005) and Javid et al., (2012).

HPLC analysis provides quick and simple measurement of the three major saffron components, with excellent linearity, selectivity, sensitivity, and accuracy. The crocetin, picrocrocin, and safranal were determined by HPLC at three wavelengths 440, 250, and 330 nm, respectively. The results were analyzed by one-way ANOVA to compare means, and DMRT was used to assess significance. The concentration of these metabolites varied significantly (Table 4.1). The variations may be attributable to the geographical origin of samples, different drying procedures, storage conditions and adulteration (Delgado *et al.,* 2005; Maghsoodi *et al.,* 2012; Biancolillo *et al.,* 2020a). The average concentration of crocin varied from 40.64 mg g^{-1} in KAE samples, 29.952 mg/g in SXR samples, 34.55mg/g in PAM samples, 28.18 mg/g in BUD samples, 35.40 mg g^{-1} in AFG samples, 35.27 mg g^{-1} in IRN samples and 34.41 mg g^{-1} in sigma sample. Safranal, one of the main components responsible for the fragrance of the spice, is soluble in polar solvents and poorly soluble in nonpolar solvents. The safranal content as per the ISO 3632 (2011) method cannot be categorized in any grade as the ISO method doesn't provide a precise classification of grades of saffron based on safranal content. The average safranal content differed significantly across KAE (0.28 mg g^{-1}), SXR (0.22 mg g^{-1}), PAM (0.28 mg g^{-1}), BUD (0.25 mg g^{-1}), AFG (0.27 mg g^{-1}), IRN (0.27 mg g^{-1}), and sigma samples (0.31 mg g^{-1}). Meanwhile, average picrocrocin content ranged from 5.40 mg g^{-1} in KAE, 3.43 mg g^{-1} in SXR, 3.62 mg g^{-1} in PAM, and 3.57 mg g^{-1} in BUD samples, 4.30 mg g^{-1} in AFG, 5.21 mg g^{-1} in IRN and 4.46 mg g^{-1} in SIG sample (Table 4.3). Crocin and picrocrocin were not detected in SXR4 sample. A biplot of samples was obtained to analyze the relation between metabolites in samples using PCA (Figure 4.2). PC1 (92.31 %) and PC2 (7.16 %) accounted for 99.47 % of the total variance of the data. The coefficient for both the principal components is given in Table 4.4.

The results obtained from UV-Vis spectroscopy showed that saffron samples from KAE were of the highest grade compared to other saffron obtained from other commercial sites. The saffron from PAM and BUD commercial sites showed a moderate range of quality. The samples from AFG and IRN fell in grade I and II as per ISO parameters. The saffron from SXR markets showed the lowest grade compared to other samples. The HPLC analysis showed a higher concentration of apocarotenoid content in KAE samples, followed by AFG and IRN

samples. The SXR samples showed the lowest quality and apocarotenoid content, which indicates an indication of adulteration.

HPLC plays a crucial role in examining nonvolatile elements and contaminants present in Saffron. This analytical method involves dissolving a sample in a mobile phase, typically a non-polar solvent, which passes through a narrow column packed with a polar stationary phase. When dealing with food samples, reverse phase HPLC is commonly employed, utilizing a polar mobile phase and a non-polar stationary phase to expedite the analysis process. The segregation of components relies on various factors such as polarity, interaction with the stationary phase, and the impact of molecule size on elution rates.

Chromatograms generate multiple peaks based on component retention times at specific wavelengths, providing data on Saffron compounds. Lozano et al (1999) employed HPLC to identify Saffron metabolites and detect artificial dyes and plant-based adulterants. Haghighi, Feizy, and Kakhki (2007) detected styles colored with natural colorants, while Campo et al. (2009) used HPLC to distinguish Saffron origins through amino acid profiles. Sabatino et al. (2011) identified adulterants in Italian Saffron, and Hajimahmoodi et al. (2013) detected synthetic food colorants. Rubert et al. (2016) differentiated Saffron origins using UHPLC-HRMS and oxidized lipids. Akbari (2015) found synthetic colors in Saffron-based foods, with Tartrazine being predominant indicates an indication of adulteration. To the best of our knowledge, HPLC analysis was conducted by Javid et al. (2012) to determine apocarotenoid content in saffron from different geographical locations in Kashmir. The findings from their study slightly differ from our research, as our study primarily examined saffron obtained from commercial stores. In contrast, the previous study by Javid et al. (2012) utilized samples sourced from cultivation sites.

Table 4.1: Floral waste percentage (wF %), moisture and volatile percentage (wMV %), UV-Vis analysis, HPLC analysis of saffron samples

Sample	wF %	wMV %	UV-Vis Analysis			HPLC analysis		
			Crocin (E1 %) 440 nm	Picrocrocin (E1 %) 257 nm	Safranal (E1 %) 330 nm	Crocin (mg g^{-1})	Picrocrocin (mg g^{-1})	Safranal (mg g^{-1})
KAE1	0.77	5.26	205[a]	85[a]	42[a]	39.32[a]	5.36[a]	0.26[bc]
KAE2	0.41	6.10	212[a]	86[a]	44[a]	43.51[a]	5.89[a]	0.31[a]
KAE3	0.66	5.15	178[a]	62[b]	28[c]	45.36[a]	6.21[a]	0.26[bc]
KAE4	2.73	7.09	203[a]	74[a]	35[a]	39.95[a]	6.01[a]	0.29[a]

KAE5	1.43	6.43	188[a]	69[b]	31[ab]	42.29[a]	4.03[b]	0.3[a]
KAE6	6.17	7.53	205[a]	79[a]	39[a]	33.43[ab]	4.91[a]	0.27[abc]
SXR1	11.51	9.34	134[b]	56[c]	24[c]	38.49[a]	4.02[b]	0.28[ab]
SXR2	4.93	6.73	179[a]	59[c]	27[c]	26.36[b]	3.16[c]	0.17[c]
SXR3	5.61	10.3	184[a]	62[b]	28[c]	32.41[ab]	3.98[b]	0.2[c]
SXR4	20.49	14.68	80[b]	43[c]	23[c]	ND	ND	0.18[c]
SXR5	9.49	11.35	162[b]	57[c]	25[c]	34.24[ab]	3.23[c]	0.29[a]
SXR6	25.3	22.35	72[b]	40[c]	16[c]	18.26[b]	2.79[c]	0.23[c]
PAM1	4.53	12.08	195[a]	69[b]	32[ab]	33.32[ab]	3.63[b]	0.29[a]
PAM2	5.68	7.84	152[b]	65[b]	29[b]	38.43[a]	3.23[c]	0.26[bc]
PAM3	7.85	7.63	201[a]	74[a]	34[bc]	42.45[a]	4.02[b]	0.28[ab]
PAM4	0.60	6.26	163[b]	72[ab]	33[bc]	30.44[ab]	3.62[bc]	0.32[a]
PAM5	1.93	8.23	189[a]	67[b]	30[b]	29.4[ab]	3.14[c]	0.26[bc]
PAM6	6.25	5.39	207[a]	82[a]	40[a]	33.31[ab]	4.11[b]	0.27[abc]
BUD1	2.48	6.19	202[a]	79[a]	38[a]	32.43[ab]	3.89[b]	0.29[a]
BUD2	2.80	7.26	185[a]	60[c]	29[b]	26.38[b]	3.77[b]	0.27[abc]
BUD3	3.91	8.15	149[b]	56[c]	25[c]	27.39[b]	3.56[c]	0.28[ab]
BUD4	16.60	10.28	105[b]	53[c]	24[c]	20.2[b]	3.04[c]	0.21[c]
BUD5	11.29	5.33	181[a]	59[c]	27[c]	30.3[ab]	3.69[b]	0.23[c]
BUD6	10.24	6.35	176[a]	58[c]	26[c]	32.41[ab]	3.51[c]	0.25[bc]
AFG1	1.56	5.68	201[a]	78[a]	37[a]	41.34[a]	5.1[a]	0.27[abc]
AFG2	1.34	5.34	208[a]	81[a]	39[a]	30.49[ab]	4.25[b]	0.3[a]
AFG3	1.97	6.63	192[a]	68[b]	31[b]	31.42[ab]	4.07[b]	0.29[a]
AFG4	3.81	7.76	188[a]	64[b]	29[bc]	38.38[a]	3.81[b]	0.25[bc]
IRN1	2.10	5.26	206[a]	84[a]	41[a]	35.42[ab]	5.33[a]	0.26[bc]
IRN2	1.92	5.59	195[a]	75[a]	36[a]	35.12[ab]	5.1[a]	0.29[a]
SIGMA	ND[*]	4.49	203[a]	72[ab]	32[ab]	34.41[ab]	4.46[ab]	0.31[a]

Means followed by the same letter within the columns are not significantly different ($p < 0.05$) using DMRT

*ND- Not Detected

Table 4.2: Quality characteristics of saffron obtained from different geographical locations using the ISO-3632 method

Sample Origin	ISO Category	Crocin (E1 %) 440 nm	Safranal (E1 %) 257 nm	Picrocrocin (E1 %) 257 nm
KAE	I (4)	203-212	28-31	62-69
	II (2)	168-178	35-42	74-84
SXR	II (2)	179-184	27-28	59-62
	III (2)	134-162	24-25	56-57
	IV* (2)	72-80	16-23	40-43
PAM	I (3)	195-207	32-40	64-82
	II (1)	189	30	67
	III (2)	152-163	29-33	65-73
BUD	I (1)	202	38	79
	II (3)	176-185	26-29	58-60

	III (1)	149	25	56
	IV* (1)	105	24	53
AFG	I (3)	192-208	31-39	68-81
	II (1)	188	29	64
IRN	I (2)	36-41	75-24	75-24
SIG	I (1)	203	32	72
Category	**Grade I**	**Grade II**	**Grade II**	**Grade IV**
Number of Samples	14	9	5	3

*Highly adulterated or counterfeit saffron samples

Table 4.3: HPLC-based concentration range of crocin, safranal and picrocrocin of saffron samples obtained from different geographical locations

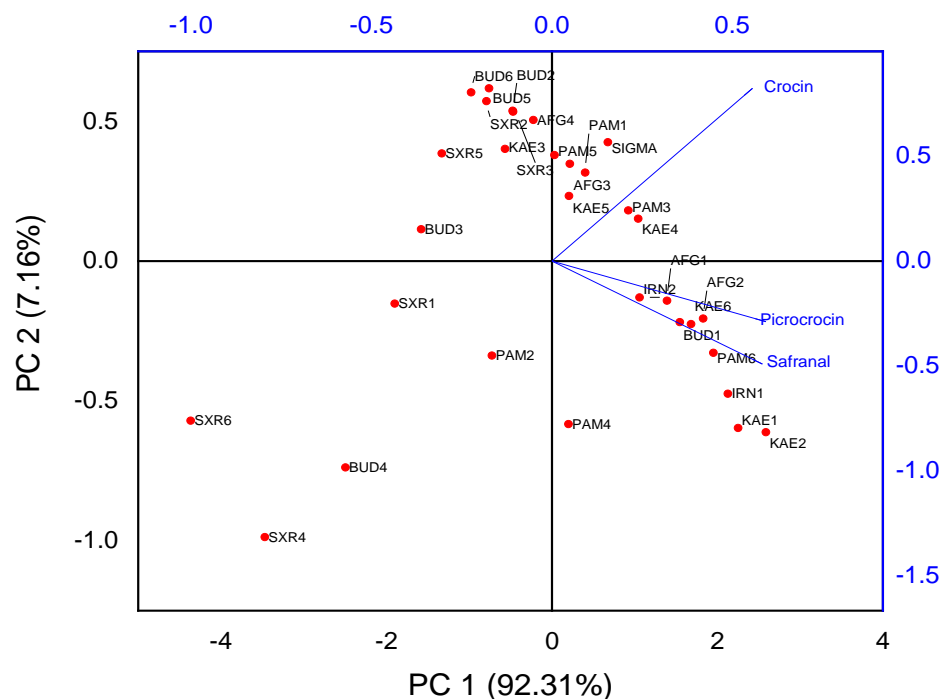| Sample Origin	Crocin (mg g^{-1})	Safranal (mg g^{-1})	Picrocrocin (mg g^{-1})
KAE	33.43-45.36	0.26-0.31	4.03-6.21
SXR	18.26-38.49	0.17-0.29	2.79-4.02
PAM	29.40-42.45	0.26-0.32	3.14-4.11
BUD	20.20-32.43	0.21-0.29	3.04-3.89
AFG	30.49-41.34	0.25-0.30	3.81-5.10
IRN	35.12-35.42	0.26-0.29	5.10-5.33
SIG	34.41	0.31	4.46

Figure 4.1: PCA analysis (biplot) of saffron samples (UV-Vis analysis)

Table 4.4: Loading of the first two principal components (PC's) for concentration of metabolites

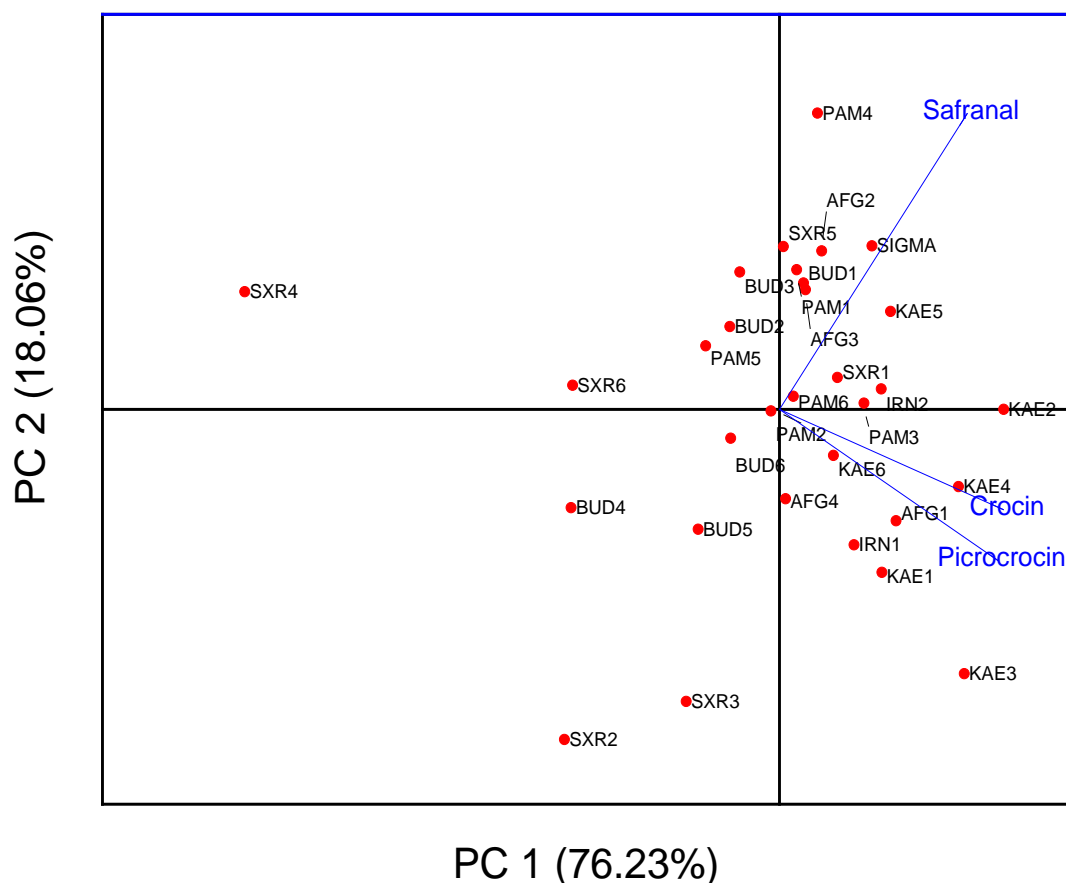| Variable	Coefficients of PC1	Coefficients of PC2
UV-Vis analysis		
Crocin	0.5555	0.82244
Safranal	0.58313	-0.49034
Picrocrocin	0.59278	-0.28836
HPLC analysis		
Crocin	0.61407	-0.28918
Safranal	0.51423	0.85245
Picrocrocin	0.59875	-0.43554

Figure 4.2: PCA analysis (biplot) of saffron samples (HPLC analysis)

Objective II

4.2. Synthesis of Molecularly Imprinted Polymer encapsulated with Quantum Dots for detection of Crocin.

The MIPs technique revolves around creating specific binding sites that closely resemble those of the template molecule. Molecularly Imprinted Polymers (MIPs) consist of target samples, functional monomers, and a cross-linker for the polymerization process (Chen et al., 2011). The functional monomer carries an active group capable of interacting with the template molecule through covalent and non-covalent means. Frequently employed monomers include itaconic acid, hydroxy methacrylate, acrylic acid, and acrylamide, among others. The cross-linker aids in the formation of a film-like layer by enveloping the functional groups around the imprinted molecule, leading to the creation of a highly interconnected polymer structure. Various cross-linker7ys such as ethylene glycol, dimethyl acrylate, and divinylbenzene are commonly used in this process.

In this study, MIP-QDs was synthesized for quantifying the crocin concentration in saffron. Crocin, a bioactive compound responsible for vivid color of saffron, necessitates accurate detection to evaluate saffron quality and prevent adulteration. To accomplish this, nanoscale probe using a combination of MIPs and CQDs was synthesized.

4.2.1. Characterization of CQDs, MIP-CQDs and NIP-CQDs

The investigation of the optical characteristics of CQDs involved the use of both UV-Vis and fluorescence spectrophotometers, as depicted in Figure 4.3. In the UV spectrum (Figure 4.3a), absorption peaks were observed for CQDs, primarily attributed to n-p and p-p* transitions initiated by molecular bonds such as C=O and C=C. Figure 4.3a illustrates the photoluminescence spectra, revealing the excitation wavelength-dependent behavior of CQDs. Notably, water-soluble CQDs exhibited fluorescence and emission characteristics dependent on the excitation wavelength.

In Figure 4.3(b), the FTIR spectrum of the synthesized CQDs is depicted. The absorption peak at 3496.8 cm-1 is attributed to the presence of a substantial amount of hydroxyl group (–OH) on the surface of the CQDs. The peaks observed at 2415.7 cm-1 are linked to the stretching vibrations of aliphatic C–H bonds, whereas those at 1644.1 cm-1 and 1210 cm-1 are indicative of C = C bonds within the structure of the CQDs. Furthermore, various functional groups were detected on the CQD surface, commonly found in CQD architecture, contributing to their water

solubility and enabling surface functionalization with other chemical groups/ligands. XPS was employed to investigate the surface chemical composition and element status of CQDs. The XPS spectrum presented in Figure 4.3(c) displays two peaks at 532.3 eV and 286 eV, corresponding to O1s, and C1s, respectively (Shan *et al*, 2019, Delwin *et al*, 2020). This indicates that CQDs are predominantly composed of carbon, and oxygen.

Figure 4.3(d) shows the XRD spectrum of CQDs, which reveals a broad diffraction peak at 18.06° and a weak peak at 25.4°. These peaks suggest that CQDs contain both an amorphous carbon phase and partially graphitized carbon. This is due to the abundance of functional groups present and the graphitization of carbon atoms, respectively. These findings confirm the existence of a graphite structure in the carbon core of CQDs. Taken together, these results indicate that small carbon dots were produced through the hydrothermal synthesis of microcrystalline cellulose with ethylenediamine, and that their carbon core structures are similar to those of graphite.
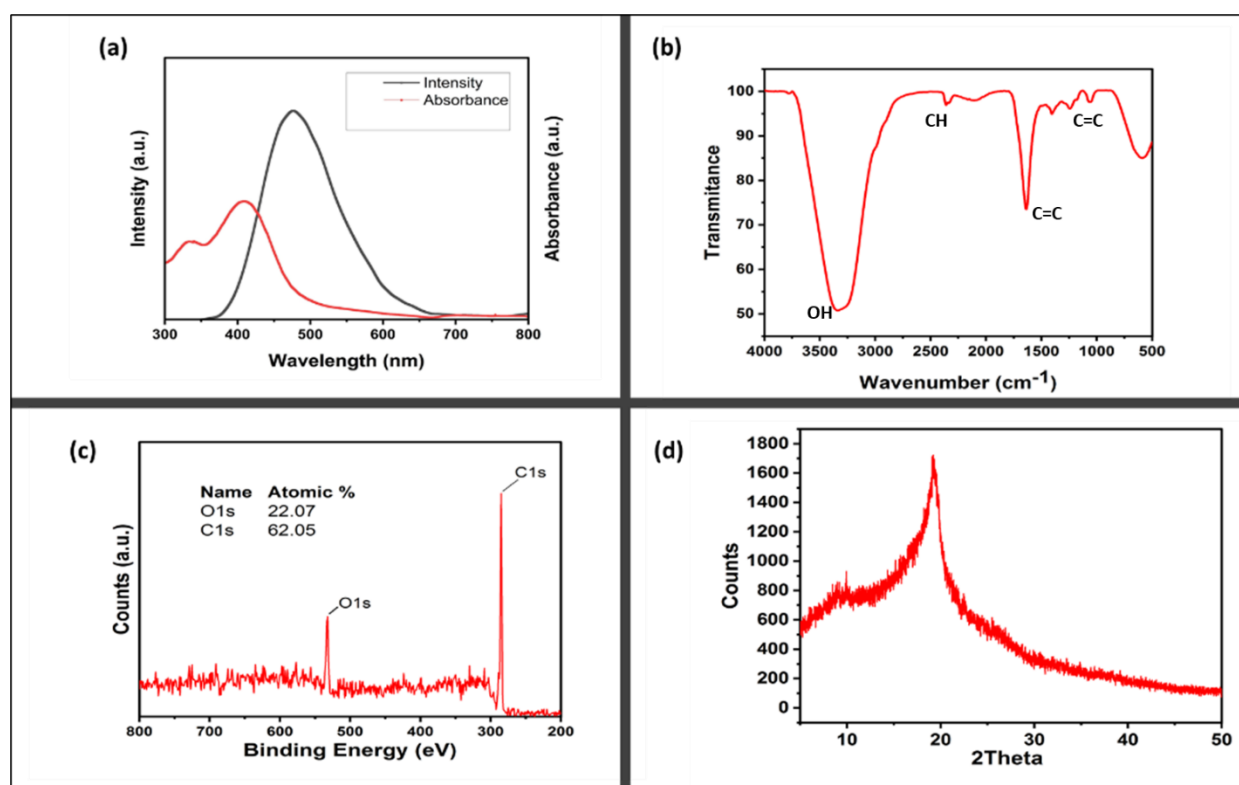

Figure 4.3. Absorption spectra and fluorescence spectra (a), FTIR spectra (b), XPS (c) and XRD (d) of CQDs.

TEM images reveal the synthesized CQDs to be quasi-spherical and monodisperse in structure, with well-separated particles [Figure 4.4 (a)]. The average size of CQDs was found to be 5.4 μM [Figure 4.4 (b)] and zeta potential potential of synthesized CQDs was found to be -04.33

[Figure 4.4 (c)]. Figure 4.5 (a) and.5 (b) depicts SEM of MIP-CQDs and NIP-CQDs respectively. The morphology and the diameter of the MIP-CQDs and NIP-CQDs were found almost similar.
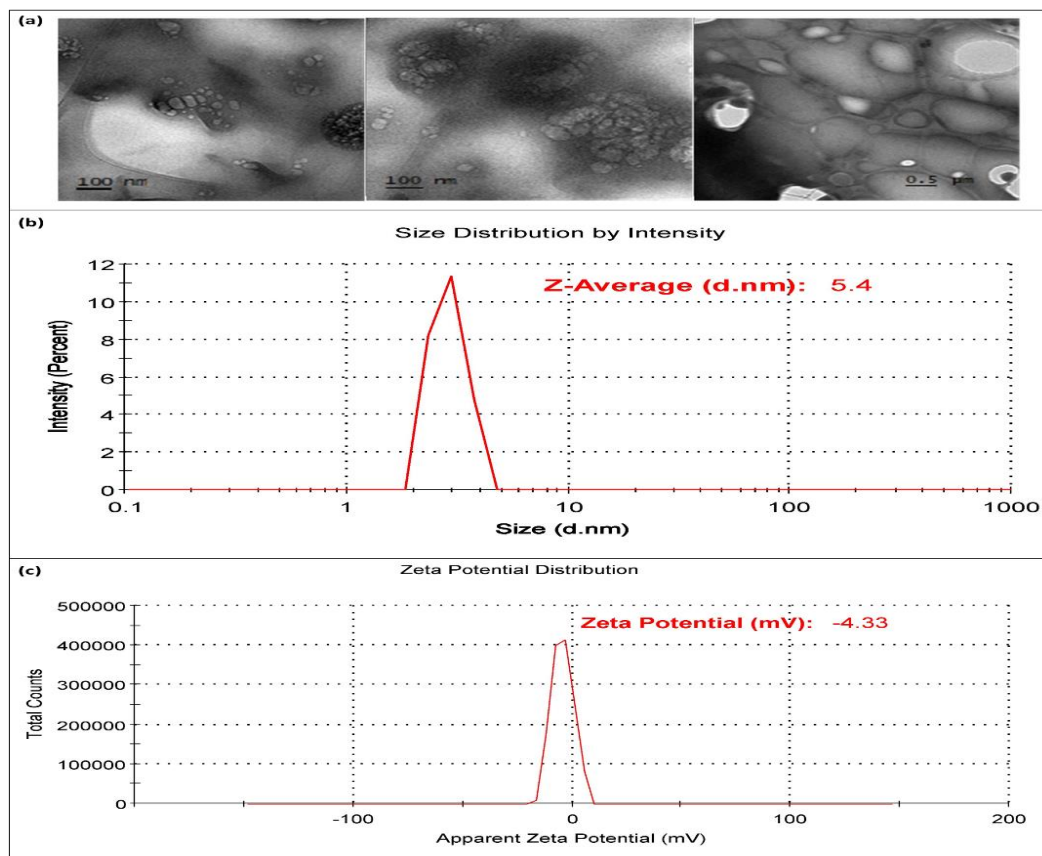

Figure 4.4. TEM images (a), Size distribution (b), zeta potential (c) of CQDs.
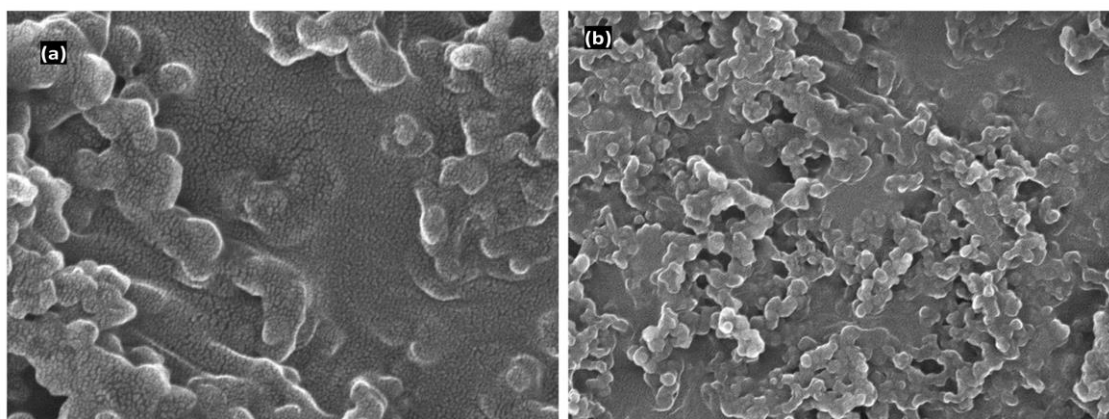

Figure 4.5. SEM image of MIP-CQDs (a) and NIP-CQDs (b).

The Figure 4.6 (a) illustrates the FT-IR fingerprint of MIP-CQDs and NIP-CQDs, providing insights into the successful chemical modifications during each synthesis. Notably, there is a distinct and broad absorption peak at 3394 cm^{-1}, indicating the stretching vibrations of the −OH group. Additionally, a peak at 2990 cm^{-1} corresponds to the CH stretching of aromatic hydrocarbons (sp2 carbon). The bands at 1730 and 1762 cm^{-1} are linked to C−O and C=H stretching vibrations, respectively. The presence of a peak at 1072 cm-1 is associated with the C-O bond. Despite the similarity in absorption peaks between MIP-CQDs and NIP-CQDs FTIR spectra, it implies the successful synthesis of the polymer and the elimination of the template molecule.

In Figure 4.6 (b) and (c), the XRD profile elucidates the nature of MIP-CQDs and NIP-CQDs. The XRD pattern for both MIPs and NIPs exhibit a comparable broad hump around 2θ = 20.4°, corresponds to the C(002) plane. This indicates their akin chemical compositions and the amorphous nature of CQDs. The similarity of the XRD patterns for both MIP-CQDs and NIP-CQDs implied comparable chemical compositions in terms of the carbon quantum dots present within their respective structures. The lack of distinct differences in the XRD patterns suggested that the core structural composition of the carbon quantum dots was consistent between the two types of samples, regardless of whether they were embedded within a molecularly imprinted polymer (MIP) or a non-imprinted polymer (NIP).
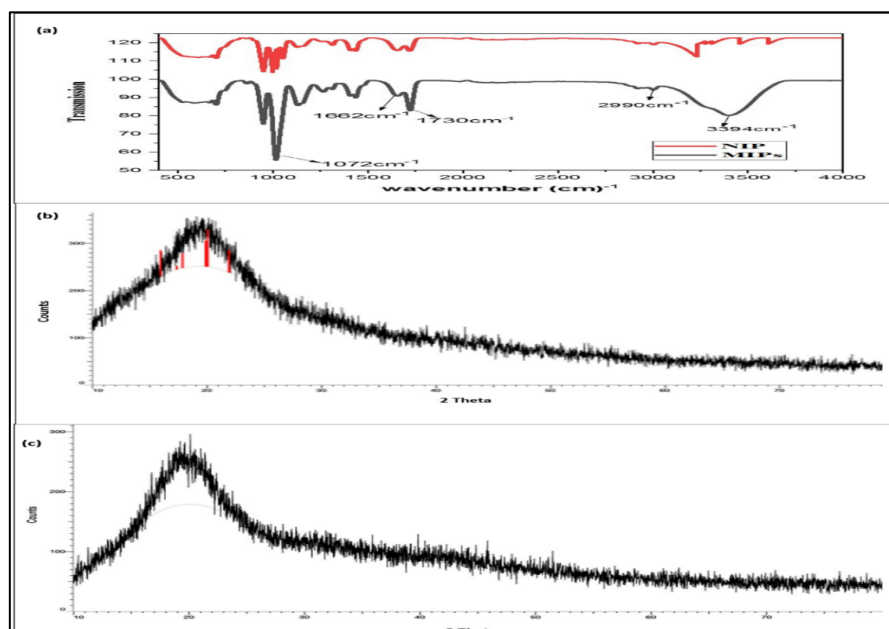

Figure 4.6. FTIR spectra of MIP-CQDs and NIP-CQDs (a), XRD of MIP-CQDs (b) and XRD of NIP-CQDs.

4.2.2. Interaction between Crocin and the FL probe

The performance evaluation of the newly developed nanosensor was conducted under optimal conditions. Different concentrations of crocin were introduced to MIP-CQDs and NIP-CQDs during a calibration series, and their fluorescence spectra were recorded (Figure 4.7). The CQDs-MIP demonstrated a significant response within a linear range of 0.2 to 175.0 μM, achieving a limit of detection (LOD) of 2.1 μM (Figure 4.7). The determination coefficient (R^2) values for CQDs-MIP and CQDs-NIP were found to be 0.995 and 0.991, respectively. Notably, the calibration curve slope for CQDs-MIP surpassed that of CQDs-NIP, indicating higher sensitivity of CQDs-MIP (Figure 4.8). This optical nanosensor, proposed for crocin trace analysis, exhibited high sensitivity with a low LOD. Fluorescence measurements for each crocin concentration were replicated five times, yielding a relative standard deviation of less than 2.9%. The quenching of fluorescence in MIP-CQDs is explained by the interaction between the crocin molecule and the functional hollow spaces. An examination of the the fluorescence emission spectrum of CQDs-MIP and UV-Vis absorption spectrum of crocin showed a significant overlap, indicating a fluorescence quenching process similar to Forster Resonance Energy Transfer (FRET) (Yang *et al*., 2017).
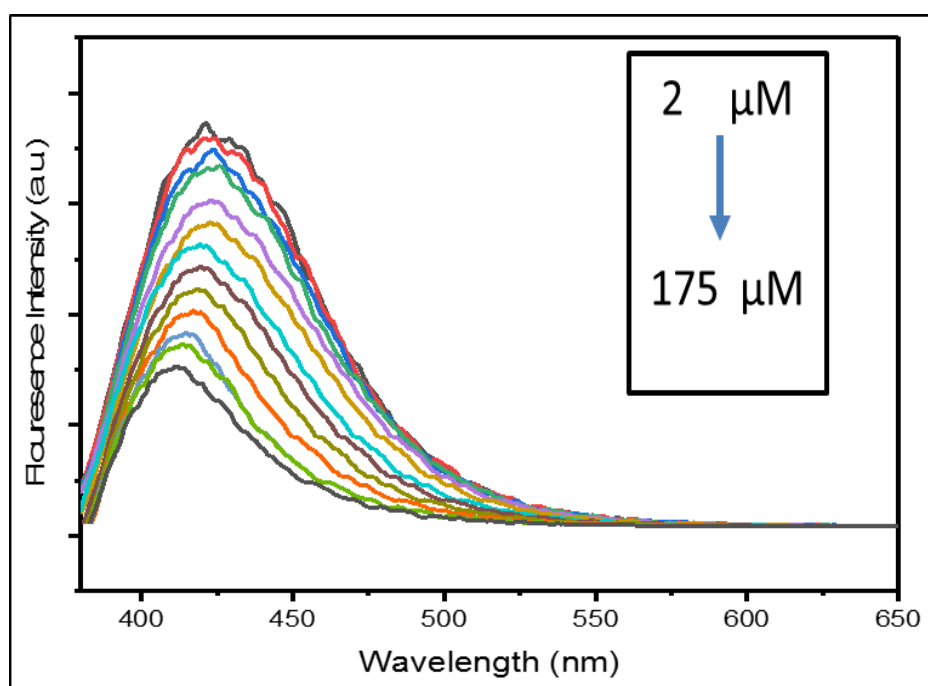

Figure 4.7- Interaction of different concentration of crocin with MIP-CQD sensor
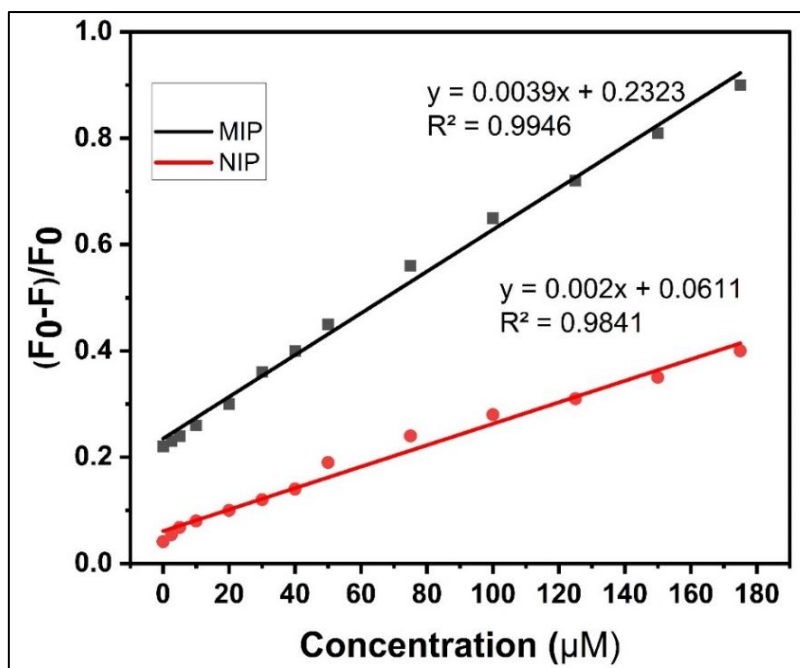
Figure 4.8- Linear range of MIP-CQDs and NIP-CQDs towards crocin

4.2.3. Optimization of parameters

The FL intensity of the nanocomposite comprising MIP-CQDs was investigated under pH range spanning from 5.0 to 9.0 (refer to Figure 4.9(a)). Briefly, 0.1 g of MIP-CQDs was dispersed in 100 ml of BR buffer for 2 hours, with the constant Crocin concentration maintained consistently for all measurements. The responsiveness of the nanosensor declined in both acidic (pH less than 7.0) and basic (pH greater than 8.0) environments. The decline in intensity under basic conditions was ascribed to a reduction in interactions between vacant sites and crocin molecules, whereas the reduction in acidic conditions was attributed to disruption in hydrogen bonding. In pH values surpassing 7, surface defects stemming from the silica layer's ionization likely led to a decrease in quenching. Consequently, a neutral pH of 7.0 was identified as the optimal condition for all measurements.

The duration for the MIP-CQDs nanocomposite to efficiently adsorb crocin was determined by gauging the reduction in fluorescence intensity (Figure 4.9(b)). The optimal conditions entailed a pH 7.0, a crocin concentration of 10.00 μM, and a temperature of $27 \pm 1\ ^0C$. The incubation time ranged from 01 to 10 minutes, with the most substantial quenching observed after 05 minutes, thus establishing 05 minutes as the optimum incubation time for crocin analysis.

75

The efficacy of the developed nanosensor in crocin measurement was assessed by examining its selectivity towards alternative compounds like safranal and picrocrocin (Figure 4.9(c)). The formulation of CQDs-MIP engendered specific binding sites on the imprinted polymer, mirroring the size, shape, and spatial arrangement of the crocin molecule. This similarity facilitated better occupancy of binding sites by crocin, resulting in a more pronounced decline in fluorescence intensity compared to its analogs. NIP-CQDs, on the other hand, exhibited negligible fluorescence quenching for crocin and other compounds, signifying poor binding between crocin and NIP-CQDs. The influence of coexisting ions on the nanosensor's performance was also scrutinized by assessing crocin detection in the presence of interfering ions (Fructose, Glucose, Fe^{3+}, Na^+, Ca^{2+}, K^+, NaCl, KCl, and Zn^{2+}) (Figure. 4.9(c)). The findings indicated that the presence of foreign ions did not significantly impact the fluorescence quenching of the probe during crocin detection.

A neutral pH of 7.0 was identified as the optimal condition for detection purposes and an incubation time of 5 minutes was found to be most effective for the adsorption of crocin onto the MIP-CQDs nanocomposite. Moreover, the nanosensor's performance remained unaffected by the presence of various co-existing ions commonly found in complex solutions. This robustness ensures accurate crocin detection even in the presence of potential interfering species. Therefore, the synthesized MIP-CQDs nanocomposite holds promise as a sensitive and specific nanosensor for crocin detection. The combination of optimal pH and incubation time, selectivity for crocin, and resistance to interference from co-existing ions highlights its potential application in real-world scenarios where precise detection of crocin is crucial. This research underscores the significance of nanocomposite design and its potential contribution to the field of molecular sensing and detection.
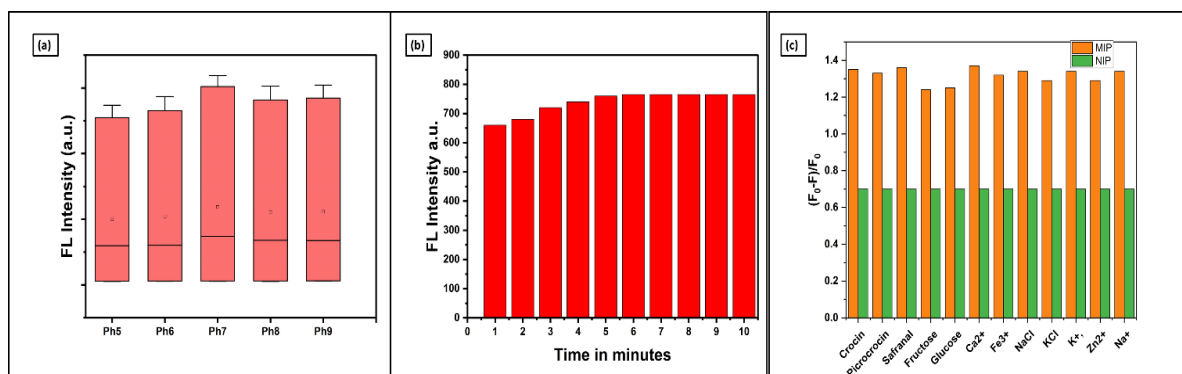

Figure 4.9- The effect of pH on the fluorescent intensity of MIP-CQDS (a), fluorescent responses of MIP-CQDs in the presence of crocin at different intervals of time (b), and selectivity of NCQDS towards crocin in the presence of interfering substances (c)

4.2.4. Analysis of crocin in saffron sample

To determine the crocin concentration in real samples of saffron from three different geographical locations, fluorescence spectra were obtained. The recovery percentage of the samples were found to be 98.6 to 99.02% (Table 4.5). Therefore, it is evident to say that the NIP-QDS can be used as an ideal candidate for the detection of crocin in saffron samples.

Table 4.5- Quantitative measurement of crocin in saffron using MIPs-NCQDS

Sample	Added (μM/L)	Final found value (μM/L)	Recovery (%)	RSD (%)
Saffron	00	45.82 ± 0.04	99.2	1.8
	00	42.50 ± 0.04	99.0	1.2
	00	48.80 ± 0.05	98.6	1.4

4.3. Development of nanomaterial-based methods for quantification and detection of various adulterants in saffron

4.3.1. Colorimetric detection of crocin in saffron based on formation of gold nanoparticle

4.3.1.1. Characterization of AuNPs

The X-ray diffraction analysis was used to confirm the crystalline size, structure, and phase purity of the synthesized AuNPs. Figure 4.10(a) depicts the XRD pattern of AuNPs. The four unique diffraction peaks of 2θ values at 38.2°, 44.4°, 64.1°, and 77.6° corresponds to 111, 200, 220, and 311. It shows that the AuNPs produced are crystalline in form. This result corresponded to JCPDS file no. 04-0784. The peak produced by (111) reflection was more intense than the other peaks, indicating that the crystallite size of AuNPs was oriented primarily along the (111) plane. The XRD analysis played a pivotal role in substantiating the crystalline characteristics, crystallographic orientations, and phase purity of the synthesized AuNPs. The distinct diffraction peaks and their intensities not only confirmed the crystalline form of the nanoparticles but also shed light on their predominant growth orientation along the (111) plane, contributing to a deeper understanding of their structural attributes.

The FTIR spectrum of gold nanoparticles is shown in Figure 4.10(b). The spectrum displayed distinct absorption bands located at specific wavenumbers, notably at 586, 1636, 2136, and 3306 cm^{-1}. The presence of aromatic compounds on the surface of the nanoparticles was notably indicated by the detection of a subtle overtone band at 2136 cm^{-1}. This overtone band was indicative of the existence of certain chemical moieties associated with aromatic rings, pointing towards the involvement of aromatic compounds in the nanoparticle's surface structure. A particularly noteworthy feature was the peak spanning the range between 1,500 and 1,700 cm^{-1}. This peak was a characteristic signature of the C=O stretching frequency, which is often attributed to carbonyl groups present in various chemical entities. The prevalence of this peak in the FTIR spectrum signified the presence of carbonyl functional groups, further substantiating the involvement of certain chemical species on the nanoparticle's surface. Additionally, the bands positioned around 3306 cm^{-1} held significance in relation to the FTIR spectrum. These bands were associated with the presence of hydroxyl functional groups, commonly found in alcohols and phenol derivatives. The detection of these bands within the FTIR spectrum provided evidence of the presence of hydroxyl groups on the AuNPs, shedding light on specific chemical functionalities incorporated into the nanoparticle's surface.

The FTIR spectrum of the generated gold nanoparticles served as a powerful tool to unveil the molecular constituents on the nanoparticle's surface. The various absorption bands at distinct wavenumbers revealed the presence of aromatic compounds, carbonyl groups, and hydroxyl functional groups, collectively contributing to a more comprehensive understanding of the chemical makeup and surface properties of the synthesized AuNPs.
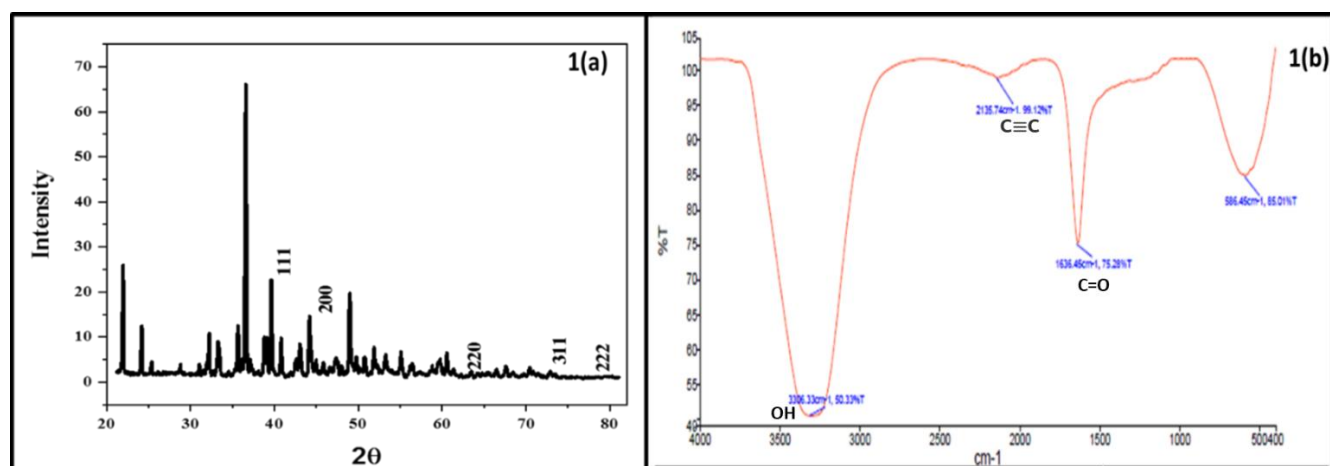

Figure 4.10. XRD (a) and FTIR (b) of Gold nanoparticles

The characterization of the structure and morphology of the AuNPs was accomplished through FE-SEM analysis, which provided valuable insights into the geometric attributes of the synthesized nanoparticles. In Figure 4.11(a), the acquired images vividly illustrated that the AuNPs exhibited a distinctive triangular and cube-like geometry, showcasing intriguing and visually captivating shapes. However, it's worth noting that these nanoparticle forms were not perfectly regular and displayed some degree of irregularity, adding an element of complexity to their morphological characteristics.

For elemental identification and distribution analysis, EDAX (Energy Dispersive X-ray Analysis) was employed. This technique allowed for the determination of the elemental composition within the synthesized material. In the context of the present study, the focus was on identifying the presence of gold nanoparticles. Figure 4.11(b) presented the EDAX spectrum, which unequivocally showcased the existence of gold within the analyzed nanoparticles. This spectrum provided a clear visual representation of the elemental distribution, confirming the successful synthesis of the desired gold nanoparticles.
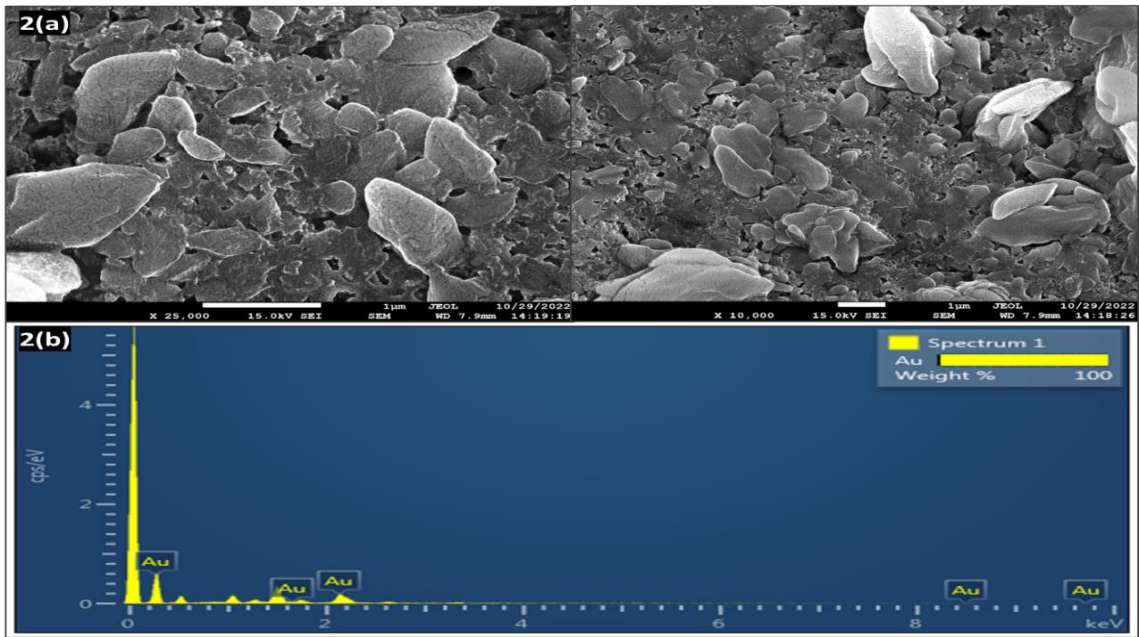
Figure 4.11. SEM (a) and EDX (b) of Gold nanoparticles

The zeta potential of gold nanoparticles was investigated. The zeta potential technique was used to assess particle charge and size. Nanoparticles having zeta potential values more than +25 m V or less than -25 m V are known to be highly stable. The as synthesized AuNPs showed slightly less zeta potential values -25m V [figure 4.12(a)], and size 50.10 nm [figure 4.12(b)] implying that they are highly stable. The zeta potential of the gold nanoparticles provided valuable information regarding their charge, size, and overall colloidal stability. The observed slightly less zeta potential values around -25 mV and the measured size of 50.10 nm underscored the high stability of the synthesized AuNPs, attributed to the repulsive forces generated by the negative charge of the particles and the well-defined size that contributed to the prevention of agglomeration and enhanced dispersion within the solution.
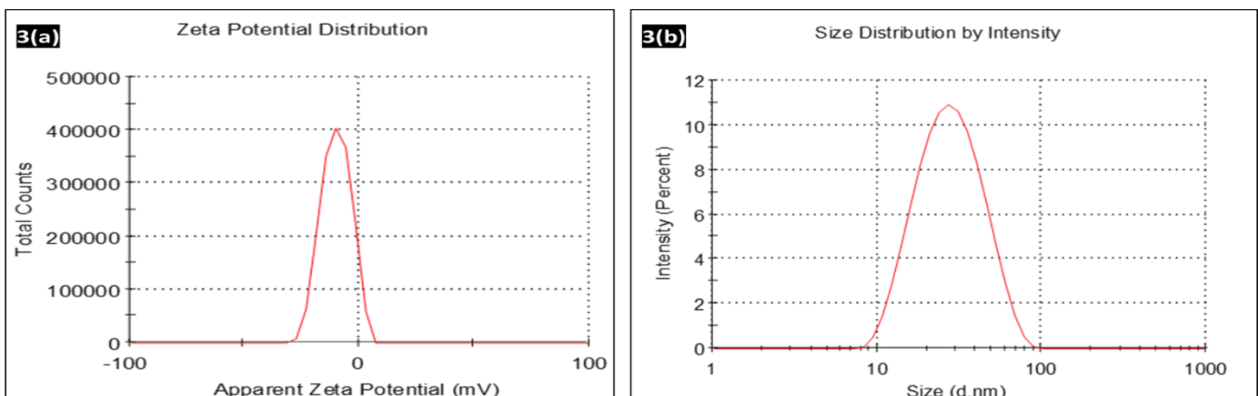

Figure 4.12. Zeta potential (a) and size distribution (b) of Gold nanoparticles

4.3.1.2. Optimization

The synthesis of AuNPs was performed under varying concentrations of $HAuCl_4$ (0 to 50 mM) and crocin concentration constant [Figure 4.13(a). It was found that at concentration of 20mM $HauCl_4$ the AuNPs were stable and given maximum yeild. Therefore, this concentration was selected as an optimal concentration of both the chemicals for the synthesis of AuNPs. The synthesis of AuNPs was performed at different pH (2-10) in order to find an optimum pH for the maximum yield of NPs. The production of gold nanoparticles was most favored at alkaline pH. and lateral size of the nanoparticles created was roughly 50 nm. At lower pH, UV-vis spectroscopy of the reaction mixture revealed only the $HAuCl_4$ absorption band at 300 nm, suggesting that no reduction was feasible at acidic pH even after a day of reaction (based on UV/visible spectroscopic observations. Maximum yield of NPs was produced at Ph. 10 [Figure 4.13(b)] with average diameter of 50 nm in size.

Figure 4.13(c) depicts the influence of reaction temperature on the production of gold nanoplates. At 40 ^0C, well-defined yield of AuNps was obtained. The reducing agents crocin, which are easily destroyed by temperature increase and increased nucleation at higher temperatures, explains the synthesis process of AuNPs using Crocin as reducing agent.

The kinetics of AuNPs production in the $AuCl_4$ reaction was investigated by altering the reaction time. At the very early stage of the reaction, the production of Au nanoparticles begins to form and the concentration of the gold nanoparticles increased upto 6 hours then remained constant. Therefore 6 hour incubation time was taken as optimum time for the synthesis of gold nanoparticles. [Figure 4.13(d)].

AuNPs were synthesized using crocin as a reducing agent under different conditions, and color intensity of synthesized NPs was been monitored by UV-vis spectroscopy. The approach to detect the concentration of crocin is based on the intensity of AuNPs, which were synthesized using crocin itself as a reducing agent. While crocin is a reducing agent, its ability to reduce gold at room temperature is limited and is accelerated by heating. It was observed that gold reduction by crocin is more effective in a basic pH environment. Based on this, AuNPs were synthesized in an alkaline medium at pH = 10 and 40 °C. It was found that all the spectra of the gold nanoparticles synthesized with different crocin concentrations for a fixed time interval of 40 minutes display the same plasmonic band, with the maximum intensity at 532 nm, and the pink color of the nanoparticles varied across all concentrations. The data demonstrate that increasing the crocin concentration leads to an increase in the plasmon band absorbance

without any shift in wavelength, which enables a relationship between the analyte concentration and the absorbance at a single wavelength to be established.
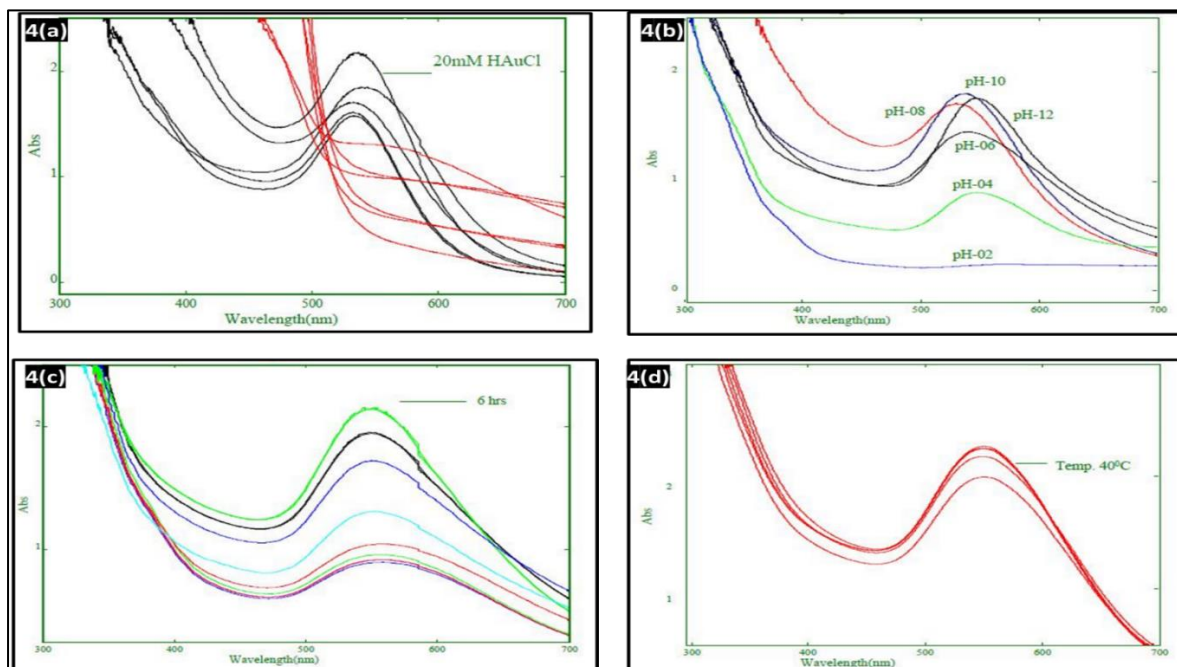
Figure 4.12. Concentration (a), pH (b), Time (c) and Temp optimization of Gold nanoparticles

The absorbance of the AuNPs solution increases with increasing crocin concentration as can be seen in figure 5(a) and 5(b) with LOD of 1.69 mM. This method is suitable for determining the presence of all crocin in many saffron or saffron containing products by determining the coloring strength of synthesized pink colored AuNP solutions.
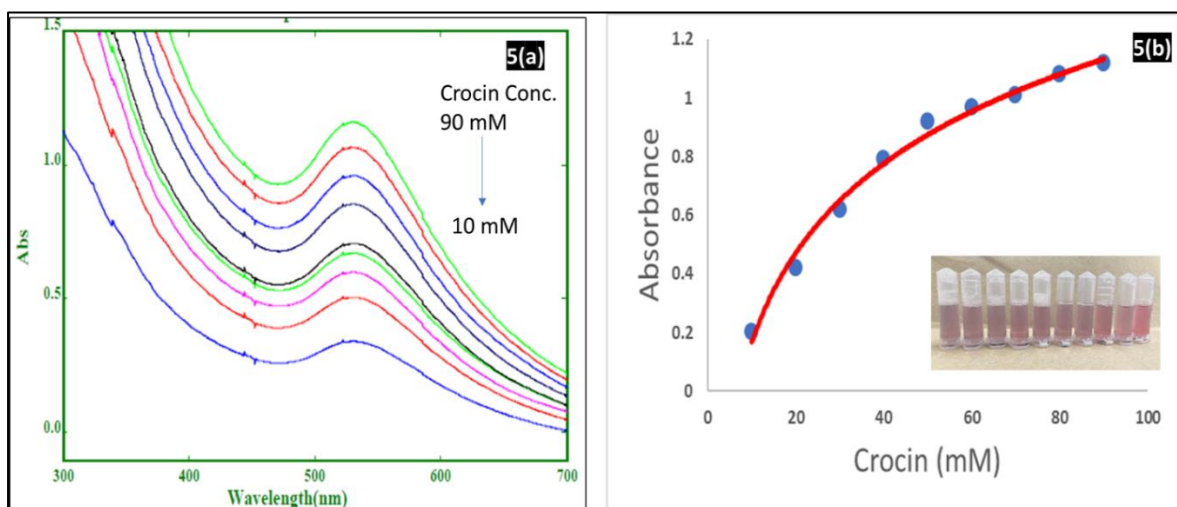
Figure 4.13. Gold nanoparticle synthesis at different concentration of crocin (a) and Absorption of Gold nanoparticle synthesis at 530 nm.

4.3.1.3. Detection in real saffron samples

In order to evaluate the analytical applicability of the proposed assays to real sample analysis, they were applied to the determination of total crocin content in saffron. Saffron extract of different concentrations in water (0.5 mg-100 mg/ml) were prepared and Uv-Vis spectra was recorded. It was found that with the decrease in the concentration of saffron extract, the color intensity also decreased, which was confirmed by UV spectrophotometer. The results showed a recovery range of 98.28-99.12%, as shown in Table 4.6.

Saffron extract with different levels of adulteration with safflower (0%-100%) were also used for the synthesis of nanoparticles. It was found that samples with higher concentration of adulteration lowered the NP synthesis as the adulteration levels increased [figure 14]

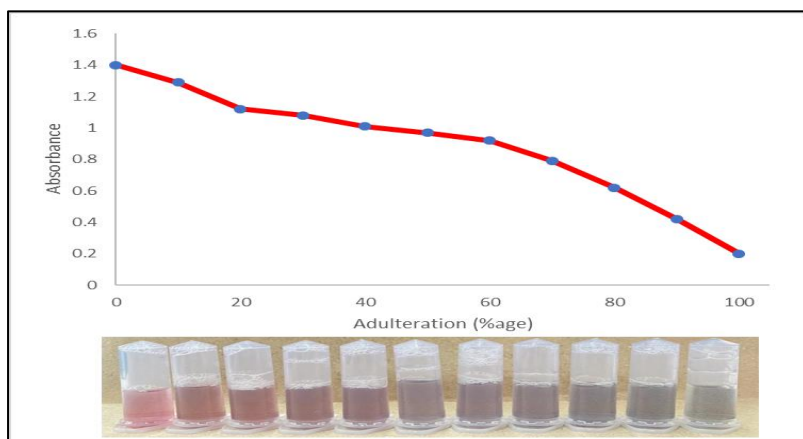Figure 4.14. Gold nanoparticle synthesis at with different levels of adulteration (0% to 100%)

.

Table 4.6. Recovery range of Crocin using gold nanoparticles

Saffron extract mg/ml	Crocin found (mg)	Recovery (%)	RSD (%)
0.5	1.74	98.28	1.8
10	2.95	98.85	1.2
20	5.36	98.66	1.4
30	7.12	98.33	1.6
40	8.48	98.94	1.7
50	9.26	99.12	1.9

4.4. Microwave-assisted Synthesis of N-Doped Carbon Quantum Dots for Detection of Methyl-Orange in Saffron

4.4.1. Characterization of NCQDs

The fluorescence emission characteristics of NCQDs are wavelength dependent. Excitation-dependent fluorescence spectra are produced by the surface state emissive trap when different excitation wavelengths are used. As the excitation wavelength increases from 280 to 440 nm, the emission peaks move from 355 to 498 nm (Figure 4.15). Furthermore, at 340 nm of excitation, the emission intensity reached maximum.
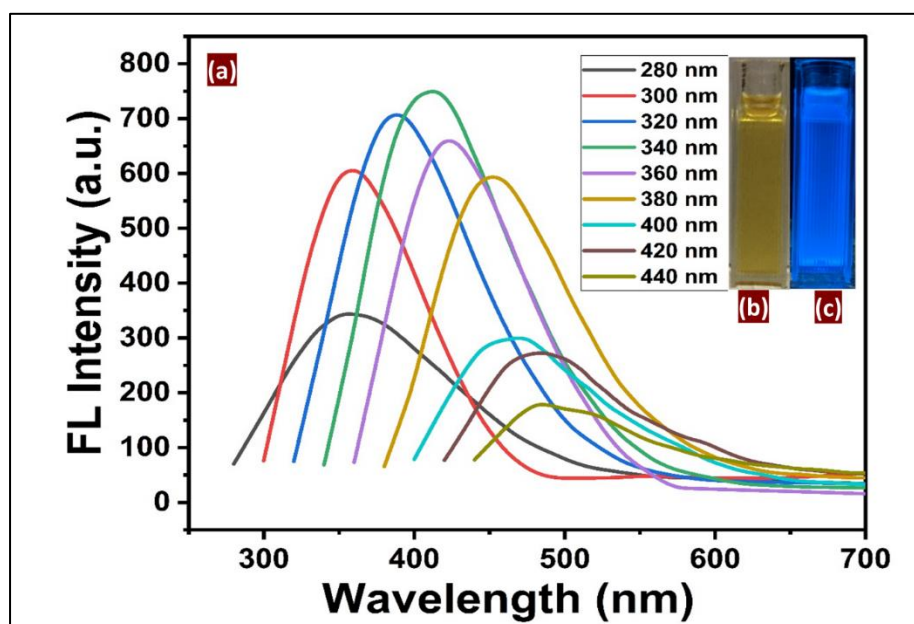
Figure 4.15- The fluorescence spectra NCQDs excited from 280 to 440 nm (a). NCQDs under visible light (b) and UV light (c)

The FTIR spectra of N-doped carbon quantum dots (NCQDs) yield valuable insights into their molecular composition and structural attributes. Figure 4.16(a) displays distinctive absorption peaks at specific wavenumbers, unraveling significant details about the chemical functionalities present within the NCQDs. Firstly, the absorption peak located at 1636 cm^{-1} is a key feature of the spectrum, corresponding to the C=O stretching vibration. This peak signifies the presence of carbonyl groups within the NCQDs, indicating the involvement of oxygen-containing functional groups in the molecular structure. This finding is consistent with the FTIR spectroscopy's ability to identify specific chemical bonds within the material.

The subsequent absorption peak observed at 2945 cm^{-1} is attributed to C-H stretching vibrations. This signal highlights the presence of carbon-hydrogen bonds, underscoring the

carbon-rich nature of the quantum dots and further characterizing their chemical composition. Likewise, the absorption peak at 3340 cm^{-1} corresponds to O-H stretching vibrations. This peak is indicative of hydroxyl functional groups present within the NCQDs, contributing to their surface properties and potential interactions with other molecules.

The narrower peak situated at 1404 cm^{-1} is attributed to the in-plane deformation of O-H bonds. This peak further confirms the presence of hydroxyl groups within the NCQDs and provides information about their structural arrangement. Additionally, the spectrum features a peak at 1066 cm^{-1}, which is attributed to the C-O stretching vibration of the C-O-C bond. This peak is a distinctive marker of ether groups, suggesting the incorporation of oxygen-containing moieties into the NCQD structure. Interestingly, the spectral region between 1210 and 1636 cm^{-1} encompasses numerous distinct bands that are associated with stretching vibrations unique to CN bonds. These bands are indicative of the presence of carbon-nitrogen bonds within the NCQDs, suggesting the successful doping of nitrogen atoms into the carbon framework.

The FTIR spectrum of NCQDs provides a comprehensive picture of their molecular composition and functional groups. The absorption peaks at specific wavenumbers reveal the presence of carbonyl, hydroxyl, and ether functional groups, as well as carbon-hydrogen and carbon-nitrogen bonds. These findings collectively contribute to a deeper understanding of the structural attributes and potential applications of N-doped carbon quantum dots.

In order to perform XRD analysis, the as-prepared NCQDs was drop-coated onto a glass sheet (1×1 cm^2), and the analysis was performed. Figure 4.16(b) depicts typical XRD patterns for as-prepared NCQDs. In the XRD patterns, a wide peak centered at around 21.02^0 can be seen, which is almost similar to the graphite lattice spacing (20.73^0). This lattice contraction in the above-mentioned range is typical for nanomaterials in the nanoscale domain, and it is most likely owing to the microwave process creating abundant active sites on the surface of NCQDs. Furthermore, XRD results confirm the 3.5 A lattice spacing. This lattice spacing metric offers a tangible measure of the interatomic distances within the crystalline configuration, serving as a corroborative indicator of the nanoscale arrangement of carbon and nitrogen atoms within the quantum dots. The discernment of this specific lattice spacing further solidifies the successful integration of nitrogen into the carbon framework of the NCQDs, confirming the deliberate doping process's effectiveness and precision.

Electrophoretic light scattering was used to determine the zeta potential of the dispersed NCQDs. Electrophoretic light scattering revealed that the zeta potentials of NCQDs were -

3.4mV (Figure 4.17(a). Each sample was subjected to comparable zeta potential and particle size distribution measurements. The zeta potential represents not only the electrical charge on the particle surface but also the stability of colloidal dispersions. The average particle size of NCQDs was found to be approximately 6 nm (Figure 4.17(b). The results of the particle size distributions agree with the zeta potential measurement.
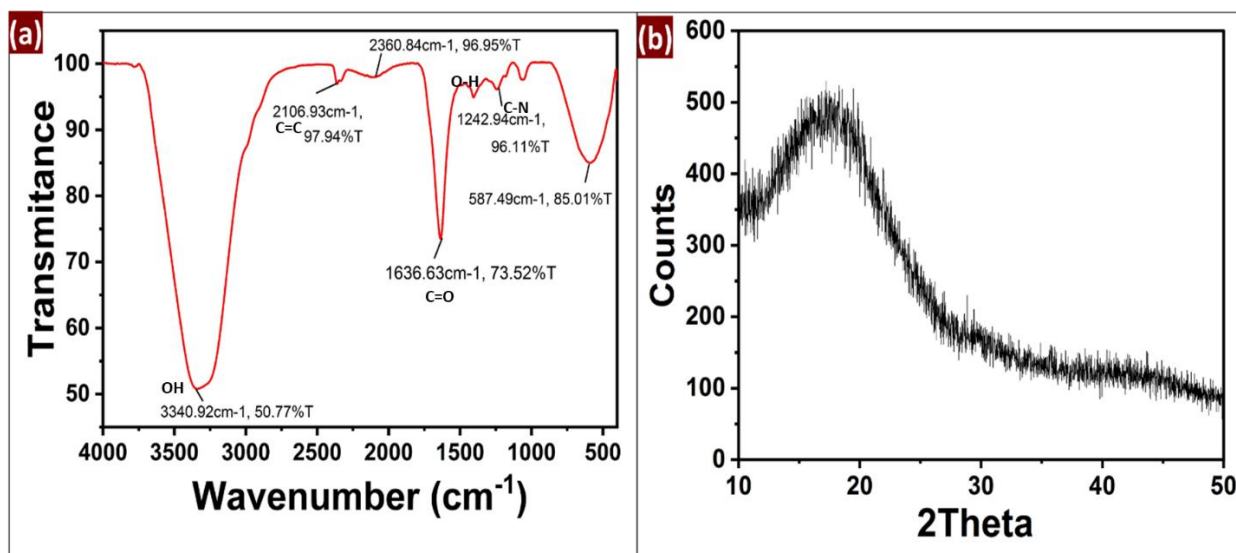
Figure 4.16- FTIR (a) and XRD (b) of NCQDs

TEM observations were used to determine the size and morphology of the prepared NCQDs. Figure 4.17(c) demonstrates that the samples are made up of a large number of spherical nano-dots with an average diameter of 6 nm. The enlarged TEM images in Figure 4.17(c) show that the quantum dots' average lateral dimension is less than 10 nm. As illustrated in Figure 4.17(d), the statistical size distribution of NCQDs shows that the size falls within the range of 3-10 nm with maximum distribution at 6 nm.
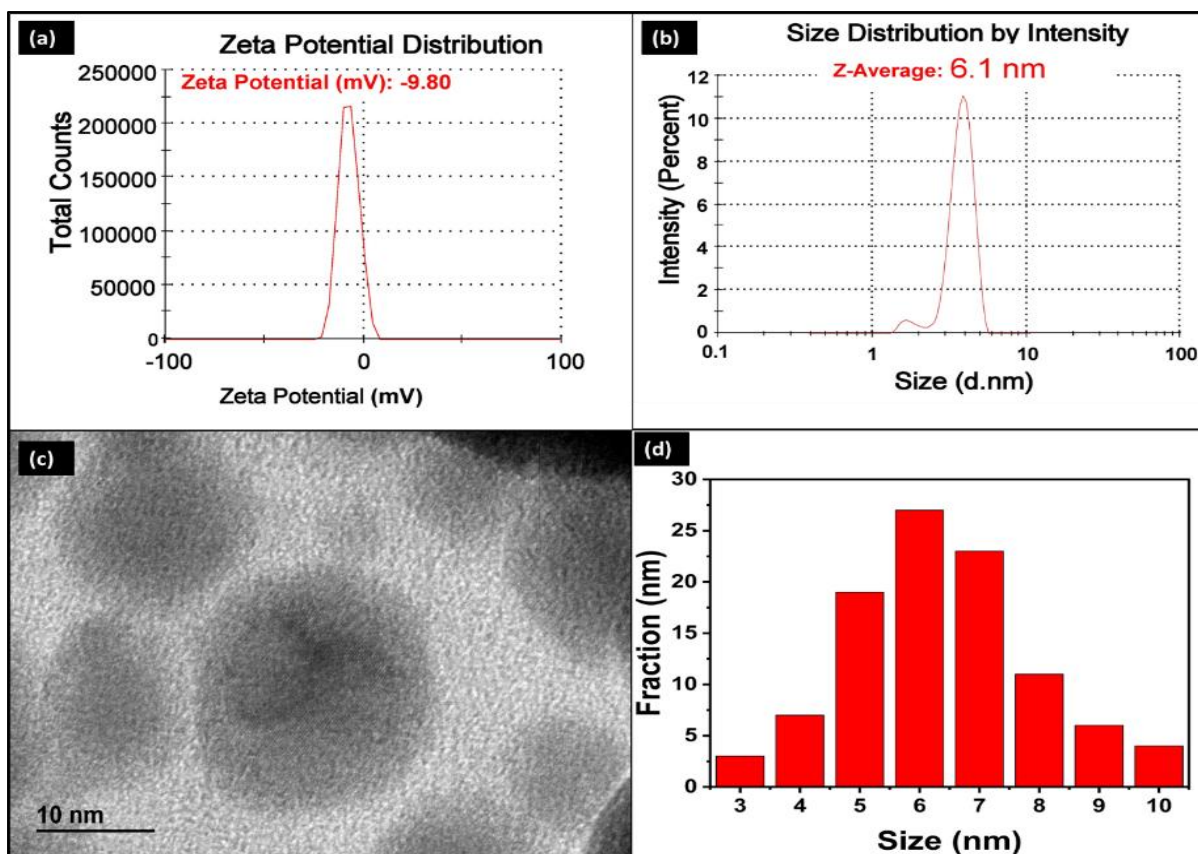
Figure 4.17-Zeta potential distribution (a), size distribution (b), TEM (c) and size distribution (d) of NCQDs

XPS was used to investigate the chemical composition and structure of the N-CDs (XPS). Figure 4.18(a) depicts a general overview of the N-CD XPS spectrum. O1s, N1s, and C1s were assigned strong binding energy peaks at 284.53, 531.24 and 399.34 eV, respectively. The N-CDs were made up of C (62.05%), N (15.88%), and O (22.07%). Moreover, in the high-resolution spectrum of C1s, two peaks at 283.14 and 287.81 eV were attributed to C-C, and C=N/C=O bonds, respectively (Figure 4.18(b)). Two central peaks in the O1s spectrum (Figure 4.18(c)) at 530.29 and 532.54 were attributed to C-O and C=O/N=O, respectively. Two notable peaks at 399.55 and 401.1 eV in the N1s spectrum were assigned to N-$(C)_3$ and O=N-C, respectively Figure 4.18(d). The XPS spectrum showed that the NCDs were composed of three different elements: carbon, nitrogen, and oxygen. Additionally, the surface of the NCDs had several oxygen-containing groups as well as nitrogen groups.
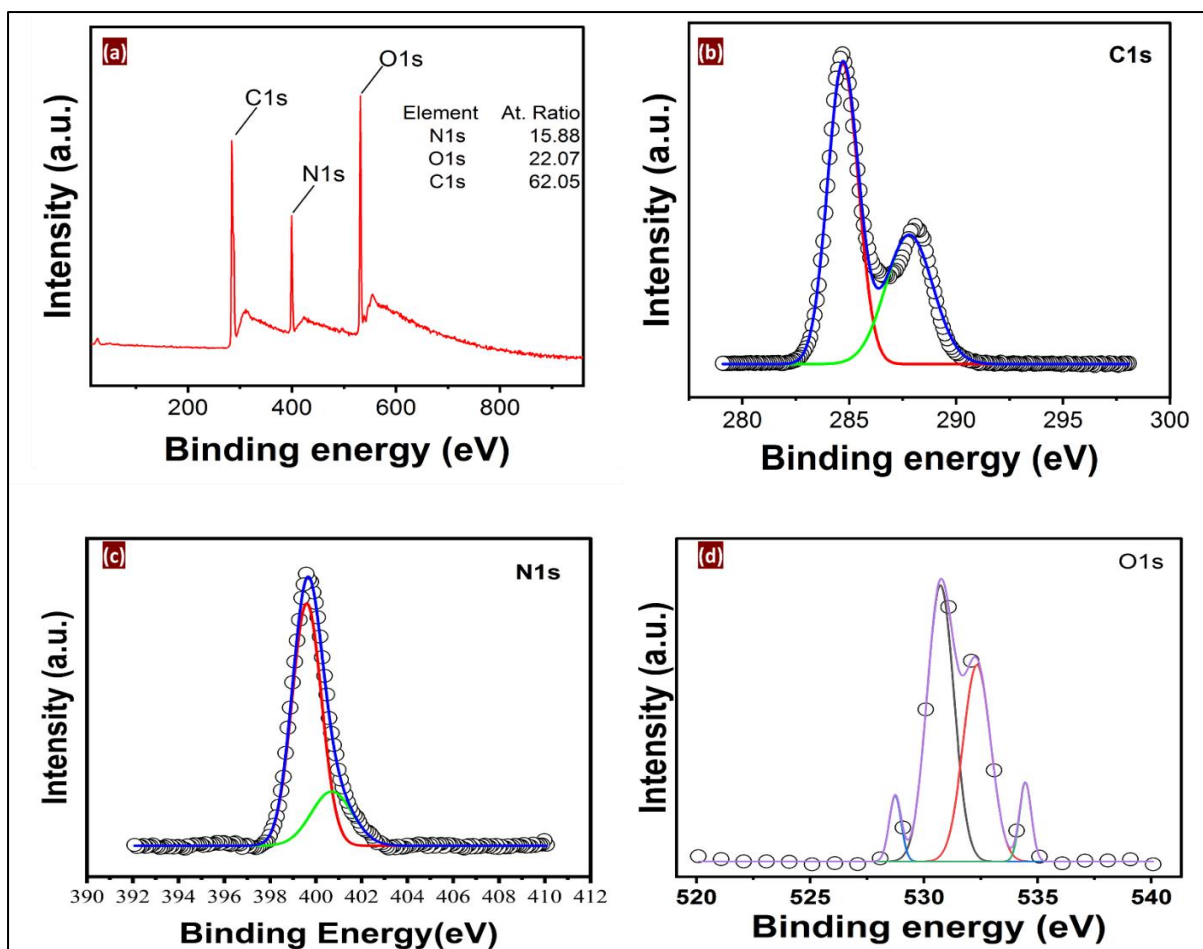
Figure 4.18- XPS full scan of NCQDs (a), High-resolution XPS spectrum of C 1s (b), N 1s (c) and O 1s

4.4.1.1. Effect of MO on the FL intensity of NCQDs

The FL intensity of NCQDs under the influence of different concentrations of MO (02 μM-200 μM) was carried out. It is evident from Figure 4.19 that the FL intensity of NCQDs decreases with the increase in the concentration of MO. The FL quenching of NCQDs with different concentrations of MO is due to charge transfer or energy transfer between the fluorophore and the quencher. Charge transfer occurs between the quencher and the excited molecule of the fluorophore. Energy transfer can occur if the fluorophore's fluorescence emission spectra and the quencher's UV absorbance spectra significantly overlap or the distance between the two is very small, often less than 10 nm. The fluorescence maxima of NCQDs can be seen at 425 nm after an excitation wavelength of 340 nm, and the maximum absorption wavelength of MO can be seen at 475 nm. It can be seen that the spectra of the two are effectively overlapped, as shown in Figure 4.20(a). Therefore, it is evident to say that the fluorescence quenching of MO on NCQDs is due to energy transfer between them.

88
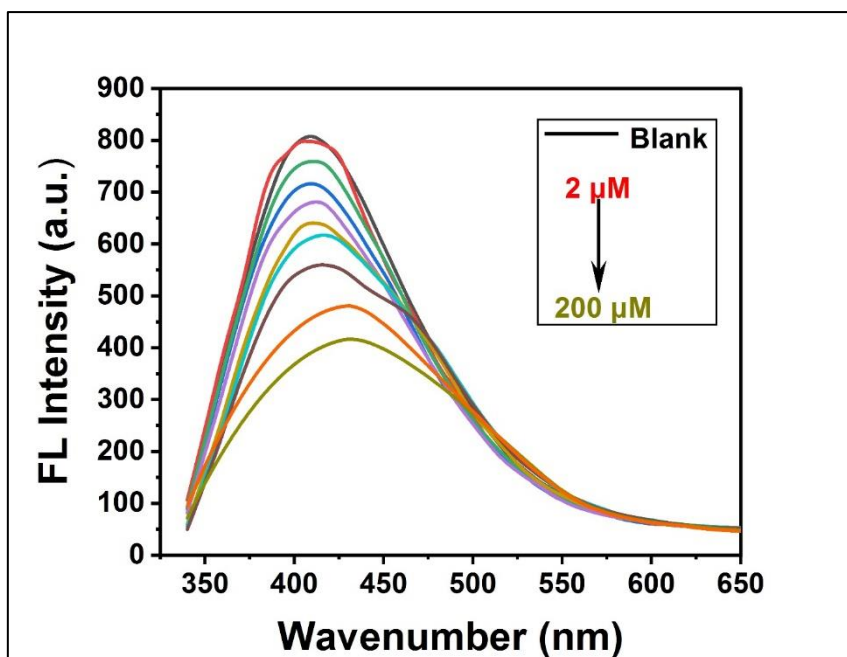
Figure 4.19- Fluorescence spectra of NCQDs in the presence of different concentrations of MO (2-200 μM)

4.4.1.2. Optimization

The effect of pH in the range of 4-10 on the FL intensity of NCQDs was investigated (Figure 4.20(a)). It was found that pH impacts the FL intensity of the NCQDs solution. While the relative FL intensity values (F_0/F) essentially remained constant throughout the entire pH range, the emission of NCQDs solution increased with the increase in pH from 4 to 8 and then decreased from 8 to 10 (Figure 4.20(b)). Therefore, pH 8 was selected as the ideal solution pH for further studies. The effects of several buffer systems, including phosphate buffer, Britton-Robinson (B-R), and Tris-HCl on F_0/F was then investigated at pH 8. Results showed that, the phosphate buffer was the most effective buffer. Additionally, the impact of incubation time on the value of FL intensity was investigated. At normal conditions, the incubation time was optimized by measuring the FL intensity of NCQDs and MO solution (pH 8) every 5 minutes. The maximum FL intensity value was attained after 15 minutes and remained almost steady for 60 minutes, as shown in Figure 4.20(c). As a result, the ideal incubation time for FL intensity was tested 10 minutes later.
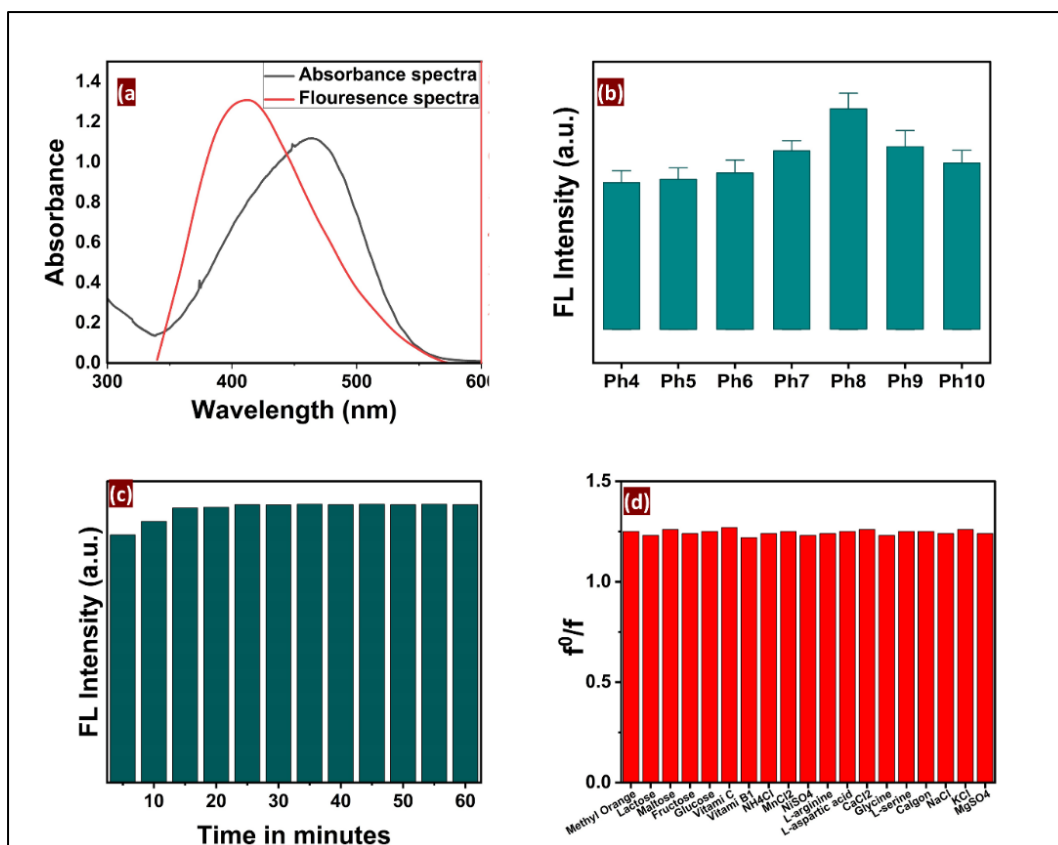
Figure 4.20- Overlap between a fluorescence spectrum of NCQDs and absorption spectrum of MO (a), the effect of pH on the fluorescent intensity of NCQDS (b), fluorescent responses of NCQDs in the presence of MO at different intervals of time (c), and selectivity of NCQDS towards MO in presence of interfering comounds (d)

To assess the specificity, the effects of some potential interfering substances L-tryptophan, L-serine, L-threonine, vitamin C, vitamin B_6, vitamin B_1, $CuCl_2$, $MgSO_4$, $NiSO_4$, NaCl, and KCl were examined. Results were obtained by combining 20.0 mmol/L of MO with NCQDs alone and 22.0 mmol/L of MO and 2000 mmol/L of possible interfering chemicals with the NCQDs, respectively. As shown in Figure 4.20(d), there was small or negligible on the ability of MO to quench fluorescence. As a result, the technique demonstrated high selectivity for MO detection.

4.4.1.3. Linear equation and Detection limit

Figure 4.21 depicts the calibration curve for the detection of MO. The FL intensity of NCQDs was found to be best described by using the Stern-Volmer equation, which goes as follows:

$F_0/F = K_{sv} [Q] + 1$

90

where F_0 and F are the fluorescence intensities of NCQDs in the presence and absence of MO, respectively; K_{sv} is a quenching constant, and *[Q]* is the concentration of quencher. The MO concentration, C, was represented by the linear regression equation *$F_0/F = 0.0103C + 1.0085$,* where C represented mmol/L. The linear range had an R_2 of 0.993 and covered the range of 2.00 to 200.00 μM/L. Based on 3s/k, the LOD was 0.77 μM /L. For 22.0 mmol/L MO, the RSD for about five replicate results was 1.3%, indicating sensitive techniques for detecting MO.
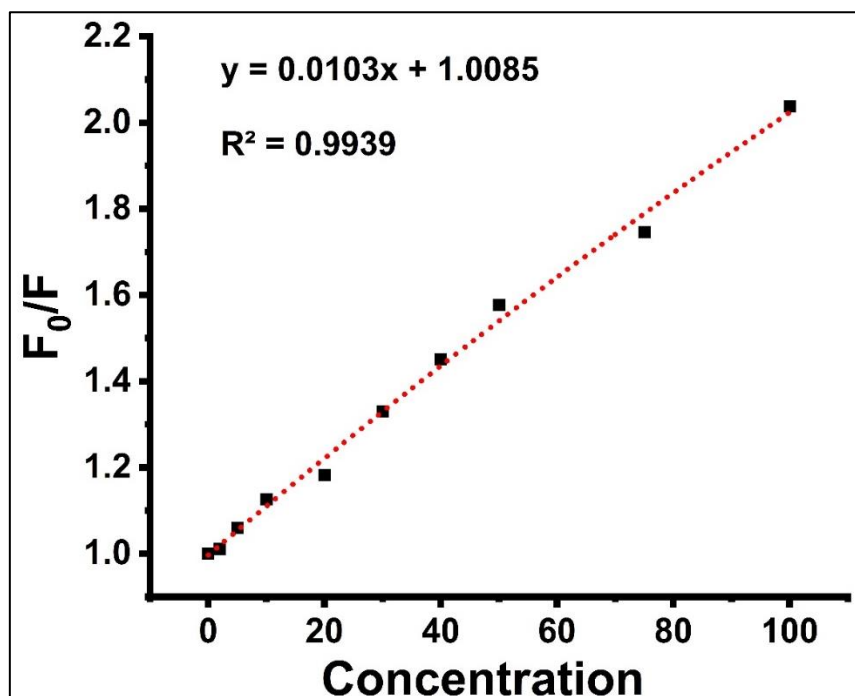
Figure 4.21- Relationship between fluorescence quenching and MO at various concentrations

4.4.1.4. Detection of MO in saffron samples

The application of NCQDs for the detection of MO in saffron samples was investigated as per the procedures mentioned in methodology section. Briefly, 100 μL of pretreated samples of saffron spiked with different concentrations of MO, and their fluorescent detection was carried out according to the procedure mentioned in section 2.6. The results showed a recovery range of 97.6-98.2%, as shown in Table 4.7. Therefore, it is evident to say that the microwave-synthesized NCQDs can be used as an ideal candidate for the detection of MO in saffron samples. A diagrammatic representation of synthesis and application of NCQDs for detection of MO is represented in Figure 4.22.

Table 4.7. - Quantitative measurement of spiked MO in saffron tea using NCQDS

Sample	MO found (μM/L)	MO Added (μM/L)	Final found value (μM/L)	Recovery (%)	RSD (%)
Saffron	0.00	10.00	9.82 ± 0.04	99.2	1.8
	0.00	25.00	24.50	99.0	1.2
	0.00	50.00	48.80 ± 0.05	98.6	1.4
	0.00	75.00	73.00	98.33	1.6
	0.00	100.00	97.90 ± 0.03	98.9	1.7

Figure 4.22- Scheme for synthesis of NCQDs and their application in detection of MO

4.4.2. Facile synthesis of S-Doped Carbon Quantum Dots and their application in the Detection of Sudan dye in saffron

4.4.2.1. Characterization of SCQDS

The fluorescence emission properties of SCQDs are dependent on the excitation wavelength. This is because the surface state emissive trap generates excitation-dependent fluorescence spectra, which causes the emission peaks to shift from 355 nm to 498 nm as the excitation wavelength increases from 305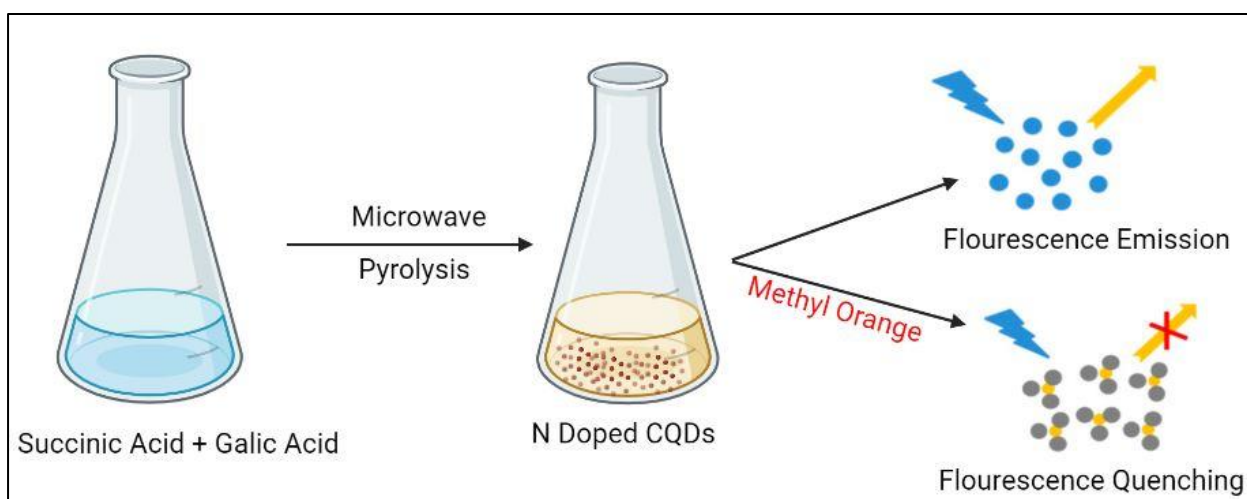 nm to 495 nm, as shown in Figure 4.23 (a). Additionally, the emission intensity reaches its peak at an excitation wavelength of approximately 340 nm [Figure 2(b)]. The UV-Vis absorption spectra of SCQDs showed peaks at 334 nm and 408 nm indicate their optical properties as shown in Figure 4.23(b). The peak at 334 nm suggests that the SCQDs have a strong absorption in the ultraviolet region, which is typical for carbon-based materials. This absorption may be attributed to the π-π* transition of the carbon core or the n-π* transition of the oxygen-containing functional groups present on the surface of the SCQDs. The peak at 408 nm indicates that the SCQDs also have an absorption in the visible region, which may be due to the presence of conjugated structures on their surface. The as synthesized quantum dots were yellowish coloured in nor day light and showed blue coloured fluorescence under UV light as shown in Figure 4.23(c) and 4.23(d).
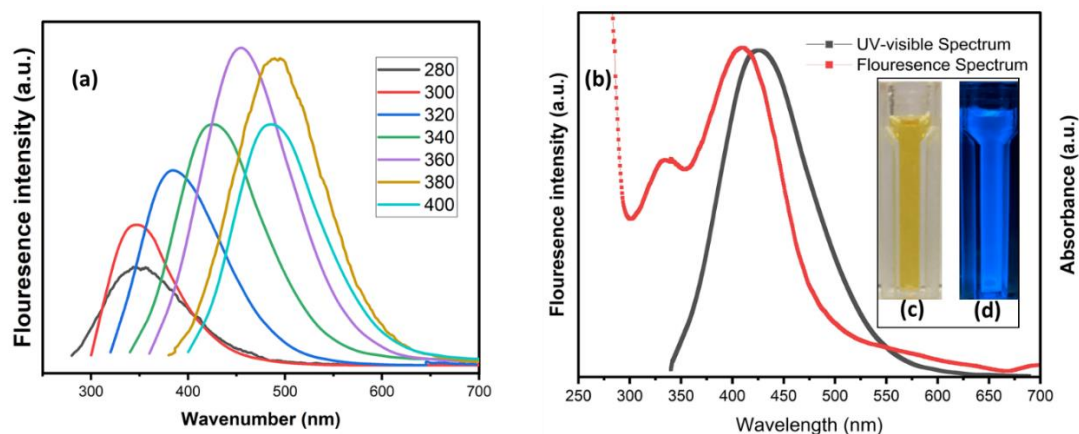
Figure 4.23- The fluorescence spectra SCQDs excited from 280 to 440 nm (a), UV-visible spectrum and fluorescence intensity of SCQDs at excitation wavelength of 340 nm (b), SCQDs under visible light (c) and SCQDs under UV light (d)

The FTIR spectrum of SCQDs [Figure 4.24] is characterized by a series of peaks that represent the various vibrational modes of the carbon-based material. Each peak in the spectrum corresponds to a particular vibrational mode, and its position and intensity are indicative of the

energy and abundance of that mode. Notably, the peak at 580.46 cm^{-1} represents the rocking mode of C-H bonds, which further supports the possibility of aliphatic chains or rings in the sample. The peak observed at 1065.43 cm^{-1} corresponds to the stretching mode of C-O bonds, implying the presence of either carboxylic acid or ester functional groups. Additionally, the peak at 1635.79 cm^{-1} corresponds to the stretching mode of C=C bonds, suggesting the presence of aromatic groups, such as benzene rings, in the sample. Another prominent peak in the spectrum observed at 2180.11 cm^{-1}, which corresponds to the stretching mode of C≡N bonds and suggests the existence of nitrile functional groups. Finally, the peak at 2360.75 cm^{-1} represents the stretching mode of C≡C bonds, which provides further evidence for the presence of alkyne groups in the quantum dots. The peak at 3335.23 cm^{-1} may correspond to the stretching vibration of O-H or N-H groups, indicating the presence of hydroxyl or amine functional groups in the SCQDs.
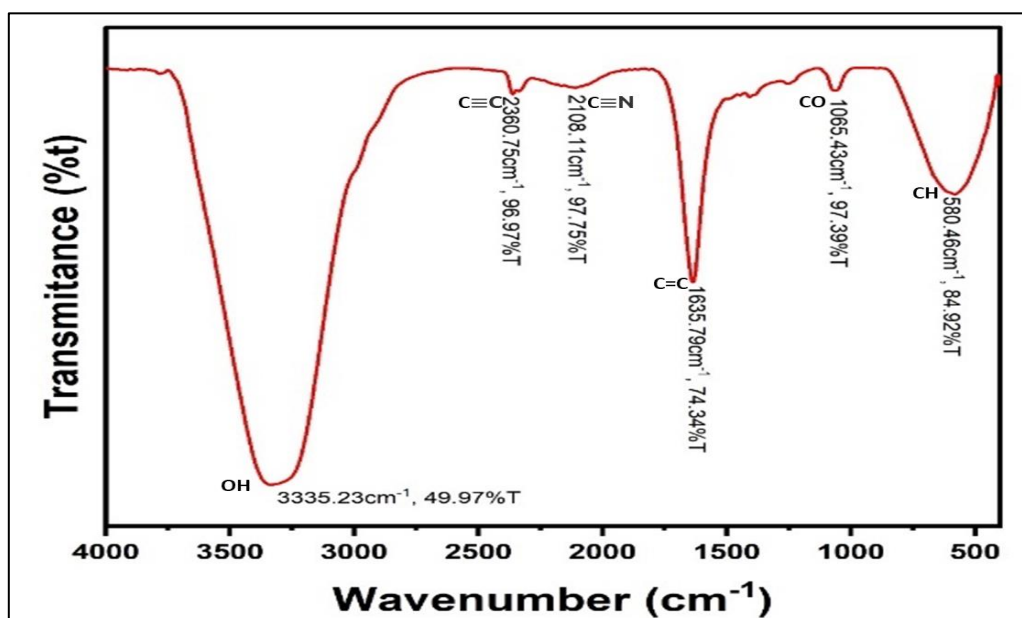
Figure 4.24. FTIR spectrum of SCQDs.

The as-prepared SCQDs were drop-coated onto an 1 cm^2 glass sheet for XRD examination. Figure 4.25(a) displays typical XRD patterns for as-prepared SCQDs. The peak at 2θ=24.6° is an important peak in the XRD pattern of SCQDs. This peak corresponds to the (002) plane of graphite. This peak indicates that the SCQDs have a highly ordered graphene-like structure, which is consistent with the reported structure of SCQDs. The (002) peak at 2θ=24.6° is a characteristic peak of graphene-based materials (Kuila *et al.,* 2012; Zhu *et al.,* 2019; Ahmed *et al.,* 2022). The intensity and width of the peak at 2θ=24.6° can provide information about the

crystallinity and size of the SCQDs. A sharp and intense peak indicates a high degree of crystallinity, while a broad peak indicates a small crystallite size.

The XPS analysis [Figure 4.25(b)] of SCQDs revealed the composition of SCQDs. The atomic percentage of carbon, sulphur and oxygen of the synthesized SCQDs was found to be 59.19, 2.78 and 37.61 per cent, respectively. XPS analysis can be used to determine the types of bonds that are present in the SCQDs. Specifically, the C1s [Figure 4.25(c)], O1s [Figure 4.25 (d)], and S2p [Figure 4.25(e)] peaks can provide information about the carbon, oxygen, and sulphur atoms in the sample, respectively. The C1s peak at 284.6 eV corresponds to C-C bond while the peak at 287.78 eV is indicative of O-C-O bonds. The peak at 288.13 eV is typically associated with carbonyl groups (C=O) and carboxyl groups (O-C=O) in the SCQDs. The O1s peak at 532.82 eV corresponds to oxygen atoms in hydroxyl (O-H) group. The peak at 535.76 eV is associated with oxygen atoms in carbonyl group (C=O). Finally, the S2p peaks at 168.06 and 170.09 eV correspond to sulphur atoms in sulfonate (-SO_3H) group and sulfonic group (S-O), respectively. These peaks indicate the presence of sulphur atoms that are chemically bonded to the carbon atoms in the SCQDs.
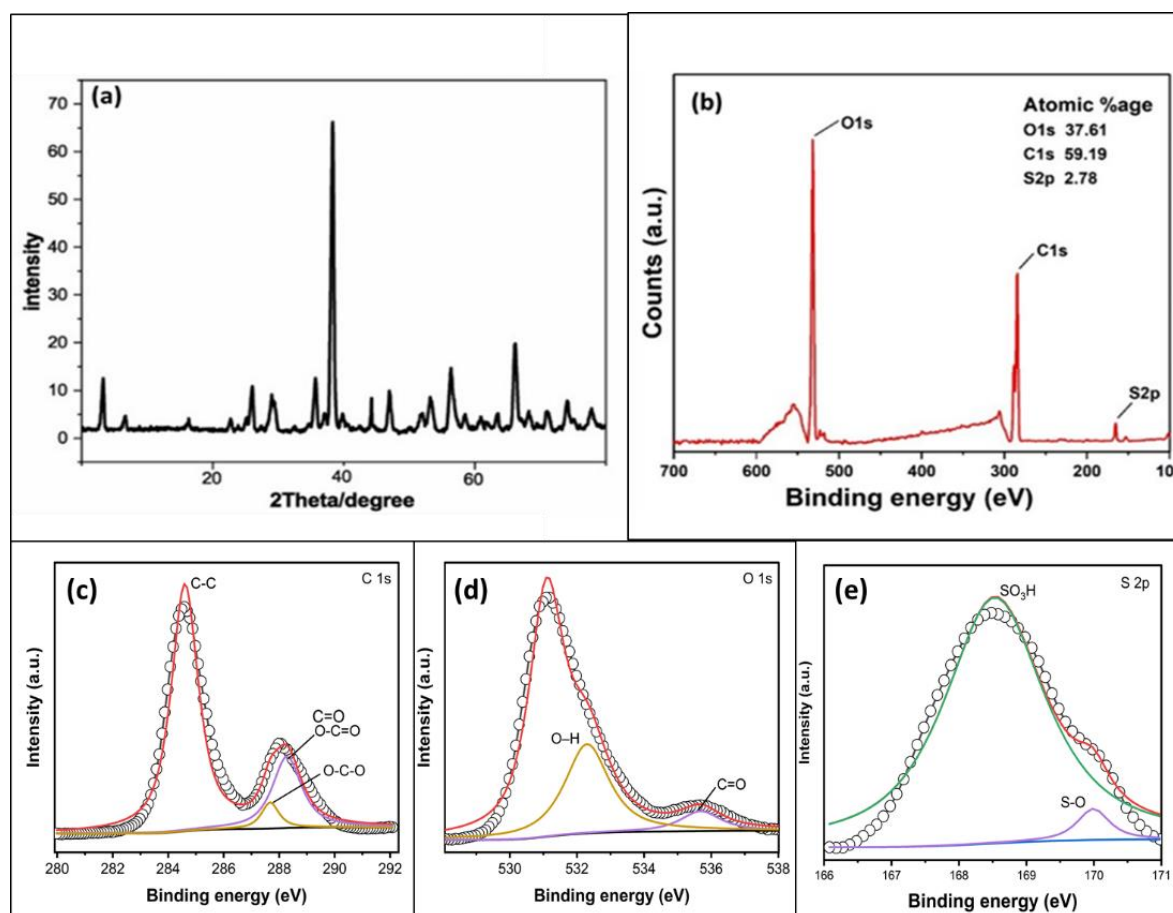
Figure 4.25. XRD (a) and XPS survey scan (b) of SCQDs, high-resolution XPS spectrum of C 1s (c), O 1s (d), and S 2p (e)

A Zeta Potential and Size Analyzer (also known as a Zetasizer) was used to determine zeta potential and size of SCQDs. As can be seen in Figure 4.26(a), zeta potential of SCQDs was found to be -13.84 mV, indicating that the surface of the SCQDs has a negative charge. Zeta potential is a measure of the electrostatic potential at the particle's surface, and it indicates the stability of the colloidal system. A negative zeta potential suggests that the SCQDs are stable in a suspension or dispersion, as like charges repel each other and prevent aggregation. Therefore, a negative zeta potential is desirable for the stability of the SCQDs in solution.

A Zetasizer can also calculate the size of quantum dots by using the dynamic light scattering (DLS) technique. DLS measures the Brownian motion of the particles suspended in a liquid to determine their size distribution. In DLS, a laser beam is directed onto the sample, and the scattered light is detected by the instrument. The intensity of the scattered light fluctuates over time due to the Brownian motion of the particles. The fluctuations in the scattered light intensity are analyzed to determine the diffusion coefficient of the particles, which is related to their size. The average particle size of SCQDs was found to be around 5.6 nm [Figure 4.26 (b)].
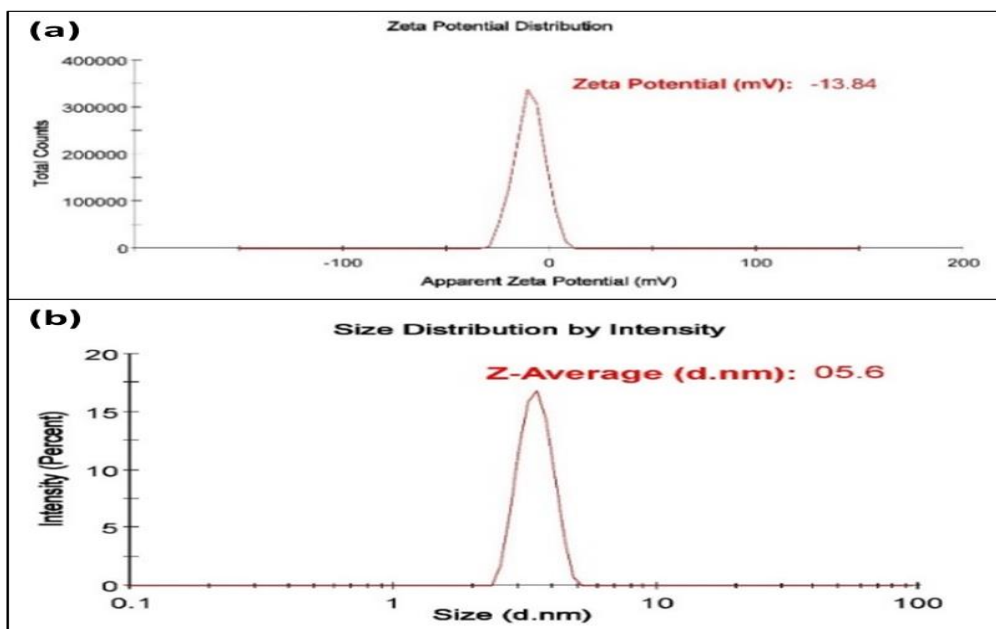
Figure 4.26 Zeta potential distribution (a), size distribution (b) of SCQDs

4.4.2.2. Effect of Sudan I on the fluorescence intensity of SCQDs

The FL intensity of SCQDs was analyzed under varying concentration of Sudan I (0.2 μM-150 μM) (Benítez-Martínez and Valcárcel 2014; Zoughi *et al.,* 2021). Figure 4.27 illustrates a decline in the FL intensity of SCQDs with an increasing concentration of Sudan I. The reduction in FL intensity at different Sudan I concentrations is attributed to either charge or energy transfer between the fluorophore and the quencher. Charge transfer occurs when the excited Sudan I molecule from the fluorophore is transferred to the quencher. Energy transfer can occur if there is a significant overlap between the fluorescence emission spectra of the fluorophore and the UV absorbance spectra of the quencher or if their distance is very small, often less than 10 nm (Algar and Krull 2007; Kadian and Manik 2020). In this study, the maximum fluorescence wavelength of SCQDs was observed at 475 nm after excitation at 340 nm, while Sudan I exhibited its maximum absorption wavelength at 475 nm as well. The efficient overlap of the two spectra is depicted in Figure 6(a). Consequently, it can be inferred that the fluorescence quenching of Sudan I on SCQDs is a result of energy transfer between them..
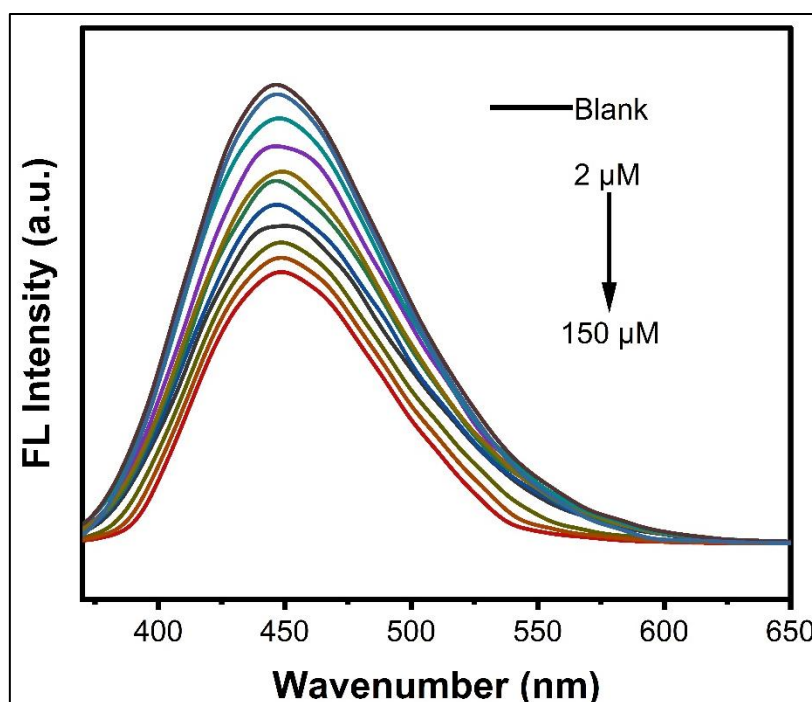
Figure 4.27- FL intensity of SCQDs with different concentration of Sudan I

4.4.2.3. Optimization

The possibility of developing a sensitive method for determining Sudan I was investigated due to the reported fluorescence quenching of SCQDs in its presence (Zoughi *et al.,* 2021b; Zhang

et al., 2022; Mir *et al.,* 2023). The impact of pH in the range of 4-10 on the FL intensity of SCQDs was studied, and it was discovered that the pH of the SCQDs solution influences its FL intensity. While the relative FL intensity values (F^0/F) were largely constant over the pH range, the emission of SCQDs solution rose from 4 to 8, then decreased from 8 to 10 [Figure 4.28(b)]. Consequently, pH 8 was chosen as the optimal pH for detection of Sudan I. At pH 8, the effects of several buffer systems, including phosphate buffer, Britton-Robinson (B-R), and Tris-HCl, on the F^0/F were examined. The phosphate buffer was shown to be effective for the buffers tested. The effect of the incubation period on the degree of FL intensity was also studied, and the incubation duration was adjusted under normal circumstances by monitoring the FL intensity of SCQDs and Sudan I solution (pH 8) every 5 minutes. As illustrated in Figure 7, the maximum FL intensity value was reached after 15 minutes and remained constant for 60 minutes, as shown in Figure 4.28(c). Therefore, the appropriate incubation period for FL intensity was determined to be 10 minutes.

The effects of putative interfering chemicals L-tryptophan, L-serine, L-threonine, vitamin C, vitamin B6, vitamin B1, CuCl2, MgSO4, NiSO4, NaCl, and KCl on specificity were investigated. The results were obtained by mixing 20.0 ml/L of Sudan I with SCQDs alone, as well as 22.0 ml/L of Sudan I and 2000 ml/L of potentially interfering compounds with the SCQDs. As seen in Figure 4.28(d), there was little to no effect on Sudan I's capacity to quench fluorescence. Therefore, this approach showed good selectivity for Sudan I detection.
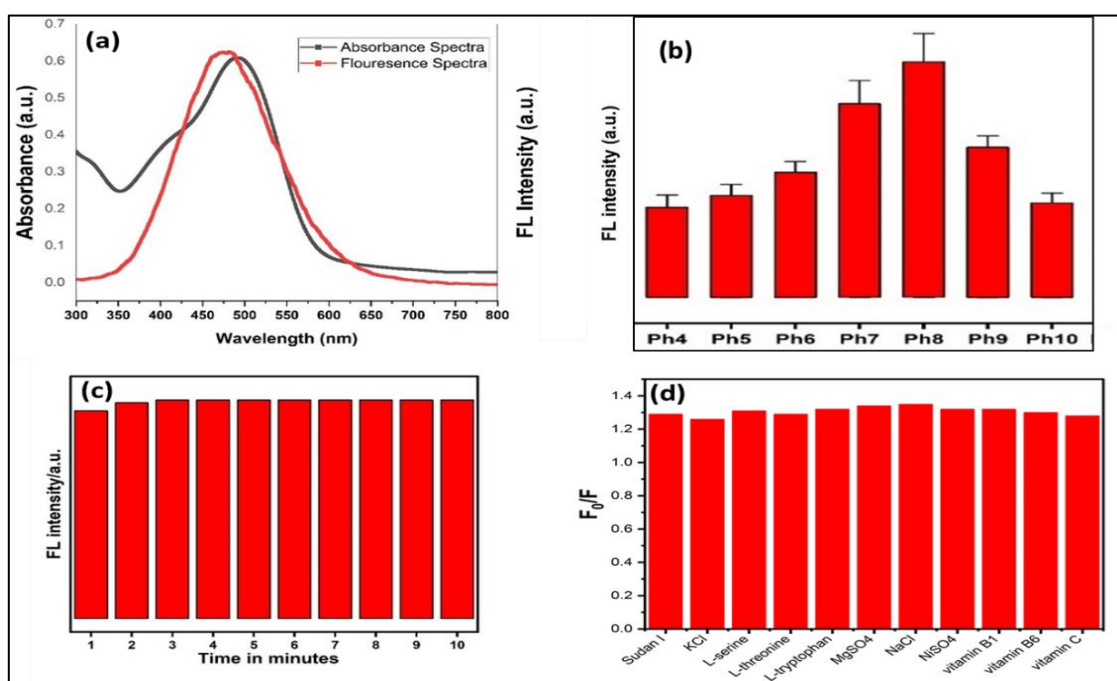
Figure 4.28- Fluorescence and Absorbance of SCQDs and Sudan I (a), pH (b) and Time (c) optimization of SCQDs as a sensor, and Selectivity of SCQDs (d)

4.4.2.4. Linear equation and Detection limit

Figure 4.29 illustrates the calibration plot designed to identify Sudan I. After analysis, it was established that the Stern-Volmer equation provided the most accurate description of the fluorescence (FL) intensity of SCQDs. This empirical equation is commonly employed to characterize the reduction in fluorescence intensity of a fluorophore caused by a quencher. It establishes a relationship between the fluorophore's fluorescence intensity without the quencher (F0) and its intensity in the presence of the quencher (F). The Stern-Volmer equation is expressed as follows::

$$\frac{F^0}{F} = 1 + Ksv\,[Q]$$

Where Ksv is the Stern-Volmer quenching constant and [Q] is the concentration of the quencher.

The Stern Volmer equation can be employed to determine the LOD of a fluorophore-quencher system. The LOD is defined as the minimum concentration of the quencher that produces a measurable change in the FL intensity. The LOD is related to the Stern-Volmer quenching constant by the following equation:

$$LOD = Ksv\,\times \frac{S}{N}$$

Where S is the standard deviation of the blank measurement and N is the slope of the calibration curve.

Therefore, the quenching mechanism can be deduced from the Stern-Volmer equation, which provides insight into the interaction between the fluorophore and the quencher. By analyzing the quenching constant and its dependence on the quencher concentration, one can infer the nature of the quenching mechanism, whether it is dynamic or static. The linear regression equation $F^0/F = 0.0073x + 1.0505$ was used to represent the Sudan I concentration, C, where C denoted ml/L. The linear range had an R^2 of 0.982, ranging from 2.00 to 150.00 μM/L [Figure 4.29]. The LOD was found to be 0.67 μM/L based on equation (iii).
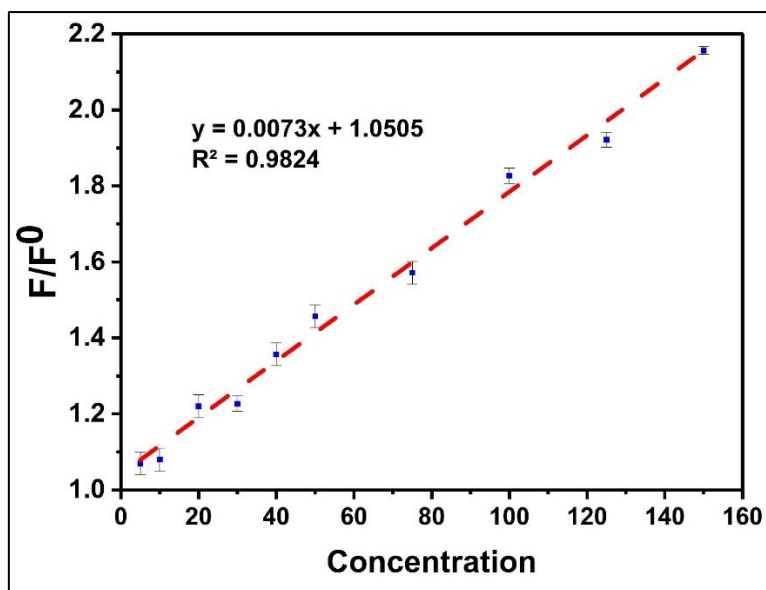
Figure 4.29- Relationship between fluorescence quenching and Sudan I at various concentrations

4.4.2.5. Detection of sudan I in saffron samples

The use of SCQDs to detect Sudan I in saffron samples was examined using the protocols outlined in Section 2.6. In brief, 100 µL of pre-treatment saffron samples were spiked with varied concentrations of Sudan I, and their fluorescence detection was performed using the technique described in section 2.6. The results showed a recovery range of 98.3-99.6%, as shown in Table 1. Therefore, it is evident to say that the microwave synthesized SCQDs can be used as an ideal candidate for the detection of Sudan I in saffron samples

Table 4.7- Quantitative measurement of spiked Sudan I in saffron using SCQDs

Sample	Sudan I found (µM)	Sudan I Added (µM)	Final found value (µM)	Recovery (%)	RSD (%)
Saffron	0.00	10.00	9.72 ± 0.04	98.6	1.9
	0.00	25.00	24.40 ± 0.05	99.2	1.2
	0.00	50.00	48.90 ± 0.03	98.4	1.8
	0.00	75.00	72.00 ± 0.04	99.6	1.5
	0.00	100.00	97.80 ± 0.05	98.3	1.6

The synthesized SCQDs served as an efficient fluorescent probe for the detection of Sudan I, with a detection limit of 0.67 μM. When applied to the detection of Sudan I in saffron samples, the as-synthesized SCQDs demonstrated outstanding performance, with a recovery range of 98.3-99.6%. Hence, our research verifies the feasibility of using S-doped carbon quantum dots to detect Sudan I in saffron.

4.5. Discussion

Saffron adulteration carries significant forensic challenge and extensive repercussions, given its status as a costly spice. Beyond its culinary and therapeutic applications, saffron holds historical, cultural, and economic significance. Nevertheless, the covert practice of adulterating saffron with foreign material substances raises several concerns that transcend mere economic fraud, encompassing matters of food safety, consumer well-being, and legal enforcement. Adulteration of saffron often involves mixing saffron with cheaper components, often sourced from plants like marigold petals, safflower petals, or turmeric. This deceptive practice not only undermines the integrity of the saffron market but also misleads consumers. To ensure equitable trade practices and safeguard the interests of both farmers and consumers, precise differentiation between genuine saffron and its adulterants is imperative. Adulterated saffron may contain poisonous or allergenic substances, posing health risks to individuals. Consumption of such tainted saffron can lead to adverse effects or allergic responses. Forensic analysis plays a pivotal role in identifying toxic contaminants, ensuring the safety of saffron products, and empowering regulatory bodies to take necessary precautions for public health. Detecting saffron adulteration becomes crucial in cases involving food fraud. Forensic experts employ several techniques to distinguish between authentic saffron and its adulterants, providing compelling evidence for legal actions against those accountable for adulteration practices. Accurate forensic analysis is indispensable to establish guilt and support legal measures aimed at curbing adulteration.

Adulteration disrupts international trade and hinders standardization efforts. Forensic analysis facilitates the development of standardized authentication procedures for saffron, fosters international collaboration, and ensures transparency in saffron trade agreements. Dependable forensic methods enable saffron-exporting nations to maintain their global reputation. The adulteration of saffron extends beyond financial losses to encompass concerns related to consumer well-being, food safety, legal accountability, cultural preservation, and international trade. Robust forensic investigations are indispensable for identifying and combating saffron

adulteration, ensuring public safety, and preserving the purity of this treasured spice with rich historical and cultural roots

The current research was an attempt to develop several sensitive techniques to determine and quantify of saffron adulteration. The first objective of this research was to investigate the purity and quality of saffron samples collected from various commercial zones in Kashmir using instrumental techniques, namely UV-Vis spectrophotometry and HPLC analysis. The study analyzed the floral waste content, moisture/volatile matter content, and apocarotenoid levels (crocin, picrocrocin, and safranal) in the saffron samples to assess their authenticity and quality. The initial step in the investigation involved determining the floral waste content in the samples. The study found significant variation in floral waste content among the different samples, with saffron from Srinagar and Budgam showing a higher range of floral waste. On the other hand, samples from Government-operated commercial emporiums (KAE) and the Sigma sample showed the lowest floral waste content. This data indicates that the purity of saffron can vary depending on its source, with KAE and Sigma samples being more likely to be pure. Next, we analyzed the moisture and volatile matter content of the saffron samples. High moisture levels in saffron can indicate improper drying and processing, which may affect the quality. The study found that samples from Srinagar, Budgam, and Pampore had higher moisture and volatile matter content compared to samples from KAE, Afghanistan, Iran, and the Sigma sample. Again, this suggests that saffron from certain commercial sources is more likely to be properly processed and of better quality.

UV-Vis spectrophotometry was used to determine the apocarotenoid content (crocin, picrocrocin, and safranal) of the saffron samples. Based on the results, they classified the samples into different quality grades following ISO guidelines. The saffron from KAE was found to be of the highest grade, while the saffron from Srinagar markets showed the lowest grade, indicating a higher likelihood of adulteration. This finding aligns with the moisture and volatile matter analysis, suggesting that saffron from Srinagar markets may be of lower quality due to inadequate processing and handling.

To further confirm the results, HPLC analysis was performed, which provided more detailed measurements of the apocarotenoid components. The results from HPLC analysis supported the findings from UV-Vis spectrophotometry, with KAE samples again showing the highest concentration of apocarotenoids, followed by Afghanistan and Iran samples. Saffron from

Srinagar markets once again exhibited the lowest quality, reinforcing the possibility of adulteration.

Based on the results, It is pertinent to say that the average concentration of crocin and picrocrocin in the Iranian samples was highest as compared to other samples, while the concentration of safranal was highest in the samples of Kashmir (KAE) samples. The highst level of adulteration was found in the samples obtained from Srinagar (SXR). This study successfully investigated the quality and authenticity of saffron samples using a combination of instrumental techniques. The results showed that saffron from different commercial sources in Kashmir can vary significantly in terms of purity and apocarotenoid content. The research highlights the importance of proper drying and processing methods in maintaining the quality of saffron and indicates the potential for adulteration in some saffron samples. These findings can be valuable for saffron producers, traders, and consumers to make informed decisions and ensure the purchase of high-quality saffron. Further research and monitoring may be necessary to address the issue of adulteration and promote the production and distribution of authentic saffron.

In the second objective MIP-QDs were synthesized to determine the crocin concentration in saffron. Crocin is a bioactive compound responsible for the vibrant color and medicinal properties of saffron, making its accurate detection essential for assessing saffron quality and preventing adulteration. To achieve this, we developed a nano probe using MIPs and Carbon Quantum Dots (CQDs).

The first step of the objective involved the meticulous synthesis and characterization of CQDs. Next Quantum dots were used in MIPs to synthesize MIPs-QDs. Gentiobiose, structurally similar to Crocin, served as a suitable template for MIP-CQDs synthesis. Various instruments were used for the characterization of the Qds and MIPs. Different concentrations of Crocin were prepared in ethanol, and their fluorescence spectra were recorded to establish a calibration series. The nanosensor exhibited impressive sensitivity, showing a linear response in the concentration range from 0.2 to 175.0 μM, with a remarkably low limit of detection (LOD) of 2.1 μM. The study also delved into optimizing various parameters (ph. Incubation time and interfering substances) to enhance the nanosensor's performance. To validate the nano sensor's practical applicability, saffron samples from different geographical locations were analyzed. The nano sensor accurately measured Crocin concentrations in the samples, and the results were compared to those obtained from the standard High-Performance Liquid Chromatography

(HPLC) method, showing excellent agreement. Therefore, this study presents a novel and sophisticated nano sensor based on MIP-CQDs for the sensitive and specific detection of Crocin in saffron. The successful synthesis and optimization of the nano sensor, along with its accuracy in saffron sample analysis, offer immense potential for applications in saffron quality control and assurance of authenticity. This research not only advances the field of food analysis but also opens doors for further exploration and potential commercialization of the nano sensor technology for various other applications in different industries.

The third objective of this research was to synthesize different nanomaterials for quantifying and detecting adulteration of saffron. The first part of this objective focuses on the synthesis of gold nanoparticles (AuNPs) synthesized using crocin as a reducing agent, with a specific emphasis on its application in detecting crocin in saffron samples. Various analytical techniques were employed to characterize the synthesized AuNPs thoroughly. X-ray diffraction (XRD) analysis confirmed the crystalline size, structure, and phase purity of the AuNPs, while Fourier transform infrared spectroscopy (FTIR) revealed the presence of aromatic compounds and functional groups on the nanoparticle surface. Field emission scanning electron microscopy (FE-SEM) provided insights into the structure and morphology, and energy-dispersive X-ray spectroscopy (EDX) confirmed the elemental distribution, establishing the presence of gold nanoparticles. Zeta potential analysis indicated that the AuNPs possessed slight negative values, suggesting high stability. Optimization studies were conducted to determine the ideal conditions for AuNPs synthesis, and it was found that an HAuCl4 concentration of 20 mM, alkaline pH of 10, temperature of 40°C, and a reaction time of 6 hours yielded the most stable and efficient AuNPs. Furthermore, the synthesized AuNPs were utilized to detect crocin in real saffron samples, resulting in a recovery range of 98.28% to 99.12% for different saffron extract concentrations, demonstrating the potential application of the colorimetric assay for saffron quality assessment and adulteration detection.

This second part of the third objective focused on synthesizing nitrogen-doped carbon quantum dots (NCQDs) and their application in the detection of Methyl orange (MO) in saffron samples. Succinic acid and gallic acid served as the carbon and nitrogen sources, respectively, for the microwave-assisted synthesis of NCQDs. To our best knowledge, no study has been done till now for the detection of MO orange in saffron using nanomaterials. The resulting NCQDs were characterized using various techniques. The fluorescence properties of NCQDs were investigated under the influence of varying concentrations of MO. The fluorescence intensity of NCQDs decreased as the concentration of MO increased, indicating fluorescence quenching

due to energy transfer between the fluorophore and the quencher. The study further optimized the experimental conditions, including pH values and incubation time, to achieve effective quenching of fluorescence upon interaction with MO. It was found that pH 8 was the ideal condition for the detection of MO. The calibration curve for the detection of MO was done using the Stern-Volmer equation. The linear range covered concentrations from 2.00 to 200.00 μM/L, with a limit of detection (LOD) of 0.77 μM/L. The method exhibited high sensitivity and selectivity for MO detection, as evidenced by minimal interference from potential interfering substances. Finally, the NCQDs were applied to detect MO in saffron samples. The saffron samples were pre-treated and analyzed using the NCQDs-based method. The results showed a recovery range of 97.6-98.2%, demonstrating the capability of the microwave synthesized NCQDs as an effective candidate for the detection of MO in saffron samples.

In this last part of third objective, we focused on the synthesis and application of S-Doped Carbon Quantum Dots (SCQDs) as a fluorescent probe for the detection of Sudan I in saffron samples. Sudan I is a synthetic dye that is commonly used as a food colorant but is banned due to its potential health hazards. The presence of Sudan I in saffron could indicate adulteration, making it essential to develop sensitive and accurate detection methods. Microwave-assisted method was employed to synthesize SCQDs using citric acid as a carbon source and thiourea as a sulfur source. The resulting SCQDs exhibited strong fluorescence properties with excitation-dependent emission spectra, making them suitable for fluorescence-based detection assays. Several instruments were employed for the characterization of as synthesized SCQDs. To optimize the performance of the SCQDs as a Sudan I probe, various factors were investigated. The pH of the SCQDs solution was found to influence its fluorescence intensity, and pH 8 was identified as the optimal pH for Sudan I detection. Additionally, the incubation time for the interaction between SCQDs and Sudan I was optimized, and a 10-minute incubation period was determined to yield the best results. The selectivity of the SCQDs probe was tested against various potentially interfering chemicals, and it showed excellent selectivity for Sudan I. We then established a calibration plot using the Stern-Volmer equation, which described the quenching of the SCQDs' fluorescence intensity by Sudan I. The linear range for Sudan I detection was found to be 2.00 to 150.00 μM/L, with a detection limit of 0.67 μM/L. In the final step, the synthesized SCQDs were applied to detect Sudan I in saffron samples. The results demonstrated high recovery percentages ranging from 98.3% to 99.6%, indicating the reliability of the SCQDs as a fluorescent probe for Sudan I detection in saffron. The study's findings suggest that the use of SCQDs as a fluorescent probe offers a sensitive and reliable

method for detecting Sudan I in saffron, ensuring its quality and authenticity in the market. The synthesized SCQDs can serve as a valuable tool for food safety and quality control in the saffron industry, helping to protect consumers from potential health risks associated with adulterated saffron products.

Chapter 5

Summary and Conclusion

Saffron, often referred to as red gold, is obtained from the stigma of *Crocus sativus* L. (Saxena 2010). *Crocus sativus* is an angiosperm plant, member of the Asparagales family. The flower of *Crocus sativus* is solitary, purple, with six petals, three stamens, one style, and three reddish-orange stigmas. Saffron grows throughout the Mediterranean–Europe, and Western Asia and is mainly cultivated in Iran, Greece, Spain, Italy, Afghanistan and India (Kashmir) (Kahriz, 2020). Saffron is quite costly because it is mainly used as a flavoring and aromatizing agent (Mir *et al*., 2022; Mzabri *et al*., 2019). Saffron contains approximately 300 volatile and non-volatile metabolites, including crocin, safranal, picrocrocin, monoterpenes, aldehydes, and various other carotenoids of therapeutic potential (Pandita 2021). It is a well-known spice that is used to cure a variety of medical conditions, including depression (Siddiqui *et al.,* 2018), cardiovascular illness (Kamalipour and Akhondzadeh 2011), asthma (Zilaee *et al.,* 2019), insomnia (Taherzadeh *et al.,* 2020), and digestive problems (Khorasany & Hosseinzadeh, 2016).

Crocin is a carotenoid chemical compound responsible for the golden yellow-orange color of saffron; picrocrocin gives bitter flavor, and safranal is responsible for the characteristic aroma of saffron. Saffron is currently known as a flavoring agent and a potent natural agent with many health advantages (Azami *et al.,* 2021; Mir *et al.,* 2022). The potential of saffron and its constituents to protect against natural and artificial poisons has enhanced its significance. Due to the high price of saffron and its great demand in the pharmaceutical industry, illegal trafficking and adulteration are prevalent nowadays (Alonso *et al*., 1998, Azami *et al.,* 2021; Mir *et al.,* 2022).

The common adulterants used in saffron include maize silk, marigold floret, horsehair, wool, saffron stamens, red dried silk fiber, and safflower (*Carthamus tinctorium* L.). Mixing low-grade saffron with high-grade saffron or old stored saffron that has lost its quality with freshly harvested saffron is also a common method of adulteration in saffron (Lowell 1964; Marieschi *et al.,* 2012; Sereshti *et al.,* 2018; Kumari *et al.,* 2021). The sale and mixing of high-grade Kashmiri saffron with lower-cost Iranian imports is common in India; the resulting mixes are then sold as pure Kashmiri saffron. This trend has deprived saffron cultivators of Kashmir of a significant portion of their revenue (Hussain, 2005). Dyes such as erythrosine, tartrazine, amaranth, sunset yellow, carmoisine, picric acid, ponceau S, methyl orange, and Sudan red are also used as adulterants in saffron (Lozano *et al.,* 1999; Petrakis *et al.,* 2015; Patel *et al.,* 2019).

Internationally, the grading of saffron is based on the standards formulated by the ISO. The ISO (ISO 3632-1:2011) certification ensures customers that the saffron they purchase is authentic and safe to consume. ISO 3632 has classified saffron into three grades (Grade I, II and III) based on the concentration of crocin, picrocrocin and safranal present in saffron. A greater concentration of these chemicals indicates a better quality of saffron. A quartz cell with a 1 cm pathway is used to measure $E_{1\%}$ at 440, 330, and 257 nm wavelengths. The results are obtained by measuring the absorption at three wavelengths using the equation; $E_{1\%}\ 1\ cm = (A \times 10000]/ (M \times (100\text{-}H)]$, where $E_{1\%}$ is the specific extinction coefficient, $1\ cm$ is the path length, A is the absorbance, M is the mass in grams of the saffron sample, H is the moisture and volatile sample material. The moisture and volatile content of the saffron is determined after drying the samples and represented as a mass fraction using the formula: *[(initial mass-constant mass)/initial mass] × 100* (Hadizadeh *et al*., 2007; *ISO - 3632-1:2011*).

The first objective of this research is to estimate the quality range and apocarotenoid content of commercial saffron in Kashmir using UV-Vis spectrophotometry and HPLC analysis.The evaluation of the quality of saffron samples was done by UV-Vis Spectroscopy according to the limit set by the ISO 3632, and the determination of apocarotenoid content was analyzed by HPLC analysis. The UV-Vis spectrophotometric results categorized the sample into different grades as per standards formulated by ISO. Only fourteen samples were identified as Grade I, and 13 samples were either grade II or grade III. The remaining 3 samples were found to be highly adulterated. The results obtained from HPLC analysis showed significant variation. The highest concentration of apocarotenoids was found in KAE samples, followed by AFG, IRN, PAM and BUD samples. Samples from SXR showed the least concentration of apocarotenoids, indicating a high level of adulteration. Adulteration in saffron is a big concern and needs to be addressed scientifically. It has an adverse effect on the saffron industry since counterfeit or adulterated saffron accounts for considerable market share. Although various instrumental methods (HPLC, GC-MS, FTIR, Raman Spectroscopy, etc.) for detecting adulteration in saffron, these methods are laboratory-based and cannot be used on a large sample size. Consequently, improvements to the existing ISO methods are suggested, and the development of a technique for on-the-spot detection of adulteration in saffron is recommended for future studies.

The second objective is development of a highly sensitive optical nanosensor for the detection of crocin using MIP-CQDs. The MIP-CQDs was prepared using APTES and TEOS with CQD nanoparticles in the presence of the template molecules. This fluorescent nanosensor has a low

detection limit of 2.01 μM, a practical linear range of 02.00-175.00 μM, strong fluorescence intensity, and minimal interference. To demonstrate the performance of the nanosensor, it was used to analyze crocin levels in saffron samples. This method is cost-effective, has low toxicity, and is simple enough to be used as chips based on the Lateral Flow technique for food analysis. Moreover, the versatility of the proposed nanocomposite could be extended to the analysis of other important targets with high accuracy.

The third objective is to synthesize AuNPs for determining the quality of saffron. The analytical applicability of the proposed sensor to real sample analysis, to determine the total crocin content in saffron. Saffron extract of different concentrations in water (0.5 mg-100 mg/ml) were used to observe the results. It was found that with the decrease in the concentration of saffron extract, the color intensity also decreased, which was confirmed by UV-Vis spectrophotometer. The results showed a recovery range of 98.28-99.12%. Saffron extract with different levels of adulteration with safflower (0%-100%) were also used for the synthesis of nanoparticles. It was found that samples with higher concentration of adulteration lowered the NP synthesis as the adulteration levels increased.

Methyl orange is one of the most common artificial colorants used in the adulteration of saffron. To prevent the sale of adulterated saffron and to make sure that food is safe and of good quality, researchers all over the world have been attempting to come up with a cheap, quick, reliable, and environmentally friendly method for determining toxic substances in foodstuff. In this research, NCQDs were synthesized by employing the microwave synthesis method using succinic acid and gallic acid as carbon and nitrogen sources, respectively. The characterization of NCQDs was done by using different instrumentation techniques such as fluorescence spectroscopy, XRD, FTIR, TEM, XPS and Zeta potential. The synthesized NCQDs were used as an effective fluorescent probe for the detection of MO with a detection limit of 0.77 μM. Moreover, the as-synthesized NCQDs showed remarkable results when used to detect MO in samples of saffron, with a recovery range of 98.6–99.2%. Therefore, this study confirms that N-doped carbon quantum dots could be used to find MO in saffron.

Sudan dye is another common dye used in adulteration of saffron. In this research, SCQDs were synthesized using Citric acid and thiourea as carbon and sulphur sources, respectively. Fluorescence spectroscopy, X-ray diffraction, Fourier transform infrared spectroscopy, X-ray photoelectron spectroscopy, and Zeta potential were used in the characterisation of as synthesized SCQDs. The synthesised SCQDs served as an efficient fluorescent probe for the detection of Sudan I, with a detection limit of 0.67 μM. When applied to the detection of Sudan

I in saffron samples, the as-synthesized SCQDs demonstrated outstanding performance, with a recovery range of 98.3-99.6%. Hence, this study also verifies the feasibility of using S-doped carbon quantum dots to detect Sudan I in saffron.

The findings of this study hold substantial social implications, primarily centered around safeguarding consumer health, preserving the integrity of the saffron industry, and advancing the field of food quality assurance. Adulteration practices in saffron, as identified through the incorporation of various adulterants like maize silk, marigold floret, and synthetic dyes, can have far-reaching consequences on public health due to the ingestion of potentially harmful substances. This concern is magnified by the global trade of saffron, where mixed-grade saffron and counterfeit blends erode consumer trust and compromise their well-being. The impact on saffron cultivators, as evidenced by the substitution of premium Kashmiri saffron with lower-cost imports, underscores the need for fair trade practices that ensure equitable revenue distribution among producers.

This study's contribution to health benefits and quality assurance is multifaceted. It addresses the need for accurate and reliable techniques to assess the quality of saffron. By employing UV-Vis spectrophotometry and HPLC analysis, the research quantifies the apocarotenoid content in saffron, an essential marker of quality and authenticity. These analyses serve to verify saffron samples according to ISO standards, enabling consumers to make informed choices and fostering confidence in the saffron market.

The development of a highly sensitive optical nanosensor using Molecularly Imprinted Polymer-Carbon Quantum Dots (MIP-CQDs) introduces a cutting-edge tool for detecting the presence of crocin, a bioactive compound responsible for saffron's color and has several health benefits. This nanosensor, characterized by its low detection limit, wide linear range, and minimal interference, revolutionizes saffron adulteration detection. It also opens avenues for broader applications in food quality assessment, aligning with global efforts to combat food fraud and ensure product authenticity. The nanosensor's potential integration into the Lateral Flow technique for food analysis brings a simplified and cost-effective solution to real-world testing, democratizing access to quality assurance even in resource-limited settings.

Moreover, the synthesis of AuNPs for saffron quality determination introduces an innovative approach that combines nanoparticles with spectrophotometry to ascertain saffron's total crocin content. This potential of this method for assessing both quality and adulteration levels emphasizes its potential in addressing the industry's challenges. The use of N-doped carbon

quantum dots and S-doped carbon quantum dots to detect specific adulterants like Sudan dye and methyl orange presents forward-looking solutions that can aid in identifying additional fraudulent practices, thereby fortifying food safety and consumer trust.

By combating adulteration and enhancing saffron quality assessment, this study contributes to a healthier populace, ensures fair economic practices for saffron producers, and sets a precedent for rigorous quality control in the food industry. The novel nanosensor technologies introduced herein not only elevate saffron authenticity verification but also hold potential for broader applications in enhancing the safety and reliability of various food products.

These as synthesized nanomaterials can be used as an effective tool for the determination and quantification of adulteration in saffron. In future, using these synthesized nano-materials, paper-based sensors can be developed to detect adulterations, and this study's findings could potentially be extended to identify target adulterants in various other food items. Furthermore, the synthesis of alternative nanomaterials may enable the detection of distinct adulterants with even lower LOD.

References:

Ahmed, F., Iqbal, S., & Xiong, H. (2022). Multifunctional dual emissive fluorescent probe based on

   europium-doped carbon dots (Eu-TCA/NCDs) for highly selective detection of

   chloramphenicol, Hg2+ and Fe3+. *Environmental Science: Nano*, *9*(8), 2624–2637.

   https://doi.org/10.1039/D2EN00376G

Ahrazem, O., Rubio-Moraga, A., Nebauer, S. G., Molina, R. V., & Gómez-Gómez, L. (2015). Saffron: Its

   Phytochemistry, Developmental Processes, and Biotechnological Prospects. *Journal of*

   Agricultural and Food Chemistry, *63*(40), 8751–8764.

   https://doi.org/10.1021/acs.jafc.5b03194

Aiello, D., Siciliano, C., Mazzotti, F., Di Donna, L., Athanassopoulos, C. M., & Napoli, A. (2020). A rapid

   MALDI MS/MS based method for assessing saffron (Crocus sativus L.) adulteration. *Food*

   Chemistry, *307*, 125527.

Akhtar, N., Wani, A. K., Mir, T.-U. G., Kumar, N., & Mannan, M. A.-U. (2021). Sapindus mukorossi:

   Ethnomedicinal USES, PHYTOCHEMISTRY, AND PHARMACOLOGICAL ACTIVITIES. *PLANT CELL*

   BIOTECHNOLOGY AND MOLECULAR BIOLOGY, 300–319.

Algar, W. R., & Krull, U. J. (2007). Towards multi-colour strategies for the detection of

   oligonucleotide hybridization using quantum dots as energy donors in fluorescence

   resonance energy transfer (FRET). *Analytica Chimica Acta*, *581*(2), 193–201.

Alonso, G. L., Salinas, M. R., & Garijo, J. (1998). Method to determine the authenticity of aroma of

   saffron (Crocus sativus L.). *Journal of Food Protection*, *61*(11), 1525–1528.

   https://doi.org/10.4315/0362-028X-61.11.1525

ALONSO, G. L., SALINAS, M. R., & GARIJO, J. (1998). Method to Determine the Authenticity of Aroma

   of Saffron (Crocus sativus L.). *Journal of Food Protection*, *61*(11), Article 11.

   https://doi.org/10.4315/0362-028X-61.11.1525

Amarowicz, R., & Pegg, R. B. (2019). Natural antioxidants of plant origin. In *Advances in Food and Nutrition Research* (Vol. 90, pp. 1–81). Academic Press Inc. https://doi.org/10.1016/bs.afnr.2019.02.011

Anastasaki, E., Kanakis, C., Pappas, C., Maggi, L., del Campo, C. P., Carmona, M., Alonso, G. L., & Polissiou, M. G. (2009). Geographical differentiation of saffron by GC-MS/FID and chemometrics. *European Food Research and Technology*, *229*(6), 899–905. https://doi.org/10.1007/s00217-009-1125-x

Ansell, R. J., Kriz, D., & Mosbach, K. (1996). Molecularly imprinted polymers for bioanalysis: Chromatography, binding assays and biomimetic sensors. *Current Opinion in Biotechnology*, *7*(1), 89–94. https://doi.org/10.1016/S0958-1669(96)80101-7

Araki, K., Maruyama, T., Kamiya, N., & Goto, M. (2005). Metal ion-selective membrane prepared by surface molecular imprinting. *Journal of Chromatography B*, *818*(2), 141–145. https://doi.org/10.1016/j.jchromb.2004.12.030

Arshad, M. S., & Batool, S. A. (2017). Natural Antimicrobials, their Sources and Food Safety. In *Food Additives*. InTech. https://doi.org/10.5772/intechopen.70197

Asgarpanah, J., Darabi-Mahboub, E., Mahboubi, A., Mehrab, R., & Hakemivala, M. (2013). In-Vitro Evaluation of Crocus Sativus L. Petals and Stamens as Natural Antibacterial Agents Against Food-Borne Bacterial Strains. In *Iranian Journal of Pharmaceutical Sciences* (Vol. 2013, Issue 9). Iranian Association of Pharmaceutical Scientists.

Ashktorab, H., Soleimani, A., Singh, G., Amr, A., Tabtabaei, S., Latella, G., Stein, U., Akhondzadeh, S., Solanki, N., Gondré-Lewis, M. C., Habtezion, A., & Brim, H. (2019). Saffron: The golden spice with therapeutic properties on digestive diseases. *Nutrients*, *11*(5). https://doi.org/10.3390/nu11050943

Ashok, V., Agrawal, N., Esteve-Romero, J., Bose, D., & Dubey, N. P. (2017). Detection of Methyl Orange in Saffron and Other Edibles Using Direct Injection Micellar Liquid Chromatography. *Food Analytical Methods*, *10*(1), 269–276. https://doi.org/10.1007/s12161-016-0578-3

Assimopoulou, A. N., Sinakos, Z., & Papageorgiou, V. P. (2005). Radical scavenging activity of Crocus

sativus L. extract and its bioactive constituents. *Phytotherapy Research*, *19*(11), 997–1000.

https://doi.org/10.1002/ptr.1749

Atchudan, R., Edison, T. N. J. I., Mani, S., Perumal, S., Vinodh, R., Thirunavukkarasu, S., & Lee, Y. R.

(2020). Facile synthesis of a novel nitrogen-doped carbon dot adorned zinc oxide composite

for photodegradation of methylene blue. *Dalton Transactions*, *49*(48), 17725–17736.

https://doi.org/10.1039/D0DT02756A

Azami, S., Shahriari, Z., Asgharzade, S., Farkhondeh, T., Sadeghi, M., Ahmadi, F., Vahedi, M. M., &

Forouzanfar, F. (2021). Therapeutic Potential of Saffron (Crocus sativus L.) in Ischemia

Stroke. *Evidence-Based Complementary and Alternative Medicine*, *2021*, e6643950.

https://doi.org/10.1155/2021/6643950

Baggiani, C., Baravalle, P., Anfossi, L., & Tozzi, C. (2005). Comparison of pyrimethanil-imprinted

beads and bulk polymer as stationary phase by non-linear chromatography. *Analytica*

Chimica Acta, *542*(1), 125–134. https://doi.org/10.1016/j.aca.2004.10.088

Bathaie, S. Z., Kermani, F. M. Z., & Shams, A. (2011). Crocin bleaching assay using purified di-

gentiobiosyl crocin (α-crocin) from Iranian saffron. *Iranian Journal of Basic Medical Sciences*,

14(5), 399–406. https://doi.org/10.22038/ijbms.2011.5034

Benítez-Martínez, S., & Valcárcel, M. (2014). Graphene quantum dots as sensor for phenols in olive

oil. *Sensors and Actuators B: Chemical*, *197*, 350–357.

Biancolillo, A., Foschi, M., & D'Archivio, A. A. (2020). Geographical Classification of Italian Saffron

(Crocus sativus L.) by Multi-Block Treatments of UV-Vis and IR Spectroscopic Data.

Molecules, *25*(10), Article 10. https://doi.org/10.3390/molecules25102332

Biancolillo, A., Maggi, M. A., De Martino, A., Marini, F., Ruggieri, F., & D'Archivio, A. A. (2020).

Authentication of PDO saffron of L'Aquila (Crocus sativus L.) by HPLC-DAD coupled with a

discriminant multi-way approach. *Food Control*, *110*, 107022.

Bogireddy, N. K. R., Lara, J., Fragoso, L. R., & Agarwal, V. (2020). One-step hydrothermal preparation

  of highly stable N doped oxidized carbon dots for toxic organic pollutants sensing and

  bioimaging. *Chemical Engineering Journal*, *401*, 126097.

  https://doi.org/10.1016/j.cej.2020.126097

Bukhari, S. I., Manzoor, M., & Dhar, M. K. (2018). A comprehensive review of the pharmacological

  potential of Crocus sativus and its bioactive apocarotenoids. In *Biomedicine and*

  Pharmacotherapy (Vol. 98, pp. 733–745). Elsevier Masson SAS.

  https://doi.org/10.1016/j.biopha.2017.12.090

Bukhari, S. I., Pattnaik, B., Rayees, S., Kaul, S., & Dhar, M. K. (2015). Safranal of Crocus sativus L.

  Inhibits Inducible Nitric Oxide Synthase and Attenuates Asthma in a Mouse Model of

  Asthma. *Phytotherapy Research*, *29*(4), 617–627. https://doi.org/10.1002/ptr.5315

Caballero-Ortega, H., Pereda-Miranda, R., Riverón-Negrete, L., Hernández, J. M., Medécigo-Ríos, M.,

  Castillo-Villanueva, A., & Abdullaev, F. I. (2004). Chemical composition of saffron (Crocus

  sativus L.) from four countries. *Acta Horticulturae*, *650*, 321–326.

  https://doi.org/10.17660/ActaHortic.2004.650.39

Cardone, L., Castronuovo, D., Perniola, M., Cicco, N., & Candido, V. (2020). Saffron (Crocus sativus

  L.), the king of spices: An overview. *Scientia Horticulturae*, *272*, 109560.

  https://doi.org/10.1016/j.scienta.2020.109560

Carmona, M., Sánchez, A. M., Ferreres, F., Zalacain, A., Tomás-Barberán, F., & Alonso, G. L. (2007).

  Identification of the flavonoid fraction in saffron spice by LC/DAD/MS/MS: Comparative

  study of samples from different geographical origins. *Food Chemistry*, *100*(2), 445–450.

  https://doi.org/10.1016/j.foodchem.2005.09.065

Cenci-Goga, B. T., Torricelli, R., Gonabad, Y. H., Ferradini, N., Venanzoni, R., Sechi, P., Iulietto, M. F.,

  & Albertini, E. (2018). In vitro bactericidal activities of various extracts of saffron (Crocus

  sativus L.) stigmas from Torbat-e Heydarieh, Gonabad and Khorasan, Iran. *Microbiology*

  Research, *9*(1), Article 1. https://doi.org/10.4081/mr.2018.7583

Chaisiwamongkhol, K., Labaidae, S., Pon-in, S., Pinsrithong, S., Bunchuay, T., & Phonchai, A. (2020). Smartphone-based colorimetric detection using gold nanoparticles of sibutramine in suspected food supplement products. *Microchemical Journal*, *158*, 105273.

Chang, L. (2022). *N, S-doped carbon quantum dots/TiO$_2$ nanocomposites for visible-light-driven photocatalytic degradation of water pollutants*.

Chen, L., Xu, S., & Li, J. (2011). Recent advances in molecular imprinting technology: Current status, challenges and highlighted applications. *Chemical Society Reviews*, *40*(5), 2922–2942. https://doi.org/10.1039/C0CS00084A

Christodoulou, E., Kadoglou, N. P., Kostomitsopoulos, N., & Valsami, G. (2015). Saffron: A natural product with potential pharmaceutical applications. *Journal of Pharmacy and Pharmacology*, *67*(12), 1634–1649. https://doi.org/10.1111/jphp.12456

Curcio, M., Cirillo, G., Parisi, O. I., Iemma, F., Picci, N., & Puoci, F. (2012). Quercetin-Imprinted Nanospheres as Novel Drug Delivery Devices. *Journal of Functional Biomaterials*, *3*(2), Article 2. https://doi.org/10.3390/jfb3020269

Cuttriss, A. J., Cazzonelli, C. I., Wurtzel, E. T., & Pogson, B. J. (2011). Carotenoids. In *Advances in Botanical Research* (Vol. 58, pp. 1–36). Academic Press Inc. https://doi.org/10.1016/B978-0-12-386479-6.00005-6

Das, I., Chakrabarty, R. N., & Das, S. (2004). Saffron can prevent chemically induced skin carcinogenesis in Swiss albino mice. *Asian Pacific Journal of Cancer Prevention: APJCP*, *5*(1), 70–76.

de Boer, T., Mol, R., de Zeeuw, R. A., de Jong, G. J., Sherrington, D. C., Cormack, P. A. G., & Ensing, K. (2002). Spherical molecularly imprinted polymer particles: A promising tool for molecular recognition in capillary electrokinetic separations. *ELECTROPHORESIS*, *23*(9), 1296–1300. https://doi.org/10.1002/1522-2683(200205)23:9<1296::AID-ELPS1296>3.0.CO;2-2

Delgado, M., Zalacain, A., Pardo, J., López, E., Alvarruiz, A., & Alonso, G. (2005). Influence of Different Drying and Aging Conditions on Saffron Constituents. *Journal of Agricultural and Food Chemistry*, *53*, 3974–3979. https://doi.org/10.1021/jf0404748

Dhar, M. K., Sharma, M., Bhat, A., Chrungoo, N. K., & Kaul, S. (2017). Functional genomics of apocarotenoids in saffron: Insights from chemistry, molecular biology and therapeutic applications. *Briefings in Functional Genomics*, *16*(6), 336–347. https://doi.org/10.1093/bfgp/elx003

Dickey, F. H. (1949). The Preparation of Specific Adsorbents. *Proceedings of the National Academy of Sciences*, *35*(5), 227–229. https://doi.org/10.1073/pnas.35.5.227

Downey, J. S., McIsaac, G., Frank, R. S., & Stöver, H. D. H. (2001). Poly(divinylbenzene) Microspheres as an Intermediate Morphology between Microgel, Macrogel, and Coagulum in Cross-Linking Precipitation Polymerization. *Macromolecules*, *34*(13), 4534–4541. https://doi.org/10.1021/ma000386y

Escribano, J., Alonso, G. L., Coca-Prados, M., & Fernández, J. A. (1996). Crocin, safranal and picrocrocin from saffron (Crocus sativus L.) inhibit the growth of human cancer cells in vitro. *Cancer Letters*, *100*(1–2), 23–30. https://doi.org/10.1016/0304-3835(95)04067-6

Ettehadi, H., Mojabi, S. N., Ranjbaran, M., Shams, J., Sahraei, H., Hedayati, M., & Asefi, F. (2013). Aqueous Extract of Saffron (Crocus sativus) Increases Brain Dopamine and Glutamate Concentrations in Rats. *Journal of Behavioral and Brain Science*, *3*(3), Article 3. https://doi.org/10.4236/jbbs.2013.33031

Fair, R. J., & Tor, Y. (2014). Antibiotics and bacterial resistance in the 21st century. *Perspectives in Medicinal Chemistry*, *6*(6), 25–64. https://doi.org/10.4137/PMC.S14459

Fairhurst, R. E., Chassaing, C., Venn, R. F., & Mayes, A. G. (2004). A direct comparison of the performance of ground, beaded and silica-grafted MIPs in HPLC and Turbulent Flow Chromatography applications. *Biosensors and Bioelectronics*, *20*(6), 1098–1105. https://doi.org/10.1016/j.bios.2004.01.020

Fatehi, M., Rashidabady, T., & Fatehi-Hassanabad, Z. (2003). Effects of Crocus sativus petals' extract on rat blood pressure and on responses induced by electrical field stimulation in the rat isolated vas deferens and guinea-pig ileum. *Journal of Ethnopharmacology*, *84*(2–3), 199–203. https://doi.org/10.1016/s0378-8741(02)00299-4

G. Gutheil, W., Reed, G., Ray, A., Anant, S., & Dhar, A. (2011). Crocetin: An Agent Derived from Saffron for Prevention and Therapy for Cancer. *Current Pharmaceutical Biotechnology*, *13*(1), 173–179. https://doi.org/10.2174/138920112798868566

Ghanbari, J., Khajoei-Nejad, G., Erasmus, S. W., & van Ruth, S. M. (2019). Identification and characterisation of volatile fingerprints of saffron stigmas and petals using PTR-TOF-MS: Influence of nutritional treatments and corm provenance. *Industrial Crops and Products*, *141*, 111803. https://doi.org/10.1016/j.indcrop.2019.111803

Giaccio, M. (2004). Crocetin from saffron: An active component of an ancient spice. *Critical Reviews in Food Science and Nutrition*, *44*(3), 155–172. https://doi.org/10.1080/10408690490441433

Gismondi, A., Serio, M., Canuti, L., & Canini, A. (2012). Biochemical, Antioxidant and Antineoplastic Properties of Italian Saffron (<i>Crocus sativus L</i>.). *American Journal of Plant Sciences*, *03*(11), 1573–1580. https://doi.org/10.4236/ajps.2012.311190

Gohari, A. R., Saeidnia, S., & Mahmoodabadi, M. K. (2013a). An overview on saffron, phytochemicals, and medicinal properties. *Pharmacognosy Reviews*, *7*(13), 61–66. https://doi.org/10.4103/0973-7847.112850

Gohari, A. R., Saeidnia, S., & Mahmoodabadi, M. K. (2013b). An overview on saffron, phytochemicals, and medicinal properties. In *Pharmacognosy Reviews* (Vol. 7, Issue 13, pp. 61–66). Pharmacogn Rev. https://doi.org/10.4103/0973-7847.112850

González, G. P., Hernando, P. F., & Alegría, J. S. D. (2006). A morphological study of molecularly imprinted polymers using the scanning electron microscope. *Analytica Chimica Acta*, *557*(1), 179–183. https://doi.org/10.1016/j.aca.2005.10.034

Guo, Y., Girmatsion, M., Li, H.-W., Xie, Y., Yao, W., Qian, H., Abraha, B., & Mahmud, A. (2021). Rapid and ultrasensitive detection of food contaminants using surface-enhanced Raman spectroscopy-based methods. *Critical Reviews in Food Science and Nutrition*, *61*(21), 3555–3568. https://doi.org/10.1080/10408398.2020.1803197

Hadizadeh, F., Mahdavi, M., Emami, S. A., Khashayarmanesh, Z., Hassanzadeh, M., Asili, J., Seifi, M., Nassirli, H., Shariatimoghadam, A., & Noorbakhsh, R. (2007). EVALUATION OF ISO METHOD IN SAFFRON QUALIFICATION. *Acta Horticulturae*, *739*, 405–410. https://doi.org/10.17660/ActaHortic.2007.739.53

Haghighi, B., Feizy, J., & Kakhki, A. H. (2007). LC Determination of Adulterated Saffron Prepared by Adding Styles Colored with Some Natural Colorants. *Chromatographia*, *66*(5–6), 325–332. https://doi.org/10.1365/s10337-007-0321-8

Haginaka, J., & Kagawa, C. (2002). Uniformly sized molecularly imprinted polymer for d-chlorpheniramine: Evaluation of retention and molecular recognition properties in an aqueous mobile phase. *Journal of Chromatography A*, *948*(1), 77–84. https://doi.org/10.1016/S0021-9673(01)01262-6

Haginaka, J., & Sakai, Y. (2000). Uniform-sized molecularly imprinted polymer material for (S)-propranolol. *Journal of Pharmaceutical and Biomedical Analysis*, *22*(6), 899–907. https://doi.org/10.1016/S0731-7085(00)00293-4

Hamidi, Z., Aryaeian, N., Abolghasemi, J., Shirani, F., Hadidi, M., Fallah, S., & Moradi, N. (2020). The effect of saffron supplement on clinical outcomes and metabolic profiles in patients with active rheumatoid arthritis: A randomized, double-blind, placebo-controlled clinical trial. *Phytotherapy Research: PTR*, *34*(7), 1650–1658. https://doi.org/10.1002/ptr.6633

Handford, C. E., Campbell, K., & Elliott, C. T. (2016). Impacts of milk fraud on food safety and nutrition with special emphasis on developing countries. *Comprehensive Reviews in Food Science and Food Safety*, *15*(1), 130–142.

Haque, Md. M., Haque, Md. A., Mosharaf, M. K., & Marcus, P. K. (2021). Decolorization, degradation and detoxification of carcinogenic sulfonated azo dye methyl orange by newly developed biofilm consortia. *Saudi Journal of Biological Sciences*, *28*(1), 793–804. https://doi.org/10.1016/j.sjbs.2020.11.012

Hatziagapiou, K., & Lambrou, G. I. (2018). The Protective Role of Crocus Sativus L. (Saffron) Against Ischemia- Reperfusion Injury, Hyperlipidemia and Atherosclerosis: Nature Opposing Cardiovascular Diseases. *Current Cardiology Reviews*, *14*(4), 272–289. https://doi.org/10.2174/1573403x14666180628095918

Haupt, K., & Mosbach, K. (2000). Molecularly Imprinted Polymers and Their Use in Biomimetic Sensors. *Chemical Reviews*, *100*(7), 2495–2504. https://doi.org/10.1021/cr990099w

Heidarbeigi, K., Mohtasebi, S. S., Foroughirad, A., Ghasemi-Varnamkhasti, M., Rafiee, S., & Rezaei, K. (2015). Detection of adulteration in saffron samples using electronic nose. *International Journal of Food Properties*, *18*(7), 1391–1401. https://doi.org/10.1080/10942912.2014.915850

Hernández-Cortez, C., Palma-Martínez, I., Gonzalez-Avila, L. U., Guerrero-Mandujano, A., Solís, R. C., & Castro-Escarpulli, G. (2017). Food Poisoning Caused by Bacteria (Food Toxins). In *Poisoning—From Specific Toxic Agents to Novel Rapid and Simplified Techniques for Analysis*. InTech. https://doi.org/10.5772/intechopen.69953

Hirayama, K., Sakai, Y., Kameoka, K., Noda, K., & Naganawa, R. (2002). Preparation of a sensor device with specific recognition sites for acetaldehyde by molecular imprinting technique. *Sensors and Actuators B: Chemical*, *86*(1), 20–25. https://doi.org/10.1016/S0925-4005(02)00107-7

Ho, K.-C., Yeh, W.-M., Tung, T.-S., & Liao, J.-Y. (2005). Amperometric detection of morphine based on poly(3,4-ethylenedioxythiophene) immobilized molecularly imprinted polymer particles prepared by precipitation polymerization. *Analytica Chimica Acta*, *542*(1), 90–96. https://doi.org/10.1016/j.aca.2005.02.036

Hosoya, K., Yoshizako, K., Shirasu, Y., Kimata, K., Araki, T., Tanaka, N., & Haginaka, J. (1996).

Molecularly imprinted uniform-size polymer-based stationary phase for high-performance

liquid chromatography structural contribution of cross-linked polymer network on specific

molecular recognition. *Journal of Chromatography A*, *728*(1), 139–147.

https://doi.org/10.1016/0021-9673(95)01165-X

Hosseinzadeh, H., bullet, P., & Khosravan, V. (2001). Anticonvulsant effect of Crocus sativus L.

stigmas aqueous and ethanolic extracts in mice. Arch Iranian Med. *Arch Iran Med*, *5*.

Hosseinzadeh, H., & Nassiri-Asl, M. (2013). Avicenna's (Ibn Sina) the canon of medicine and saffron

(Crocus sativus): A review. In *Phytotherapy Research* (Vol. 27, Issue 4, pp. 475–483).

https://doi.org/10.1002/ptr.4784

Hosseinzadeh, H., & Sadeghnia, H. R. (2005). Safranal, a constituent of Crocus sativus (saffron),

attenuated cerebral ischemia induced oxidative damage in rat hippocampus. *Journal of

Pharmacy & Pharmaceutical Sciences: A Publication of the Canadian Society for

Pharmaceutical Sciences, Societe Canadienne Des Sciences Pharmaceutiques*, *8*(3), 394–399.

Hosseinzadeh, H., & Sadeghnia, H. R. (2007). Protective effect of safranal on pentylenetetrazol-

induced seizures in the rat: Involvement of GABAergic and opioids systems. *Phytomedicine:

International Journal of Phytotherapy and Phytopharmacology*, *14*(4), 256–262.

https://doi.org/10.1016/j.phymed.2006.03.007

Hosseinzadeh, H., & Talebzadeh, F. (2005). Anticonvulsant evaluation of safranal and crocin from

Crocus sativus in mice. *Fitoterapia*, *76*(7), 722–724.

https://doi.org/10.1016/j.fitote.2005.07.008

Husaini, A., bullet, Kamili, A., Wani, bullet, & Bhat, bullet. (2010). *Sustainable Saffron (Crocus

sativus Kashmirianus) Production: Technological and Policy Interventions for Kashmir*.

Hussain, A. (2005, January 28). Saffron industry in deep distress. *BBC NEWS*.

http://news.bbc.co.uk/2/hi/south_asia/4216493.stm

Iman Yousefi Javan, & Yousef Hosseinzadehgonabad. (2017). Isolation of Main Genes Involved in

   Flowering of Saffron (Crocus sativus L.) in Order to Study Effective Flowering Protein. *Journal*

   of Food Science and Engineering, *7*(8). https://doi.org/10.17265/2159-5828/2017.08.003

Inbaraj, B. S., & Chen, B. (2016). Nanomaterial-based sensors for detection of foodborne bacterial

   pathogens and toxins as well as pork adulteration in meat products. *Journal of Food and*

   Drug Analysis, *24*(1), 15–28.

ISO - ISO 3632-1:2011—Spices—Saffron (Crocus sativus L.)—Part 1: Specification. (n.d.). Retrieved

   December 17, 2019, from https://www.iso.org/standard/44523.html

Jalali-Heravi, M., Parastar, H., & Ebrahimi-Najafabadi, H. (2009). Characterization of volatile

   components of Iranian saffron using factorial-based response surface modeling of ultrasonic

   extraction combined with gas chromatography-mass spectrometry analysis. *Journal of*

   Chromatography A, *1216*(33), 6088–6097. https://doi.org/10.1016/j.chroma.2009.06.067

Jana, J., Ganguly, M., & Pal, T. (2016). Enlightening surface plasmon resonance effect of metal

   nanoparticles for practical spectroscopic application. *RSC Advances*, *6*(89), 86174–86211.

Javanmardi, N., Bagheri, A., Moshtaghi, N., Sharifi, A., & Kakhki, A. H. (2011). *Identification of*

   Safflower as a fraud in commercial Saffron using RAPD / SCAR marker. *3*(February 2015), 31–

   37.

Kaavya, R., Pandiselvam, R., Mohammed, M., Dakshayani, R., Kothakota, A., Ramesh, S., Cozzolino,

   D., & Ashokkumar, C. (2020). Application of infrared spectroscopy techniques for the

   assessment of quality and safety in spices: A review. *Applied Spectroscopy Reviews*, *55*(7),

   593–611.

Kadian, S., & Manik, G. (2020a). A highly sensitive and selective detection of picric acid using

   fluorescent sulfur-doped graphene quantum dots. *Luminescence*, *35*(5), 763–772.

Kadian, S., & Manik, G. (2020b). Sulfur doped graphene quantum dots as a potential sensitive

   fluorescent probe for the detection of quercetin. *Food Chemistry*, *317*, 126457.

Kahriz, P. P. (2020). Saffron (Crocus sativus L.) Cultivation in Turkey. In *Saffron* (pp. 33–43). Elsevier.

Kamalipour, M., & Akhondzadeh, S. (2011). Cardiovascular effects of saffron: An evidence-based review. *The Journal of Tehran Heart Center*, *6*(2), Article 2.

Kanakis, C. D., Tarantilis, P. A., Tajmir-Riahi, H. A., & Polissiou, M. G. (2007). Crocetin, dimethylcrocetin, and safranal bind human serum albumin: Stability and antioxidative properties. *Journal of Agricultural and Food Chemistry*, *55*(3), 970–977. https://doi.org/10.1021/jf062638l

Karimi, E., Oskoueian, E., Hendra, R., & Jaafar, H. Z. E. (2010a). Evaluation of Crocus sativus L. stigma phenolic and flavonoid compounds and its antioxidant activity. *Molecules*, *15*(9), 6244–6256. https://doi.org/10.3390/molecules15096244

Karimi, E., Oskoueian, E., Hendra, R., & Jaafar, H. Z. E. (2010b). Evaluation of Crocus sativus L. Stigma Phenolic and Flavonoid Compounds and Its Antioxidant Activity. *Molecules*, *15*(9), Article 9. https://doi.org/10.3390/molecules15096244

Karimi, S., Feizy, J., Mehrjo, F., & Farrokhnia, M. (2016a). Detection and quantification of food colorant adulteration in saffron sample using chemometric analysis of FT-IR spectra. *RSC Advances*, *6*(27), 23085–23093. https://doi.org/10.1039/c5ra25983e

Karimi, S., Feizy, J., Mehrjo, F., & Farrokhnia, M. (2016b). Detection and quantification of food colorant adulteration in saffron sample using chemometric analysis of FT-IR spectra. *RSC Advances*, *6*(27), 23085–23093.

Keller, M., Fankhauser, S., Giezendanner, N., König, M., Keresztes, F., Danton, O., Hamburger, M., Butterweck, V., & Potterat, O. (2019). Saponins from saffron corms inhibit the secretion of pro-inflammatory cytokines at both protein and gene levels. *Planta Med*, *85*(18), SL A-03.

Khalili, M., Kiasalari, Z., Rahmati, B., & Narenjkar, J. (2010). *Behavioral and histological analysis of Crocus sativus effect in intracerebroventricular streptozotocin model of Alzheimer disease in rats*.

Khazdair, M. R., Boskabady, M. H., Hosseini, M., Rezaee, R., & M Tsatsakis, A. (2015). The effects of Crocus sativus (saffron) and its constituents on nervous system: A review. *Avicenna Journal of Phytomedicine*, *5*(5), 376–391. https://doi.org/10.22038/ajp.2015.4503

Khorasany, A. R., & Hosseinzadeh, H. (2016). Therapeutic effects of saffron (Crocus sativus L.) in digestive disorders: A review. *Iranian Journal of Basic Medical Sciences*, *19*(5), 455–469.

Khurshid Wani, A., Akhtar, N., Mir, T.-U. G., & Singh, R. (2021). *Extraction designs and therapeutic attributes associated with limonene: A review Plant Plant Archives EXTRACTION DESIGNS AND THERAPEUTIC ATTRIBUTES ASSOCIATED WITH LIMONENE: A REVIEW*. https://doi.org/10.51470/PLANTARCHIVES.2021.v21.S1.254

Khurshid Wani, A., Singh, R., Mir, T.-U. G., & Akhtar, N. (2022). *Limonene extraction from the zest of Citrus sinensis, Citrus limon, Vitis vinifera and evaluation of its antimicrobial activity*. *16*, 309–314.

Kooyman, R. P. (2008). Physics of surface plasmon resonance. *Handbook of Surface Plasmon Resonance*, *1*.

Kosar, M., Demirci, B., Goger, F., Kara, I., & Baser, K. H. C. (2017). Volatile composition, antioxidant activity, and antioxidant components in saffron cultivated in Turkey. *International Journal of Food Properties*, *20*(sup1), S746–S754. https://doi.org/10.1080/10942912.2017.1311341

Kriz, D., Ramström, O., & Mosbach, K. (2011). *Peer Reviewed: Molecular Imprinting: New Possibilities for Sensor Technology* (world). https://doi.org/10.1021/ac971657e

Kubiak, A., Ciric, A., & Biesaga, M. (2020). Dummy molecularly imprinted polymer (DMIP) as a sorbent for bisphenol S and bisphenol F extraction from food samples. *Microchemical Journal*, *156*, 104836. https://doi.org/10.1016/j.microc.2020.104836

Kuila, T., Bose, S., Khanra, P., Mishra, A. K., Kim, N. H., & Lee, J. H. (2012). A green approach for the reduction of graphene oxide by wild carrot root. *Carbon*, *50*(3), 914–921. https://doi.org/10.1016/j.carbon.2011.09.053

Kumar, N., Seth, R., & Kumar, H. (2014). Colorimetric detection of melamine in milk by citrate-stabilized gold nanoparticles. *Analytical Biochemistry*, *456*, 43–49.

Kumari, L., Jaiswal, P., & Tripathy, S. (2021a). Various techniques useful for determination of adulterants in valuable saffron: A review. *Trends in Food Science & Technology*, *111*. https://doi.org/10.1016/j.tifs.2021.02.061

Kumari, L., Jaiswal, P., & Tripathy, S. S. (2021b). Various techniques useful for determination of adulterants in valuable saffron: A review. *Trends in Food Science & Technology*, *111*, 301–321. https://doi.org/10.1016/j.tifs.2021.02.061

Lei, J.-D., & Tong, A.-J. (2005). Preparation of Z-l-Phe-OH-NBD imprinted microchannel and its molecular recognition study. *Spectrochimica Acta Part A: Molecular and Biomolecular Spectroscopy*, *61*(6), 1029–1033. https://doi.org/10.1016/j.saa.2004.06.001

Li, H., Li, Y., & Cheng, J. (2010). Molecularly Imprinted Silica Nanospheres Embedded CdSe Quantum Dots for Highly Selective and Sensitive Optosensing of Pyrethroids. *Chemistry of Materials*, *22*(8), 2451–2457. https://doi.org/10.1021/cm902856y

Li, H., Li, Y., Wang, D., Wang, J., Zhang, J., Jiang, W., Zhou, T., Liu, C., & Che, G. (2021). Synthesis of hydrophilic SERS-imprinted membrane based on graft polymerization for selective detection of L-tyrosine. *Sensors and Actuators B: Chemical*, *340*, 129955. https://doi.org/10.1016/j.snb.2021.129955

Li, P., Rong, F., & Yuan, C. (2003). Morphologies and binding characteristics of molecularly imprinted polymers prepared by precipitation polymerization. *Polymer International*, *52*(12), 1799–1806. https://doi.org/10.1002/pi.1381

Liu, D.-D., Ye, Y.-L., Zhang, J., Xu, J.-N., Qian, X.-D., & Zhang, Q. (2014). Distinct pro-apoptotic properties of Zhejiang saffron against human lung cancer via a caspase-8-9-3 cascade. *Asian Pacific Journal of Cancer Prevention: APJCP*, *15*(15), 6075–6080. https://doi.org/10.7314/apjcp.2014.15.15.6075

Liu, H., Row, K. H., & Yang, G. (2005). Monolithic Molecularly Imprinted Columns for

Chromatographic Separation. *Chromatographia*, *61*(9), 429–432.

https://doi.org/10.1365/s10337-005-0531-x

Lopresti, A. L., Smith, S. J., Metse, A. P., & Drummond, P. D. (2020). Effects of saffron on sleep quality

in healthy adults with self-reported poor sleep: A randomized, double-blind, placebo-

controlled trial. *Journal of Clinical Sleep Medicine*, *16*(6), 937–947.

https://doi.org/10.5664/jcsm.8376

Lowell, G. (1964). Saffron Adulteration. *Journal of Association of Official Agricultural Chemists*, *47*(3),

538. https://doi.org/10.1093/jaoac/47.3.538

Lozano, P., Castellar, M. R., Simancas, M. J., & Iborra, J. L. (1999a). A quantitative high-performance

liquid chromatographic method to analyse commercial saffron (Crocus sativus L.) products.

Journal of Chromatography A, *830*(2), 477–483. https://doi.org/10.1016/S0021-

9673(98)00938-8

Lozano, P., Castellar, M. R., Simancas, M. J., & Iborra, J. L. (1999b). A quantitative high-performance

liquid chromatographic method to analyse commercial saffron (Crocus sativus L.) products.

Journal of Chromatography A, *830*(2), Article 2. https://doi.org/10.1016/S0021-

9673(98)00938-8

Ma, X. Q., Zhu, D. Y., Li, S. P., Dong, T. T. X., & Tsim, K. W. K. (2001). Authentic identification of

Stigma Croci (stigma of Crocus sativus) from its adulterants by molecular genetic analysis.

Planta Medica, *67*(2), 183–186. https://doi.org/10.1055/s-2001-11533

Madikizela, L., Tavengwa, N., & Pakade, V. (2017). Molecularly Imprinted Polymers for

Pharmaceutical Compounds: Synthetic Procedures and Analytical Applications. In *Recent

Research in Polymerization*. IntechOpen. https://doi.org/10.5772/intechopen.71475

Magesh, V., DurgaBhavani, K., Senthilnathan, P., Rajendran, P., & Sakthisekaran, D. (2009). In vivo

protective effect of crocetin on benzo(a)pyrene-induced lung cancer in Swiss albino mice.

Phytotherapy Research: PTR, *23*(4), 533–539. https://doi.org/10.1002/ptr.2666

Magesh, V., Singh, J. P. V., Selvendiran, K., Ekambaram, G., & Sakthisekaran, D. (2006). Antitumour activity of crocetin in accordance to tumor incidence, antioxidant status, drug metabolizing enzymes and histopathological studies. *Molecular and Cellular Biochemistry*, *287*(1–2), 127–135. https://doi.org/10.1007/s11010-005-9088-0

Maggi, L., Sánchez, A. M., Carmona, M., Kanakis, C. D., Anastasaki, E., Tarantilis, P. A., Polissiou, M. G., & Alonso, G. L. (2011). Rapid determination of safranal in the quality control of saffron spice (Crocus sativus L.). *Food Chemistry*, *127*(1), 369–373. https://doi.org/10.1016/j.foodchem.2011.01.028

Maghsoodi, V., Kazemi, A., & Akhondi, E. (2012). Effect of Different Drying Methods on Saffron (Crocus Sativus L) Quality. *IRANIAN JOURNAL OF CHEMISTRY & CHEMICAL ENGINEERING-INTERNATIONAL ENGLISH EDITION*, *31*, 85–89.

Mahmoudabady, M., Neamati, A., Vosooghi, S., & Aghababa, H. (2013). Hydroalcoholic extract of Crocus sativus effects on bronchial inflammatory cells in ovalbumin sensitized rats. *Avicenna Journal of Phytomedicine*, *3*(4), 356–363.

Malavi, D., Nikkhah, A., Alighaleh, P., Einafshar, S., Raes, K., & Van Haute, S. (2024). Detection of saffron adulteration with *Crocus sativus* style using NIR-hyperspectral imaging and chemometrics. *Food Control*, *157*, 110189. https://doi.org/10.1016/j.foodcont.2023.110189

Marieschi, M., Torelli, A., & Bruni, R. (2012). Quality Control of Saffron (Crocus sativus L.): Development of SCAR Markers for the Detection of Plant Adulterants Used as Bulking Agents. *Journal of Agricultural and Food Chemistry*, *60*(44), 10998–11004. https://doi.org/10.1021/jf303106r

MATSUI, J., MIYOSHI, Y., MATSUI, R., & TAKEUCHI, T. (1995). Rod-Type Affinity Media for Liquid Chromatography Prepared by in-situ-Molecular Imprinting. *Analytical Sciences*, *11*(6), 1017–1019. https://doi.org/10.2116/analsci.11.1017

Mecker, L. C., Tyner, K. M., Kauffman, J. F., Arzhantsev, S., Mans, D. J., & Gryniewicz-Ruzicka, C. M. (2012). Selective melamine detection in multiple sample matrices with a portable Raman

instrument using surface enhanced Raman spectroscopy-active gold nanoparticles. *Analytica Chimica Acta*, *733*, 48–55.

Mehri, S., Abnous, K., Khooei, A., Mousavi, S. H., Shariaty, V. M., & Hosseinzadeh, H. (2015). Crocin reduced acrylamide-induced neurotoxicity in wistar rat through inhibition of oxidative stress. *Iranian Journal of Basic Medical Sciences*, *18*(9), 902–908. https://doi.org/10.22038/ijbms.2015.5213

Mgbeahuruike, E. E., Yrjönen, T., Vuorela, H., & Holm, Y. (2017). Bioactive compounds from medicinal plants: Focus on Piper species. In *South African Journal of Botany* (Vol. 112, pp. 54–69). Elsevier B.V. https://doi.org/10.1016/j.sajb.2017.05.007

Milajerdi, A., Djafarian, K., & Hosseini, B. (2016). The toxicity of saffron (Crocus sativus L.) and its constituents against normal and cancer cells. In *Journal of Nutrition and Intermediary Metabolism* (Vol. 3, pp. 23–32). Elsevier Inc. https://doi.org/10.1016/j.jnim.2015.12.332

Mir, T. ul G., Shukla, S., Malik, A. Q., Singh, J., & Kumar, D. (2023). Microwave-assisted synthesis of N-doped carbon quantum dots for detection of methyl orange in saffron. *Chemical Papers*. https://doi.org/10.1007/s11696-023-02726-2

Mir, T. ul G., Wani, A. K., Singh, J., & Shukla, S. (2022). Therapeutic application and toxicity associated with Crocus sativus (saffron) and its phytochemicals. *Pharmacological Research - Modern Chinese Medicine*, *4*, 100136. https://doi.org/10.1016/j.prmcm.2022.100136

Mir, T.-U. G., Khurshid Wani, A., Shukla, S., & Singh, J. (2022). *Crocus Sativus: Comprehensive Pharmacological Significance and Forensic Identification of Saffron in Illegal Trade*. *14*. https://doi.org/10.21088/ijfmp.0974.3383.14221.38

Moallem, S. A., Hariri, A. T., Mahmoudi, M., & Hosseinzadeh, H. (2014). Effect of aqueous extract of Crocus sativus L. (saffron) stigma against subacute effect of diazinon on specific biomarkers in rats. *Toxicology and Industrial Health*, *30*(2), 141–146. https://doi.org/10.1177/0748233712452609

Mohajeri, S. A., Malaekeh-Nikouei, B., & Sadegh, H. (2012). Development of a pH-responsive

imprinted polymer for diclofenac and study of its binding properties in organic and aqueous

media. *Drug Development and Industrial Pharmacy*, *38*(5), 616–622.

https://doi.org/10.3109/03639045.2011.621126

Mollazadeh, H., Emami, S. A., & Hosseinzadeh, H. (2015). Razi's Al-Hawi and saffron (Crocus sativus):

A review. *Iranian Journal of Basic Medical Sciences*, *18*(12), 1153–1166.

Mottaghipisheh, J., Mahmoodi Sourestani, M., Kiss, T., Horváth, A., Tóth, B., Ayanmanesh, M.,

Khamushi, A., & Csupor, D. (2020). Comprehensive chemotaxonomic analysis of saffron

crocus tepal and stamen samples, as raw materials with potential antidepressant activity.

Journal of Pharmaceutical and Biomedical Analysis, *184*, 113183.

https://doi.org/10.1016/j.jpba.2020.113183

Mykhailenko, O., Kovalyov, V., Goryacha, O., Ivanauskas, L., & Georgiyants, V. (2019). Biologically

active compounds and pharmacological activities of species of the genus Crocus: A review. In

Phytochemistry (Vol. 162, pp. 56–89). Elsevier Ltd.

https://doi.org/10.1016/j.phytochem.2019.02.004

Mzabri, I., Addi, M., & Berrichi, A. (2019a). Traditional and Modern Uses of Saffron (Crocus Sativus).

Cosmetics, *6*(4), Article 4. https://doi.org/10.3390/cosmetics6040063

Mzabri, I., Addi, M., & Berrichi, A. (2019b). Traditional and Modern Uses of Saffron (Crocus Sativus).

Cosmetics, *6*(4), Article 4. https://doi.org/10.3390/cosmetics6040063

Naeimi, M., Shafiee, M., Kermanshahi, F., Khorasanchi, Z., Khazaei, M., Ryzhikov, M., Avan, A., Gorji,

N., & Hassanian, S. M. (2019). Saffron (*Crocus sativus*) in the treatment of gastrointestinal

cancers: Current findings and potential mechanisms of action. *Journal of Cellular*

Biochemistry, *120*(10), 16330–16339. https://doi.org/10.1002/jcb.29126

Nakamura, M., Ono, M., Nakajima, T., Ito, Y., Aketo, T., & Haginaka, J. (2005). Uniformly sized

molecularly imprinted polymer for atropine and its application to the determination of

atropine and scopolamine in pharmaceutical preparations containing Scopolia extract.

Journal of Pharmaceutical and Biomedical Analysis, *37*(2), 231–237.

https://doi.org/10.1016/j.jpba.2004.10.017

Nazari, S. H., & Keifi, N. (2007). Saffron and various fraud manners in its production and trades. *Acta Horticulturae*, *739*, 411–416. https://doi.org/10.17660/actahortic.2007.739.54

Ohno, Y., Nakanishi, T., Umigai, N., Tsuruma, K., Shimazawa, M., & Hara, H. (2012). Oral administration of crocetin prevents inner retinal damage induced by N-methyl-D-aspartate in mice. *European Journal of Pharmacology*, *690*(1–3), 84–89.

https://doi.org/10.1016/j.ejphar.2012.06.035

O'Mahony, J., Molinelli, A., Nolan, K., Smyth, M. R., & Mizaikoff, B. (2006). Anatomy of a successful imprint: Analysing the recognition mechanisms of a molecularly imprinted polymer for quercetin. *Biosensors & Bioelectronics*, *21*(7), 1383–1392.

https://doi.org/10.1016/j.bios.2005.05.015

Ordoudi, S., Cagliani, L., Melidou, D., Tsimidou, M., & Consonni, R. (2017). Uncovering a challenging case of adulterated commercial saffron. *Food Control*, *81*, 147–155.

Pandita, D. (2021a). Saffron (Crocus sativus L.): Phytochemistry, therapeutic significance and omics-based biology. In *Medicinal and Aromatic Plants* (pp. 325–396). Elsevier.

https://doi.org/10.1016/b978-0-12-819590-1.00014-8

Pandita, D. (2021b). Saffron (Crocus sativus L.): Phytochemistry, therapeutic significance and omics-based biology. In *Medicinal and Aromatic Plants* (pp. 325–396). Elsevier.

Pang, X., Cheng, G., Li, R., Lu, S., & Zhang, Y. (2005). Bovine serum albumin-imprinted polyacrylamide gel beads prepared via inverse-phase seed suspension polymerization. *Analytica Chimica Acta*, *550*(1), 13–17. https://doi.org/10.1016/j.aca.2005.06.067

Parmar, I., Gehlot, P., Modi, V., & Patel, D. (2022). Recent developments in food adulteration analytical techniques. *International Journal of Pharmaceutical Science and Research*, *13*(5), 2001–2012.

Patel, K., Maguigan, K., & Shoulders, B. (2019). 648: EVALUATION OF BETA-LACTAM
    CONCENTRATIONS ASSOCIATED WITH EXTENDED DAILY DIALYSIS. *Critical Care Medicine*,
    47(1), 304. https://doi.org/10.1097/01.ccm.0000551400.16360.6c

Petrakis, E. A., Cagliani, L. R., Polissiou, M. G., & Consonni, R. (2015). Evaluation of saffron (Crocus
    sativus L.) adulteration with plant adulterants by 1H NMR metabolite fingerprinting. *Food
    Chemistry*, *173*, 890–896. https://doi.org/10.1016/j.foodchem.2014.10.107

Piacham, T., Josell, Å., Arwin, H., Prachayasittikul, V., & Ye, L. (2005). Molecularly imprinted polymer
    thin films on quartz crystal microbalance using a surface bound photo-radical initiator.
    Analytica Chimica Acta, *536*(1), 191–196. https://doi.org/10.1016/j.aca.2004.12.067

Purushothuman, S., Nandasena, C., Peoples, C. L., El Massri, N., Johnstone, D. M., Mitrofanis, J., &
    Stone, J. (2013). Saffron Pre-Treatment Offers Neuroprotection to Nigral and Retinal
    Dopaminergic Cells of MPTP-Treated mice. *Journal of Parkinson's Disease*, *3*(1), 77–83.
    https://doi.org/10.3233/JPD-130173

Rajabi, F., Rahimi, M., Sharbafchizadeh, M., & Tarrahi, M. (2020). Saffron for the management of
    premenstrual dysphoric disorder: A randomized controlled trial. *Advanced Biomedical
    Research*, *9*(1), 60. https://doi.org/10.4103/abr.abr_49_20

Rameshrad, M., Razavi, B. M., & Hosseinzadeh, H. (2018). Saffron and its derivatives, crocin, crocetin
    and safranal: A patent review. In *Expert Opinion on Therapeutic Patents* (Vol. 28, Issue 2, pp.
    147–165). Taylor and Francis Ltd. https://doi.org/10.1080/13543776.2017.1355909

Rani, S., Das, R. K., Jaiswal, A., Singh, G. P., Palwe, A., Saxena, S., & Shukla, S. (2023). 4D nanoprinted
    sensor for facile organo-arsenic detection: A two-photon lithography-based approach.
    Chemical Engineering Journal, *454*, 140130.

Ravichandran, R. (2010). Nanotechnology applications in food and food processing: Innovative green
    approaches, opportunities and uncertainties for global market. *International Journal of
    Green Nanotechnology: Physics and Chemistry*, *1*(2), P72–P96.

Ravindran, N., Kumar, S., CA, M., Thirunavookarasu S, N., & CK, S. (2021). Recent advances in Surface Plasmon Resonance (SPR) biosensors for food analysis: A review. *Critical Reviews in Food Science and Nutrition*, 1–23.

Razak, S. I. A., Hamzah, M. S. A., Yee, F. C., Kadir, M. R. A., & Nayan, N. H. M. (2017). A Review on Medicinal Properties of Saffron toward Major Diseases. *Journal of Herbs, Spices & Medicinal Plants*, *23*(2), 98–116. https://doi.org/10.1080/10496475.2016.1272522

Razavi, B. M., & Hosseinzadeh, H. (2017). Saffron: A promising natural medicine in the treatment of metabolic syndrome. In *Journal of the Science of Food and Agriculture* (Vol. 97, Issue 6, pp. 1679–1685). John Wiley and Sons Ltd. https://doi.org/10.1002/jsfa.8134

Ren, X., Liu, H., & Chen, L. (2015). Fluorescent detection of chlorpyrifos using Mn(II)-doped ZnS quantum dots coated with a molecularly imprinted polymer. *Microchimica Acta*, *182*(1), 193–200. https://doi.org/10.1007/s00604-014-1317-3

Rimmer, S. (1998). Synthesis of molecular imprinted polymer networks. *Chromatographia*, *47*(7), 470–474. https://doi.org/10.1007/BF02466483

Rubio-Moraga, Á., Gerwig, G. J., Castro-Díaz, N., Jimeno, M. L., Escribano, J., Fernández, J.-A., & Kamerling, J. P. (2011). Triterpenoid saponins from corms of Crocus sativus: Localization, extraction and characterization. *Industrial Crops and Products*, *34*(3), 1401–1409. https://doi.org/10.1016/j.indcrop.2011.04.013

Rubio-Moraga, Á., Gómez-Gómez, L., Trapero, A., Castro-Díaz, N., & Ahrazem, O. (2013). Saffron corm as a natural source of fungicides: The role of saponins in the underground. *Industrial Crops and Products*, *49*, 915–921. https://doi.org/10.1016/j.indcrop.2013.06.029

Rückert, B., Hall, A. J., & Sellergren, B. (2002). Molecularly imprinted composite materials via iniferter-modified supports. *Journal of Materials Chemistry*, *12*(8), 2275–2280. https://doi.org/10.1039/B203115A

Sabatino, L., Scordino, M., Gargano, M., Belligno, A., Traulo, P., & Gagliano, G. (2011). HPLC/PDA/ESI-MS evaluation of saffron (Crocus sativus L.) adulteration. *Natural Product Communications*, *6*(12), 1934578X1100601220.

Sadi, R., Mohammad-Alizadeh-Charandabi, S., Mirghafourvand, M., Javadzadeh, Y., & Ahmadi-Bonabi, A. (2016). Effect of saffron (Fan Hong Hua) on the readiness of the uterine cervix in term pregnancy: A placebo-controlled randomized trial. *Iranian Red Crescent Medical Journal*, *18*(10), 27241. https://doi.org/10.5812/ircmj.27241

Samarghandian, S., Azimi-Nezhad, M., & Farkhondeh, T. (2017). Immunomodulatory and antioxidant effects of saffron aqueous extract (Crocus sativus L.) on streptozotocin-induced diabetes in rats. *Indian Heart Journal*, *69*(2), 151–159. https://doi.org/10.1016/j.ihj.2016.09.008

Samarghandian, S., & Borji, A. (2014). Anticarcinogenic effect of saffron (Crocus sativus L.) and its ingredients. In *Pharmacognosy Research* (Vol. 6, Issue 2, pp. 99–107). Pharmacognosy Network Worldwide. https://doi.org/10.4103/0974-8490.128963

SAMBE, H., HOSHINA, K., & HAGINAKA, J. (2005). Retentivity and Enantioselectivity of Uniformly-sized Molecularly Imprinted Polymers for (S)-Nilvadipine in Aqueous and Non-Aqueous Mobile Phases. *Analytical Sciences*, *21*(4), 391–395. https://doi.org/10.2116/analsci.21.391

Saxena, R. (2010). Botany, taxonomy and cytology of Crocus sativus series. *AYU (An International Quarterly Journal of Research in Ayurveda)*, *31*(3), 374. https://doi.org/10.4103/0974-8520.77153

Saxena, R. B. (2010). Botany, taxonomy and cytology of Crocus sativus series. *AYU (An International Quarterly Journal of Research in Ayurveda)*, *31*(3), Article 3. https://doi.org/10.4103/0974-8520.77153

Say, R., Erdem, M., Ersöz, A., Türk, H., & Denizli, A. (2005). Biomimetic catalysis of an organophosphate by molecularly surface imprinted polymers. *Applied Catalysis A: General*, *286*(2), 221–225. https://doi.org/10.1016/j.apcata.2005.03.015

Seifi, A., & Shayesteh, H. (2020). Molecular biology of Crocus sativus. In *Saffron* (pp. 247–258). Elsevier. https://doi.org/10.1016/b978-0-12-818638-1.00015-0

Sellergren, B., Rückert, B., & Hall, A. J. (2002). Layer-by-Layer Grafting of Molecularly Imprinted Polymers via Iniferter Modified Supports. *Advanced Materials*, *14*(17), 1204–1208. https://doi.org/10.1002/1521-4095(20020903)14:17<1204::AID-ADMA1204>3.0.CO;2-O

Semiond, D., Dautraix, S., Desage, M., Majdalani, R., Casabianca, H., & Brazier, J. L. (1996). Identification and isotopic analysis of safranal from supercritical fluid extraction and alcoholic extracts of saffron. *Analytical Letters*, *29*(6), 1027–1039. https://doi.org/10.1080/00032719608001453

Sereshti, H., Poursorkh, Z., Aliakbarzadeh, G., & Zarre, S. (2018). Quality control of saffron and evaluation of potential adulteration by means of thin layer chromatography-image analysis and chemometrics methods. *Food Control*, *90*, 48–57. https://doi.org/10.1016/j.foodcont.2018.02.026

Shafat A., M., Javeed I.A., B., Rouf Ahmad, B., Bilal A., B., Hafiz ul, I., Shakeel, A. D., Ishrat, B., & Gowhar, R. (2021). Cytogenetic and bioactive attributes of Crocus sativus (Saffron): A tool to unfold its medicinal mystery. In *Medicinal and Aromatic Plants* (pp. 145–167). Elsevier. https://doi.org/10.1016/b978-0-12-819590-1.00007-0

Shahi, T., Assadpour, E., & Jafari, S. M. (2016). Main chemical compounds and pharmacological activities of stigmas and tepals of 'red gold'; saffron. *Trends in Food Science & Technology*, *58*, 69–78. https://doi.org/10.1016/j.tifs.2016.10.010

Shanker Sahu, R., Dubey, A., & Shih, Y. (2021). Novel metal-free in-plane functionalized graphitic carbon nitride with graphene quantum dots for effective photodegradation of 4-bromophenol. *Carbon*, *182*, 89–99. https://doi.org/10.1016/j.carbon.2021.05.033

Sharma, M., Thakur, R., & Sharma, M. (2020). Ethnomedicinal, phytochemical and pharmacological properties of Crocus sativus (saffron). *The Journal of Indian Botanical Society*, *99*, 115–126. https://doi.org/10.5958/2455-7218.2020.00017.0

Shati, A. A., Elsaid, F. G., & Hafez, E. E. (2011). Biochemical and molecular aspects of aluminium chloride-induced neurotoxicity in mice and the protective role of Crocus sativus L. extraction and honey syrup. *Neuroscience*, *175*, 66–74. https://doi.org/10.1016/j.neuroscience.2010.11.043

Shea, K. J., & Sasaki, D. Y. (1989). On the control of microenvironment shape of functionalized network polymers prepared by template polymerization. *Journal of the American Chemical Society*, *111*(9), 3442–3444. https://doi.org/10.1021/ja00191a059

Siavash, H. C., Fadzilah, A. A. M., Mohamad, R. S., Ehsan, T., & Saleh, S. (2010). Impact of saffron as an anti-cancer and anti-tumor herb. *African Journal of Pharmacy and Pharmacology*, *4*(11), 834–840.

Siddiqui, M. J., Saleh, M. S. M., Basharuddin, S. N. B. B., Zamri, S. H. B., Mohd Najib, M. H. bin, Che Ibrahim, M. Z. bin, binti Mohd Noor, N. A., Binti Mazha, H. N., Mohd Hassan, N., & Khatib, A. (2018). Saffron (Crocus sativus L.): As an Antidepressant. *Journal of Pharmacy & Bioallied Sciences*, *10*(4), Article 4. https://doi.org/10.4103/JPBS.JPBS_83_18

Siddiqui, M., Saleh, M. M. M., Basharuddin, S. B. B., Zamri, S. B., Mohd Najib, M. bin, Che Ibrahim, M., binti Mohd Noor, N., Binti Mazha, H., Mohd Hassan, N., & Khatib, A. (2018). Saffron (Crocus sativus L.): As an antidepressant . *Journal of Pharmacy And Bioallied Sciences*, *10*(4), 173. https://doi.org/10.4103/jpbs.jpbs_83_18

Silvestri, D., Borrelli, C., Giusti, P., Cristallini, C., & Ciardelli, G. (2005). Polymeric devices containing imprinted nanospheres: A novel approach to improve recognition in water for clinical uses. *Analytica Chimica Acta*, *542*(1), 3–13. https://doi.org/10.1016/j.aca.2004.12.005

Soffritti, G., Busconi, M., Sánchez, R. A., Thiercelin, J. M., Polissiou, M., Roldán, M., & Fernández, J. A. (2016a). Genetic and epigenetic approaches for the possible detection of adulteration and auto-adulteration in saffron (Crocus sativus L.) Spice. *Molecules*, *21*(3), 1–16. https://doi.org/10.3390/molecules21030343

Soffritti, G., Busconi, M., Sánchez, R. A., Thiercelin, J.-M., Polissiou, M., Roldán, M., & Fernández, J. A. (2016b). Genetic and epigenetic approaches for the possible detection of adulteration and auto-adulteration in saffron (Crocus sativus L.) spice. *Molecules*, *21*(3), 343.

Sreenivasan, K. (2006). Surface imprinted polyurethane film as a chiral discriminator. *Talanta*, *68*(3), 1037–1039. https://doi.org/10.1016/j.talanta.2005.05.005

Srivastava, R., Ahmed, H., Dixit, R., Dharamveer, & Saraf, S. (2010). Crocus sativus L.: A comprehensive review. In *Pharmacognosy Reviews* (Vol. 4, Issue 8, pp. 200–208). Wolters Kluwer -- Medknow Publications. https://doi.org/10.4103/0973-7847.70919

Sujata, V., Ravishankar, G. A., & Venkataraman, L. V. (1992). Methods for the analysis of the saffron metabolites crocin, crocetins, picrocrocin and safranal for the determination of the quality of the spice using thin-layer chromatography, high-performance liquid chromatography and gas chromatography. *Journal of Chromatography A*, *624*(1–2), 497–502. https://doi.org/10.1016/0021-9673(92)85699-T

Sunanda, B., Rammohan, B., Amitabh, K., & Kudagi, B. (2014). The effective study of aqueous extract of Crocus sativus Linn. In chemical induced convulsants in rats. *World Journal of Pharmacy and Pharmaceutical Sciences (WJPPS)*, *3*(8), 1175–1182.

Surugiu, I., Danielsson, B., Ye, L., Mosbach, K., & Haupt, K. (2001). Chemiluminescence Imaging ELISA Using an Imprinted Polymer as the Recognition Element Instead of an Antibody. *Analytical Chemistry*, *73*(3), 487–491. https://doi.org/10.1021/ac0011540

Taherzadeh, Z., Khaluyan, H., Iranshahy, M., Rezaeitalab, F., Ghalibaf, M. H. E., & Javadi, B. (2020). Evaluation of sedative effects of an intranasal dosage form containing saffron, lettuce seeds and sweet violet in primary chronic insomnia: A randomized, double-dummy, double-blind placebo controlled clinical trial. *Journal of Ethnopharmacology*, *262*, 113116.

Tamayo, F. G., Titirici, M. M., Martin-Esteban, A., & Sellergren, B. (2005). Synthesis and evaluation of new propazine-imprinted polymer formats for use as stationary phases in liquid

chromatography. *Analytica Chimica Acta*, *542*(1), 38–46.

https://doi.org/10.1016/j.aca.2004.12.063

Thakar, M., & Sharma, T. (2018). MICROWAVE ASSISTED EXTRACTION OF BIOLOGICAL COMPONENTS

OF CROCUS SATIVUS WITH DNA BARCODING TECHNOLOGY. *International Journal of*

Pharmaceutical Sciences and Research, *47*, 82.

Thangaraju, S., Modupalli, N., & Natarajan, V. (2021). Food Adulteration and Its Impacts on Our

Health/Balanced Nutrition. In *Food Chemistry* (pp. 189–216). John Wiley & Sons, Ltd.

https://doi.org/10.1002/9781119792130.ch7

Torelli, A., Marieschi, M., & Bruni, R. (2014a). Authentication of saffron (Crocus sativus L.) in

different processed, retail products by means of SCAR markers. *Food Control*, *36*(1), 126–

131. https://doi.org/10.1016/j.foodcont.2013.08.001

Torelli, A., Marieschi, M., & Bruni, R. (2014b). Authentication of saffron (Crocus sativus L.) in

different processed, retail products by means of SCAR markers. *Food Control*, *36*(1), 126–

131.

Trapero, A., Ahrazem, O., Rubio-Moraga, A., Jimeno, M. L., Gómez, M. D., & Gómez-Gómez, L.

(2012). Characterization of a glucosyltransferase enzyme involved in the formation of

kaempferol and quercetin sophorosides in Crocus sativus. *Plant Physiology*, *159*(4), 1335–

1354. https://doi.org/10.1104/pp.112.198069

ul Gani Mir, T., Malik, A. Q., Singh, J., Shukla, S., & Kumar, D. (2022). An Overview of Molecularly

Imprinted Polymers Embedded with Quantum Dots and Their Implementation as an

Alternative Approach for Extraction and Detection of Crocin. *ChemistrySelect*, *7*(21),

e202200829. https://doi.org/10.1002/slct.202200829

Varliklioz Er, S., Eksi-Kocak, H., Yetim, H., & Boyaci, I. H. (2017). Novel Spectroscopic Method for

Determination and Quantification of Saffron Adulteration. *Food Analytical Methods*, *10*(5),

1547–1555. https://doi.org/10.1007/s12161-016-0710-4

Ventola, C. L. (2015). The antibiotic resistance crisis: Causes and threats. *P & T Journal*, *40*(4), 277–283. https://doi.org/Article

Visciano, P., & Schirone, M. (2021). Food frauds: Global incidents and misleading situations. *Trends in Food Science & Technology*, *114*, 424–442. https://doi.org/10.1016/j.tifs.2021.06.010

Wang, H.-F., He, Y., Ji, T.-R., & Yan, X.-P. (2009). Surface Molecular Imprinting on Mn-Doped ZnS Quantum Dots for Room-Temperature Phosphorescence Optosensing of Pentachlorophenol in Water. *Analytical Chemistry*, *81*(4), 1615–1621. https://doi.org/10.1021/ac802375a

Wani, A. K., Akhtar, N., Datta, B., Pandey, J., & Amin-ul Mannan, M. (2021). Chapter 14 - Cyanobacteria-derived small molecules: A new class of drugs. In A. Kumar, J. Singh, & J. Samuel (Eds.), *Volatiles and Metabolites of Microbes* (pp. 283–303). Academic Press. https://doi.org/10.1016/B978-0-12-824523-1.00003-1

Wani, A. K., Akhtar, N., Sher, F., Navarrete, A. A., & Américo-Pinheiro, J. H. P. (2022). Microbial adaptation to different environmental conditions: Molecular perspective of evolved genetic and cellular systems. *Archives of Microbiology*, *204*(2), 144. https://doi.org/10.1007/s00203-022-02757-5

Wei, X., Hao, T., Xu, Y., Lu, K., Li, H., Yan, Y., & Zhou, Z. (2016). Facile polymerizable surfactant inspired synthesis of fluorescent molecularly imprinted composite sensor via aqueous CdTe quantum dots for highly selective detection of λ-cyhalothrin. *Sensors and Actuators B: Chemical*, *224*, 315–324. https://doi.org/10.1016/j.snb.2015.10.048

Wu, L., Liu, X., Lv, G., Zhu, R., Tian, L., Liu, M., Li, Y., Rao, W., Liu, T., & Liao, L. (2021). Study on the adsorption properties of methyl orange by natural one-dimensional nano-mineral materials with different structures. *Scientific Reports*, *11*(1), Article 1. https://doi.org/10.1038/s41598-021-90235-1

Xi, L., & Qian, Z. (n.d.). *Pharmacological Properties of Crocetin and Crocin (Digentiobiosyl Ester of Crocetin) from Saffron*.

Ye, L., Cormack, P. A. G., & Mosbach, K. (2001). Molecular imprinting on microgel spheres. *Analytica Chimica Acta*, *435*(1), 187–196. https://doi.org/10.1016/S0003-2670(00)01248-4

Ye, L., Surugiu, I., & Haupt, K. (2002). Scintillation Proximity Assay Using Molecularly Imprinted Microspheres. *Analytical Chemistry*, *74*(5), 959–964. https://doi.org/10.1021/ac015629e

Yildirim, M. U., Sarihan, E. O., & Khawar, K. M. (2020). Chapter 2—Ethnomedicinal and Traditional Usage of Saffron (Crocus sativus L.) in Turkey. In M. Sarwat & S. Sumaiya (Eds.), *Saffron* (pp. 21–31). Academic Press. https://doi.org/10.1016/B978-0-12-818462-2.00002-4

Yin, J., Yang, G., & Chen, Y. (2005). Rapid and efficient chiral separation of nateglinide and its l-enantiomer on monolithic molecularly imprinted polymers. *Journal of Chromatography A*, *1090*(1), 68–75. https://doi.org/10.1016/j.chroma.2005.06.078

Yoshino, F., Yoshida, A., Umigai, N., Kubo, K., & Lee, M.-C.-I. (2011). Crocetin reduces the oxidative stress induced reactive oxygen species in the stroke-prone spontaneously hypertensive rats (SHRSPs) brain. *Journal of Clinical Biochemistry and Nutrition*, *49*(3), 182–187. https://doi.org/10.3164/jcbn.11-01

Zalacain, A., Ordoudi, S. A., Blázquez, I., Díaz-Plaza, E. M., Carmona, M., Tsimidou, M. Z., & Alonso, G. L. (2005). Screening method for the detection of artificial colours in saffron using derivative UV-Vis spectrometry after precipitation of crocetin. *Food Additives and Contaminants*, *22*(7), 607–615. https://doi.org/10.1080/02652030500150051

Zengin, G., Aumeeruddy, M. Z., Diuzheva, A., Jekő, J., Cziáky, Z., Yıldıztugay, A., Yıldıztugay, E., & Mahomoodally, M. F. (2019). A comprehensive appraisal on Crocus chrysanthus (Herb.) Herb. Flower extracts with HPLC–MS/MS profiles, antioxidant and enzyme inhibitory properties. *Journal of Pharmaceutical and Biomedical Analysis*, *164*, 581–589. https://doi.org/10.1016/j.jpba.2018.11.022

Zhang, L., Cheng, G., & Fu, C. (2003). Synthesis and characteristics of tyrosine imprinted beads via suspension polymerization. *Reactive and Functional Polymers*, *56*(3), 167–173. https://doi.org/10.1016/S1381-5148(03)00054-3

Zhang, M., Yu, H., Tang, X., Zhu, X., Deng, S., & Chen, W. (2022). Multifunctional Carbon Dots-Based

Fluorescence Detection for Sudan I, Sudan IV and Tetracycline Hydrochloride in Foods.

Nanomaterials, *12*(23), 4166.

Zhou, T., Ding, L., Che, G., Jiang, W., & Sang, L. (2019). Recent advances and trends of molecularly

imprinted polymers for specific recognition in aqueous matrix: Preparation and application

in sample pretreatment. *TrAC Trends in Analytical Chemistry*, *114*, 11–28.

https://doi.org/10.1016/j.trac.2019.02.028

Zhu, J., Li, Y., Huang, Y., Ou, C., Yuan, X., Yan, L., Li, W., Zhang, H., & Shen, P. K. (2019). General

Strategy To Synthesize Highly Dense Metal Oxide Quantum Dots-Anchored Nitrogen-Rich

Graphene Compact Monoliths To Enable Fast and High-Stability Volumetric Lithium/Sodium

Storage. *ACS Applied Energy Materials*, *2*(5), 3500–3512.

https://doi.org/10.1021/acsaem.9b00279

Zilaee, M., Hosseini, S. A., Jafarirad, S., Abolnezhadian, F., Cheraghian, B., Namjoyan, F., & Ghadiri, A.

(2019a). An evaluation of the effects of saffron supplementation on the asthma clinical

symptoms and asthma severity in patients with mild and moderate persistent allergic

asthma: A double-blind, randomized placebo-controlled trial. *Respiratory Research*, *20*(1).

https://doi.org/10.1186/s12931-019-0998-x

Zilaee, M., Hosseini, S. A., Jafarirad, S., Abolnezhadian, F., Cheraghian, B., Namjoyan, F., & Ghadiri, A.

(2019b). An evaluation of the effects of saffron supplementation on the asthma clinical

symptoms and asthma severity in patients with mild and moderate persistent allergic

asthma: A double-blind, randomized placebo-controlled trial. *Respiratory Research*, *20*(1),

39. https://doi.org/10.1186/s12931-019-0998-x

Zoughi, S., Faridbod, F., Amiri, A., & Ganjali, M. R. (2021). Detection of tartrazine in fake saffron

containing products by a sensitive optical nanosensor. *Food Chemistry*, *350*, 129197.